DEFORMATION ANALYSIS OF CONCRETE FACED AYDIN KARACASU DAM AND COMPARISON OF THEORETICAL RESULTS WITH MEASUREMENTS

A THESIS SUBMITTED TO
THE GRADUATE SCHOOL OF NATURAL AND APPLIED SCIENCES
OF
MIDDLE EAST TECHNICAL UNIVERSITY

BY

TUĞÇE TÜTÜNCÜBAŞI TOSUN

IN PARTIAL FULFILLMENT OF THE REQUIREMENTS
FOR
THE DEGREE OF MASTER OF SCIENCE
IN
CIVIL ENGINEERING

JUNE 2015

Approval of the thesis:

“DEFORMATION ANALYSIS OF CONCRETE FACED AYDIN KARACASU DAM AND COMPARISON OF THEORETICAL RESULTS WITH MEASUREMENTS”

Submitted by **TUĞÇE TÜTÜNCÜBAŞI TOSUN**in partial fulfillment of the requirements for the degree of **Master of Science in Civil Engineering Department, Middle East Technical University** by,

Prof. Dr. Gülbin Dural Ünver Dean, Graduate School of **Natural and Applied Sciences**	____________________
Prof. Dr. Ahmet CevdetYalçiner Head of Department, **Civil Engineering**	____________________
Prof. Dr. ErdalÇokça Supervisor, **Civil Engineering Dept., METU**	____________________
Prof. Dr. M. Yener Özkan Co-Supervisor,**Civil Engineering Dept., METU**	____________________

Examining Committee Members

Prof. Dr. Ufuk Ergun Civil Engineering Dept., METU	____________________
Prof. Dr. ErdalÇokça Civil Engineering Dept., METU	____________________
Prof. Dr. M. Yener Özkan Civil Engineering Dept., METU	____________________
Doc. Dr. Zeynep Gülerce Civil Engineering Dept., METU	____________________
GülruSaadet Yıldız, MSc Free Lance	____________________ Date: 29.06.2015

I hereby declare that all information in this document has been obtained and presented in accordance with academic rules and ethical conduct. I also declare that, as required by these rules and conduct, I have fully cited and referenced all material and results that are not original to this work.

Name, Last name: Tuğçe Tütüncübaşı Tosun

Signature:

ABSTRACT

DEFORMATION ANALYSIS OF CONCRETE FACED AYDIN KARACASU DAM AND COMPARISON OF THEORETICAL RESULTS WITH MEASUREMENTS

Tütüncübaşı Tosun, Tuğçe
M.S., Department of Civil Engineering
Supervisor: Prof. Dr. Erdal Çokça
Co-Supervisor: Prof. Dr. M. Yener Özkan

June 2015, 121 Pages

The improvement in design technologies has enhanced the use of different fill materials in construction of the embankment dams. Rockfill is one of the most preferred fill materials for embankment dam. Also, use of different fill material such as sand-gravel has been preferred in recent years. Previous studies on concrete faced sand-gravel fill dam, results of the laboratory experiments and in-situ testing analysis display that using sand-gravel as a fill material is not only cost-effective but also safe and provides high quality natural construction material. In this study, settlement of Karacasu Dam, which is the first concrete faced sand-gravel fill dam in Turkey, is examined during "end of construction" period and "reservoir impoundment" period. Total stresses and deformations are determined by computing two dimensional finite element analyses. Hardening soil model is utilized to obtain non-linear, stress dependent and inelastic behavior of the sand-gravel fill material. As a first approach, model parameters of sand-gravel fill are selected mainly according to the previous works on the concrete faced dams. Then, back analyses are conducted to obtain optimal values. Finally, deformations and stresses, which are calculated by finite element analyses, are compared with the data observed by General Directorate of State Hydraulic Works (DSİ) for both end of the construction and reservoir impoundment periods. The comparison of the results indicates that calculated deformations are generally compatible with the observed ones.

Keywords: sand-gravel fill, deformation, two dimensional finite element model, end of construction, reservoir impoundment, hardening soil model

ÖZ

ÖN YÜZÜ BETON KAPLI AYDIN KARACASU BARAJININ DEFORMASYON ANALİZİ VE ÖLÇÜMLERLE TEORİK BULGULARIN KARŞILAŞTIRILMASI

Tütüncübaşı Tosun, Tuğçe

Yüksek Lisans, İnşaat Mühendisliği Bölümü

Tez Yöneticisi: Prof. Dr. Erdal Çokça

Ortak Tez Yöneticisi: Prof. Dr. M. Yener Özkan

Haziran 2015, 121 Sayfa

Dizayn teknolojilerindeki gelişim, farklı dolgu malzemelerin baraj inşaatlarında kullanımını arttırmaktadır. Dolgu barajlar için kaya, dolgu malzemesi olarak en çok tercih edilenlerden birisidir. Fakat son yıllarda kum-çakıl da dolgu malzemesi olarak kullanılmaya başlanmıştır. Ön yüzü beton kaplı kum-çakıl dolgu barajlar üzerine yapılan daha önceki çalışmalar, laboratuvar deneyleri ve test sonuçlarının da gösterdiği üzere, kum-çakılın dolgu malzemesi olarak kullanılması sadece ekonomik açıdan avantaj sağlamamakta, bunun yanında daha güvenli ve yüksek kaliteli baraj tasarımına olanak sağlamaktadır. Bu çalışmada Türkiye'nin ilk ön yüzü beton kaplı kum-çakıl dolgu barajı olan Aydın Karacasu Barajı'nın inşa aşamasında ve rezervuar dolumu sırasında oturma davranışı incelenmiştir. Toplam gerilmeler ve deformasyonlar iki boyutlu sonlu elemanlar yöntemi ile belirlenmiştir. Sertleşen zemin modeli, kum-çakıl dolgu malzemesinin doğrusal, gerilime bağımlı, elastik olmayan davranışını belirlemek için kullanılmıştır. Kum-çakılın malzeme model parametreleri, ön yüzü beton kaplı dolgu barajlar üzerine yapılan çalışmalar nezdinde seçilmiştir. Daha sonra, geri analiz yapılarak en ideal parametreler bulunmuştur. Sonuç olarak, sonlu elemanlar analiz sonuçlarından elde edilen değerler ile Devlet Su İşleri Genel Müdürlüğünden alınan değerlerin karşılaştırması yapılarak doğru malzeme parametrelerin ortaya konması sağlanmıştır. Bu karşılaştırmalardan çıkan sonuçlar, sonlu elemanlar modeli ile elde edilen deformasyonların genellikle T. C. Devlet Su İşleri Genel Müdürlüğü tarafından gözlenen deformasyonlar ile uyumlu olduğunu göstermiştir.

Anahtar Kelimeler: kum-çakıl dolgu, deformasyon, iki boyutlu sonlu elemanlar modeli, inşa aşaması, rezervuar dolumu, sertleşen malzeme modeli

To my daughter and husband

Masal Asya Tosun ve Oğuzhan Tosun’a

ACKNOWLEDGMENTS

First of all, I would like to express my sincere attitude to my supervisor, Prof. Dr. Erdal ÇOKÇA and co-supervisor Prof. Dr. M. Yener ÖZKAN for their extreme patience, support, advise, encouragement and warm-hearted cooperation that they have provided me during my whole graduate study. Their guidance helped throughout the research and writing phase of this thesis. I am thankful for their great interest and help.

I would like to give my special thanks to İlker PEKER and Gülru S. YILDIZ, M.Sc. for their valuable support and advises. They helped me patiently throughout the study. I am thankful for their precious advises encouragement, insight and excellent guidance.

I am thankful to my grand family Ali AYKANAT, Saadet AYKANAT and Naide ÇALTI for their limitless help, patience and self-abnegation. They come Ankara from Eskişehir in order to look after my baby whenever I call. This study would have never been completed without their support. I am also thankful to my dear family Nesrin TÜTÜNCÜBAŞI, Murat TÜTÜNCÜBAŞI, Fatma TOSUN, Cemil TOSUN, Aybike TOSUN, Gönül ÇALTI and Sevil ÇALTI for their tolerations, help and encouragements. They hardly get permission from their work and come to Ankara from İstanbul to look after my baby whenever I call. They always give me a back throughout this study. I would never have accomplished this study without their love and belief in me. Especially, I would like to thank to my dear sister Aybüke TÜTÜNCÜBAŞI for her help during whole thesis. Her limitless support and toleration help me through this difficult period. I consider myself lucky to be having a nice family.

I also would like to express my thanks to my supervisors, colleagues from Ziraat Bank and my dear fellow Duygu DİNÇ for their help and their belief in me during this study and graduation. In addition, I want to specially thank to Didem Gamze ÖGET, Yaşam

KIZILDAĞ, Kübra BEZGİN, Miray ARCA, Furkan KAVASOĞLU, Tuğçe ÇELİK who have supported me and helped me stay focused on my study.

Last but not least, I wish to show my intimate appreciation to my spouse equivalent Oğuzhan TOSUN, who has always helped selflessly and motivated me throughout this study. He supported almost at every stage of this study and without his support this study would have never finished. In addition, I would like to thank to my dear daughter Masal Asya TOSUN. She shows limitless patience during this difficult and long process despite being a baby. This thesis is dedicated to them and without their love, patience and belief in me I would never have completed this. Hence, I am grateful for having my family.

TABLE OF CONTENTS

LIST OF FIGURES

FIGURES

LIST OF TABLES

TABLES

CHAPTER 1

INTRODUCTION

1.1. Problem Statement

The unregulated water resources need to be managed in order to satisfy the needs of mankind. For this purpose, people have been constructing dams for water supply and irrigation since the beginning of civilization. The oldest known dam in the world is Jawa Dam, constructed in BC 3000 at Jordan. Dams are the sources of water which are constructed for many purposes among which are flood control, hydro-power, irrigation, drinking water. Water utilization is a sign of development in civil life.

With technological development and increased perfection in dam engineering, concrete face sand-gravel dams (CFSGD) are widely used in today’s world. Due to economic aspects, the application of sand-gravel fill materials, mostly alluvial deposits, is gaining more and more relevance for the selection of the dam fill materials. Safety of CFSGDs is based on construction, appropriate design, and observation of actual behavior during the construction and during the operation of the structure. The most important problems encountered at CFSGDs are cracking of impervious face and deformation behavior of dam body, because cracking can cause leakage (Haselsteiner et al., 2011).

1.2.Thesis Objective

Finite element method has been used, starting with Clough at 1967, as the most powerful method to calculate the stresses and deformation in earth; both at end of construction period and at water impoundment period. Before finite element method, predictions were made by linear elastic model which does not overlap with real behavior of earth. Today, the behavior of earth can be modeled as nonlinear and inelastic models, which agree with real soil behavior, by using technological computers and more complex methods.

The main objective of this study is to determine the deformation and stress behavior of the Karacasu Dam, the first concrete faced sand-gravel dam in Turkey, by utilizing two dimensional finite element model. Within this context, the focus is given to material model parameters that affect the deformation behavior of the soil. Another objective is the comparison of the calculated results, taken from two dimensional finite element analyses, with observed data, obtained from General Directorate of State Hydraulic Works (DSİ). It is expected that calculated results and observed data will be compatible. Figure 1.1 represents the methodology of the study.

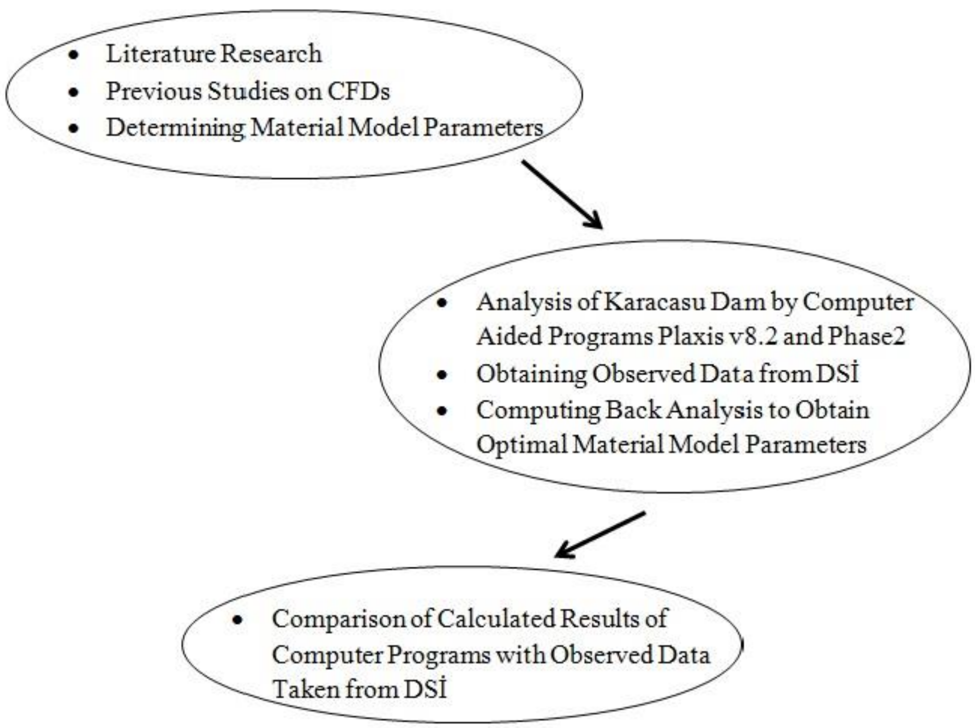

Figure 1.1 Schematic representation of the methodology of the study

In this study, stresses and deformations are calculated for both construction period and water impoundment period with the computer aided programs Plaxis v8.2 and Phase 2. The results taken from finite element analysis and observed data, obtained from General Directorate of State Hydraulic Works (DSİ), are compared. Hardening soil model is used to represent sand-gravel material behavior in Plaxis v8.2 during analyses since hardening soil model is a nonlinear and inelastic model. Mohr-Coulomb Model is also used to represent sand-gravel material behavior in Phase2. Indeed, material model parameters, which are used as an input in computer, aided programs, Plaxis v8.2 and Phase2, carry importance, since they directly affect the deformation behavior of the dam. Thus, in the scope of our study, the literature work related to estimations of material model parameters is carefully examined.

1.3.Thesis Scope

This thesis contains a total of five chapters: (1) Introduction, (2) A Review of Literature, (3) General Information about Concrete Faced Aydın Karacasu Dam and Instrumentation, (4) Settlement Analyses of Concrete Faced Aydın Karacasu Dam, (5) Results of Analyses, and (6) Summary, Conclusions and Future Studies.

In Chapter 2, the literature works related to concrete faced dams are presented. In this regard, characteristics of concrete faced dams (CFD) and specific examples are given. In Chapter 3, general information about concrete faced Aydın Karacasu dam and instrumentation are presented. Chapter 4 covers the settlement analyses of Karacasu Dam and nonlinear material models are summarized. In Chapter 5, the results obtained from finite element models are given and a comparison of the results, which are computed by Plaxis v8.2 and Phase2, and observed data taken from DSİ is provided at the end. The last chapter summarizes the whole work explained in this study. It comprises of the summary of the study as well as the major findings. Also, the conclusions of all analyses are given in this chapter. Finally, the chapter gives a brief idea for the future studies.

CHAPTER 2

A REVİEW OF LITERATURE

The implementation of concrete faced dams has increased all over the world during last decades. In today's world, concrete faced dam (CFD) types have become popular and competed with roller compacted concrete dam types when the general limitation are proper for both types concerning mainly geology and fill material (Haselsteiner et al., 2011).

Some properties of the CFDs differ from other type of dams. Slope of the CFDs are usually steeper than other embankment dam types. Because it is assumed that no pore pressure and limited seepage flow occur in the main body. However, experiences have displayed that serious seepage flow may occur as a result of cracking in the concrete membrane. This cracking forms frequently during first reservoir impoundment (Haselsteiner et al., 2011).

CFDs can be divided in two categories with respect to construction material for the main fill; (1) concrete faced rockfill dams (CFRD), (2) concrete faced sand-gravel fill dams (CFSGD). Rockfill is provided from rock quarries. Sand-gravel fill material is generally supplied in the form of river deposits (alluvium). Occasionally, differentiating of two types is not obvious because the majority of CFSGDs includes rockfill material, which is utilized in corresponding zones (Haselsteiner et al., 2011).

Zoning of CFDs has to be determined for each project in terms of applied zonings, available materials and other constraints. Typical cross-section of a CFRD is given in the Figure 2.1.

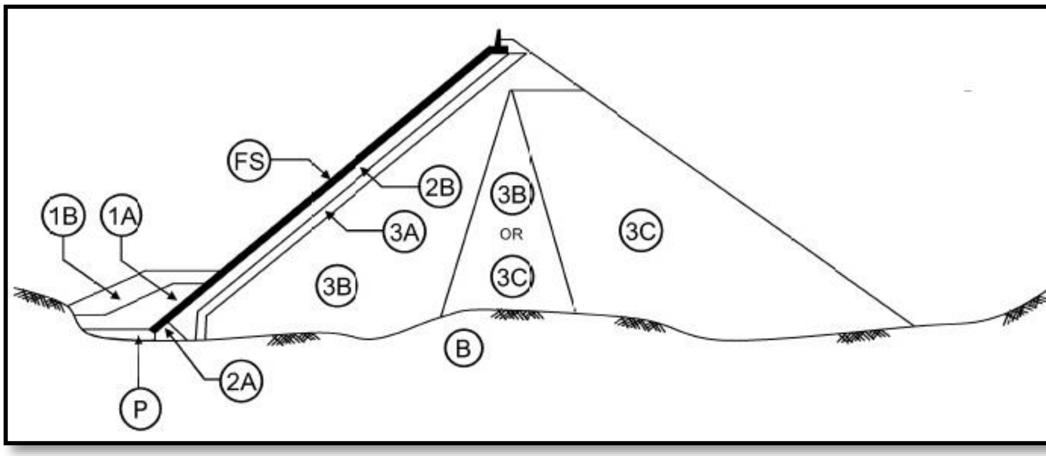

Figure 2.1 Typical CFRD cross-section/zoning (ICOLD, 2005)

Where,

3A : Filter Zone,
3B : Rockfill (well compacted),
3C : Rockfill,
1A : Self-Healing Fill,
1B : Protection Fill,

2A : Perimeter Zone
2B : Cushion Zone
P : Plinth
FS : Concrete Face Slab
B : Bedrock

A uniform zoning is not available. However, Fell et al. (2005), stated that the most widespread classification is displayed that corresponds nearly to the section of ICOLD. Recently, gravel or sand-gravel soils are implemented as main fill materials on behalf of coarse rockfill material. Design and construction procedure of the CFSGDs types shows similarity with CFRDs. However some aspects have to be examined and handled differently. Later, in this study, differences between CFSGD and CFRD will be explained. Typical cross-section of a CFSGD is given in the Figure 3. Cracks in the dam body cause seepage flow. L-shaped drain/filter controls the seepage flow. As seen in the

Figure 2.2, zones, which contain different fill material, are separated by a filter/L-shaped drain.

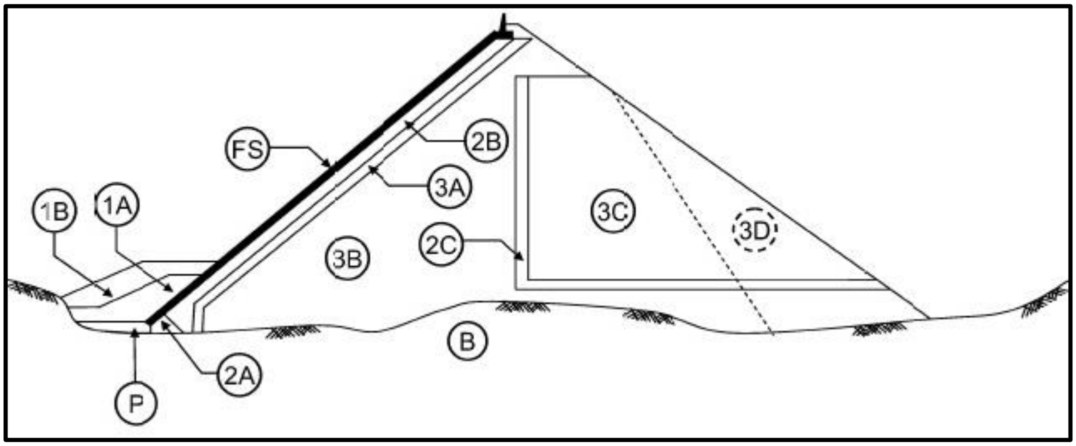

Figure 2.2 Typical CFSGD cross-section (Fell et al., 2005)

Where,

3A : Filter Zone,
3B : Sand-Gravel Fill,
3C : Sand-Gravel Fill (dirty)
3D : Rockfill,
1A : Self-Healing Fill,
1B : Protection Fill,

2A : Perimeter Zone
2B : Cushion Zone
2C : Filter
P : Plinth
FS : Concrete Face Slab
B : Bedrock

Selecting dam type CFRD or CFSGD depends on the availability of granular fill material and clay layer location within the construction area. In the following a main features of CFD dams are outlined.

2.1. A Brief History of CFD Dams

"Impervious membrane type dams originated and were developed in the Sierra Mountains of California, USA in 1850s to meet the requirements of gold miners. The dams were needed in remote, inaccessible locations and in the glaciated granite of Sierra no earth was available. The miners were quite familiar with rock blasting, and used their skill to build dams of quarried rock with impervious facing made from locally available timber." (Singh et al, 1995) The success of technique is accepted by engineering organizations and some major dams of this type were built in 1940s, among which two remarkable examples are 84m high Dix River Dam and 100m high Salt Springs Dam, both in USA. During this period; sound, hard rock was used and rock particles were obtained as large in size as possible by extracting them from large heights. The purpose was to acquire stable contacts between rock particles and to decrease future deformations that could cause leakage and cracking in the impervious membrane.

The period, which improvement of rockfill dams both with impervious membrane and earth cores was made is between 1940 and 1965, which was called as transition period. The major problems of this period were the unavailability of construction sites where comprise of rock having required hardness and the compressibility of dumped fill material (Singh et al, 1995).

With 1950s, earth and rock materials have started to be used together which create rockfill dams with earth cores. In 1938, San Gabriel no: 1 Dam was completed; similarly, in 1950, South Houston with the height of 87m is completed with the same techniques of using earth and rock material together (Singh et al., 1995).

The post of 1965 period can be thought as the modern period of rockfill dam construction. The use of well graded and compacted rockfill was increased. This has provided an increased confidence which caused the construction of dams in unexpected heights. Some outstanding examples are Cethana in Autralia (height of 110 m, completed in 1970) and Foz de Areia in Brazil (height of 160 m, completed in 1980) which is the highest existing concrete faced dam in its time (Keming et al, 1999).

2.2. General Characteristics of CFRDs

Rockfill dams are fundamentally embankment dams. High ratio of stability and high permeability are their special features. The site conditions are important considerations on selection of the dam type. Imperviousness in CFRDs is provided either by an earth core or an impervious membrane.

There are some advantages selecting membrane types instead of earth core types. Selecting "concrete faced rockfill dams" instead of "rockfill dams with earth cores", is more reasonable when the soil for earth core is not available, as for example in high rocky areas. Slopes of fill dams with impervious membrane can be designed steeper than those for the dams with earth core. The weather conditions are also important considerations on selecting the type of dam, because in continuously rainy weather, it is hard to keep proper moisture control for compaction of earth cores and there is no such a problem in concrete faced rockfill type. Placement of concrete membrane requires open air; however, it takes shorter time. In sand-gravel dams and at locations where there is unavailability of large size stones to provide wave protection is not available, a membrane can act as wave protector (Singh et al., 1995).

When compared membrane and earth core types of rockfill dams, membrane ones have the following advantages; greater stability, greater tolerance for leakage, accessibility, speed of construction and stage construction facility. However there are some factors unfavorable to membranes relative to earth cores; which are limited life, higher cost, limitation on height and possibility of leakage (Singh et al., 1995).

"Safety of the CFRDs depends in the proper design, construction, and monitoring of actual behavior during the construction and during the operation of the structure" (Chrzanowski et. al, 2008). The construction of the concrete membrane is an important aspect, especially during first filling of the reservoir and earthquake. When the drainage and sealing system is fully working and no significant seepage intrusion from the dam abutments occurs, concrete faced dams usually display favorable seepage condition.

2.2.1. Deformation Behavior of Rockfill Dams

Rockfill comprises of voids in different sizes and rock fragments. Rock may contact with rock by its edges, surfaces or points. Pore pressures and total stresses change during construction of a dam body and creep takes place. As a result, internal deformation occurs in a dam body. Additionally, load transfer between different zones of the dam and foundation deformations affect dam body deformations. Important movements on the crest may occur during first reservoir impoundment, after the dam construction is completed. The rate of deformation generally reduces with time; although, time-dependent creep may continue at a decreasing rate for several years. The movements may be examined in “vertical direction, horizontal in the upstream-downstream direction normal to the dam axis, horizontal in the cross-valley direction, parallel to the dam axis” (Singh et al., 1995).

2.2.1.1. Importance of Deformations

Monitoring of settlement behavior of dam carries importance for the safety of the dam. Failures give warning signals like increased rate of settlement, cracking, leakage and strain discontinuities. Cracking of the concrete membrane may require expensive repairs. Another significant benefit is that many valuable data accumulates for the design of future dams (Singh et al., 1995).

If water impoundment does not occur too rapidly, the important proportion of deformation will form during construction. Sowers and his colleagues (1975) made a research on deformation behavior of fourteen of the earlier rockfill dam. The results showed that settlements of dam changed from 0.25% to 1% of height in ten years and sluicing have a significant effect on decreasing settlements during construction. Lawton and Lester (1964) worked on settlements of several rockfill dams. They concluded that the settlements could be explained by a formulation:

$$S = 0.001H^{3/2} \qquad \textbf{\textit{Eqn.}}\,(\mathbf{2.1})$$

Where,

S : Settlement (in meters)

H : The dam Height (in meters)

As it can be seen from *Eqn. (2.1)*, the settlement will be calculated as 1% of the dam height for 100 m high dam. According to the equation, the percentage will change with respect to dam height since the relationship between settlement and dam height is not linear (Singh et al., 1995).

The maximum concrete membrane deformation gives an idea about the overall deformation behavior of dam. Salt Spring Dam is a concrete faced rockfill dam with 100 m high in California. According to the case studies on Salt Spring Dam, dam settles extreme values of over 1.0% of the dam height. The reason of extreme deformation is the implementation of dumped rockfill to the Salt Spring Dam. With respect to the case studies, dams settle within a smaller range of 0.05-0.5% of dam height (Haselsteiner et al., 2011). For instance, Shuibuya is a concrete faced rockfill dam with 233m high in China. Settlement value of the Shuibuya Dam was about 0.5% of its height (Haselsteiner et al., 2011).

Horizontal deformations occur as cross-valley movements under the dam own weight. Direction of the cross-valley movements is from the dam abutments towards the deepest part of the valley. Horizontal deformation have been predicted by finite element model and observed on actual dams. Settlements in the upstream and downstream parts and normal to the dam axis mainly occur as a result of first filling of the reservoir. For concrete faced dams, water pressure acts on the upstream face, which causes additional vertical deformations and downstream movement of the crest.

Nobari and Duncan (1972), claimed that more serious vertical and horizontal deformations occur as a result of first reservoir filling. Water loads acting on the upstream membrane and softening of the fill material causes such important deformations. Softening of the fill material is not expected for the rockfill or sand-gravel fill dams. It poses danger for the stability of earth dams. In the *Figure 2.3*, the effect of reservoir impoundment on dam movement is seen.

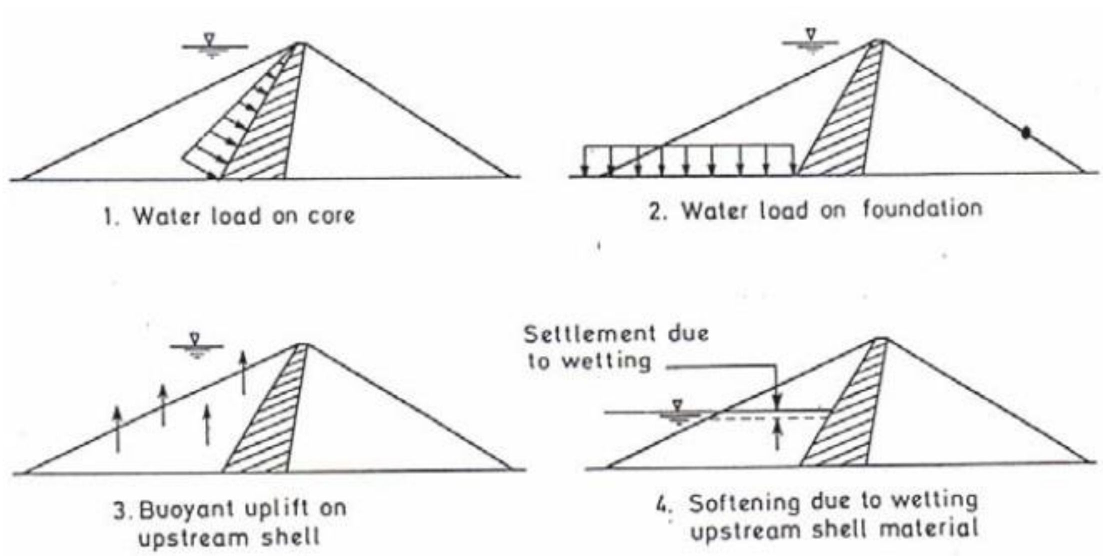

Figure 2.3 The effect of reservoir impoundment on a rockfill dam (Duncan et al., 1972)

2.2.2. Determination of Elasticity Modulus of Rockfill

Settlement behavior of rockfill was determined by Fitzpatric et al. (1985) by using two different elasticity modulus, E_{rc} and $E_{rf.}$ Where,

E_{rf} : Elasticity modulus using to determine first reservoir filling behavior (in MPa)

E_{rc} : Elasticity modulus to determine construction behavior (in MPa)

$$E_{rc} = \frac{\gamma * H * d}{\delta_s} \qquad \textbf{Eqn. (2.2)}$$

$$E_{rf} = \frac{\gamma_w * H * d}{\delta_n} \qquad \textbf{Eqn. (2.3)}$$

Where (Figure 2.4),

γ : $Unit\ weight\ of\ the\ fill\ material\ (in\ kN/m^3)$

$\boldsymbol{\delta_n}$: $Settlement(in\ mm) of\ the\ concrete\ membrane\ at\ a\ depth$ "h" due to reservoir filling

$\boldsymbol{\delta_s}$: $Settlement(in\ mm) of\ the\ thickness\ d\ due\ to\ construction\ (Hunter\ and\ Fell,$ 2003)

In the *Figure 2.4,* Eqn 2.2 and Eqn 2.3 are depicted.

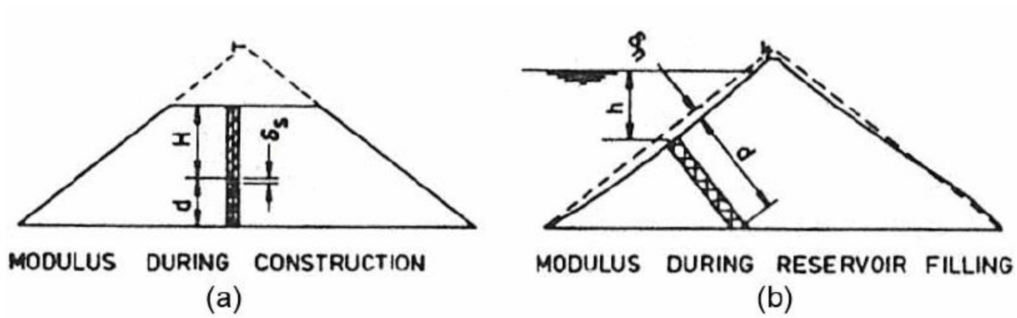

Figure 2.4 Determination of elasticity modulus of rockfill (Fitzpatrick et al., 1985)

2.2.3. Settlement Analysis of CFRDs

Concrete faced rockfill dams are analyzed to determine deformation and stress behavior both in the foundation and dam body. Stage construction is applied in the construction of CFDs. Finite element analysis is used to predict the real behavior of the dam. Clough and Woodward (1967), carried out the finite element method to predict a 30.5 m high homogeneous dam. The purpose of the study is to determine the impact of foundation elasticity and stage construction on settlements and stresses in the dam body. Constant "E" and "ν" values were utilized in settlement analyses. "Single lift analysis" and "10 lift analysis" are computed for the same embankment. Settlements occurred due to dead weight for both analyses. The horizontal displacements calculated by both analyses were close to each other. However, important differences were observed in the distribution pattern and magnitude of the vertical settlement. The maximum vertical settlement was observed at the top of the dam in a "Single lift analysis", whereas small vertical settlement values were observed at the same location in a “10 lift analysis” and the maximum vertical settlement value was observed at the mid-height of the dam. In the *Figure 2.5*, settlement distributions for both analyses can be seen.

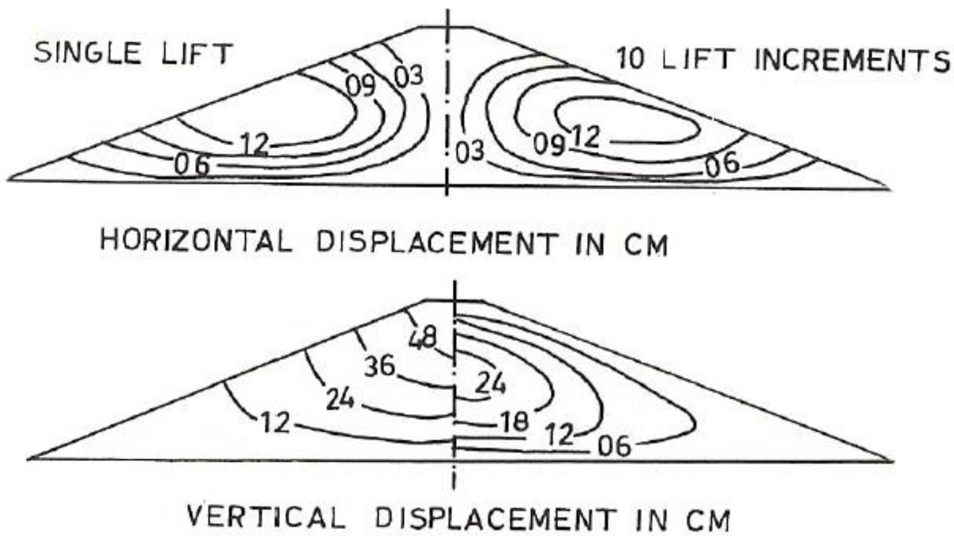

Figure 2.5 Displacement contours of the dam both for single lift analysis and 10 lift increments (Clough et al., 1967)

2.3. General Characteristics of CFSGDs

The implementation of sand-gravel fill material is gaining more and more importance, because CFSGDs may be economical with respect to other alternatives whenever sand-gravel material is available. Salvajina Dam (Colombia) is 148 m high and Golillas Dam (Colombia) is 125 m high concrete face gravel fill dams. Fill material of these dams are exploited from alluvial deposits. Aguamilpa Dam (Mexico) is 187 m high dam. In the construction of Aguamilpa Dam, both rockfill and alluvial material were used. The main fill material of the dam was sand and gravel, so, it is thought to be the highest CFSGD in its time.

Generally, CFSGD types are designed as CFRD. Design and construction approach of CFRDs and CFSGDs are related to each other. On the other side, settlement and seepage behavior of CFRDs and CFSGDs show difference. First of all, the occurrence of cracks depends on applied fill material and measured engineering parameters like elasticity modulus. Sand-gravel fill material display a more favorable deformation behavior, because “the achievable deformation modulus” of sand-gravel are significantly higher than for rockfill materials (Haselsteiner et al., 2011).

In the *Figure 2.6,* elasticity modulus for construction and for first reservoir filling, which is obtained from several case studies, is seen. Elasticity modulus of sand-gravel fill display higher values than the elasticity modulus of rockfill. Oroville Dam is 244 m high. Elasticity modulus of fill material was taken as 365 MPa. Aguamilpa Dam is sand-gravel fill dam. The elasticity modulus of fill material used in construction of Aguamilpa Dam was taken a value of 250 MPa. When elasticity modulus of rockfill was taken between 70-240 MPa, rockfill material was thought to have very high strength. Generally, “gravel-rockfills” are expected to display smaller post construction deformations by a factor of up to 10 when compared to rockfill material having medium strength (Haselsteiner et al., 2011).

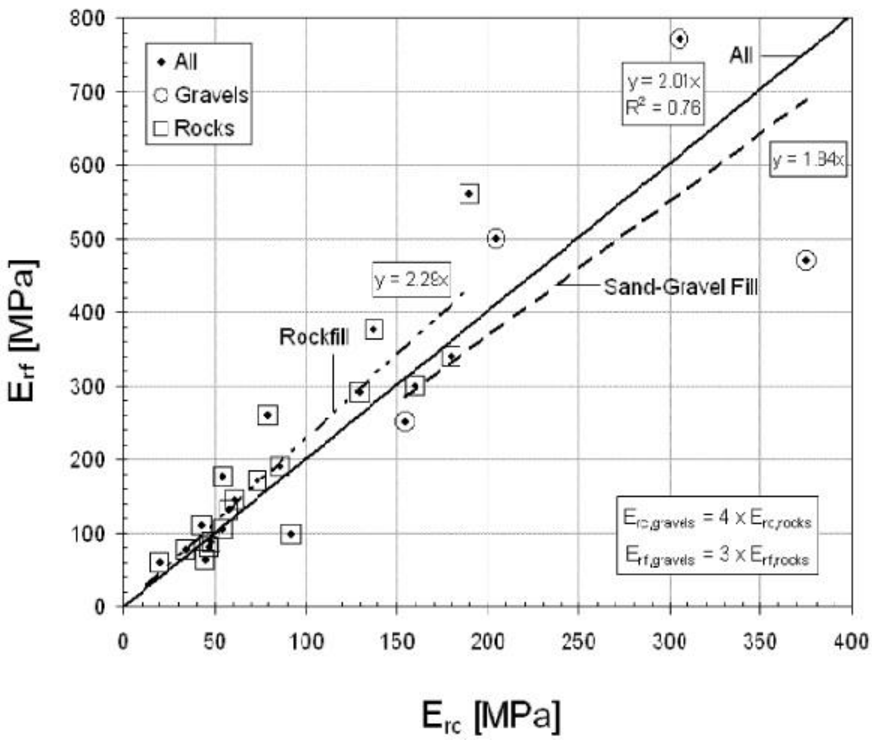

Figure 2.6 Elasticity modulus for construction versus pseudo modulus for first reservoir filling for rocks and gravels (Hunter & Fell, 2002)

Where,

$\mathbf{E_{rf}}$ **:**Pseudo modulus for first reservoir filling

$\mathbf{E_{rc}}$ **:** Elasticity modulus for construction

"When the face slab cracks, seepage may infiltrate into the dam body causing partial saturation of affected zones and corresponding pore water pressures within the dam body. The effective stresses are reduced by the pore water pressure within the affected zones."(Haselsteiner et al., 2011). When dam body does not have enough draining capacity in order to control the seepage conditions, the slope stability of the dam may not be provided. If rockfill material is saturated, it may be exposed to saturation settlements. On the other side, if sand-gravel fill composes of alluvial deposits, sand-gravel fill does not behave as sensitively to saturation as rockfill material (Haselsteiner et al., 2011).

Sand and gravel fill material does not display a free draining feature. Permeability is less than $k=10^{-4}$ m/s. Hence, complicated dam design which comprises extra draining zones is required for concrete faced sand-gravel fill dams (CFSGD). Construction material affects this difference. Where ‘dirty’ sand and gravel fills are utilized to control seepage, drainage systems and to provide zoning for the long-term stability of dam (Haselsteiner et al., 2011).

Another important point is that sand-gravel fill material is generally acquired from alluvial deposits of the river or lateral valleys. When alluvium display significant depth under the dam body and the plinth is not be directly installed on suitable bedrock, which has low compressibility, more serious deformations occur as expected compared to the dam built directly on bedrock.

2.3.1. Observed Deformation Behavior of CFSGDs

Settlement behavior of embankment dams depends on several factors such as fill material, design procedure, construction period and site constraints. A case study is selected to explain the settlement behavior of CFSGD dam for end of construction (EOC) and reservoir impoundment (RI) period. Settlement analyses were studied by Zeng Fanlie (2000) for these conditions in Gudongkou Dam. Sand-gravel is primarily used as a fill material in the construction of Gudongkou Dam.

Gudongkou Dam was built on Gufu River, upstream part of the Xiangxi River. Gudongkou Dam is located in the Xingshan Country in the border of Hubei Province. Catchment area of the dam site is 965 km^2. Reservoir storage is 148 million m^3. Height of the dam is 117.6 m. Crest length is 193 m with upstream slope 1:1.5 and downstream slope 1:1.4. Normal water level is 325.0 m. (Fanlie, 2000)

The section of the Gudongkou Dam was determined according to valuable studies. The dam body consists of six zones and all of the zones were filled with sand-gravel. For economical purpose and convenience in transportation and quality of the material, the natural sand-gravel quarry was selected.

Unconfined compressive strength of sand-gravel in Gudongkou Dam is 25-44 kPa. Dry unit weight of the gravel is 2.76 g/cm^3. Angle of response is 34^o under water level and 38^o above the water level. Average dry density is between 2.28 g/cm^3 and 2.36 g/cm^3. Coefficient of permeability is between 4.0x10^{-4} and 3.9x10^{-3} cm/s and compressibility modulus is taken between 200 and 420 MPa.

Certain number of instrumentation devices was installed at Gudongkou Dam to control the stability and construction quality. Instrumentation devices measured stress, settlement and seepage in Gudongkou Dam. As seen in the Figure ,Pipe type settlement gauges (GS) and steel wire horizontal displacement meters (GY) are installed at elevation of 253.0 m, elevation of 277.0 m and elevation of 302 m. in six different axis (A_1-A_1, A_2-A_2, A_3-A_3, A_4-A_4, A_5-A_5, A_6-A_6) at the maximum cross-section of Gudongkou Dam. Axes are shown in the *Figure 2.7*(Fanlie, 2000).

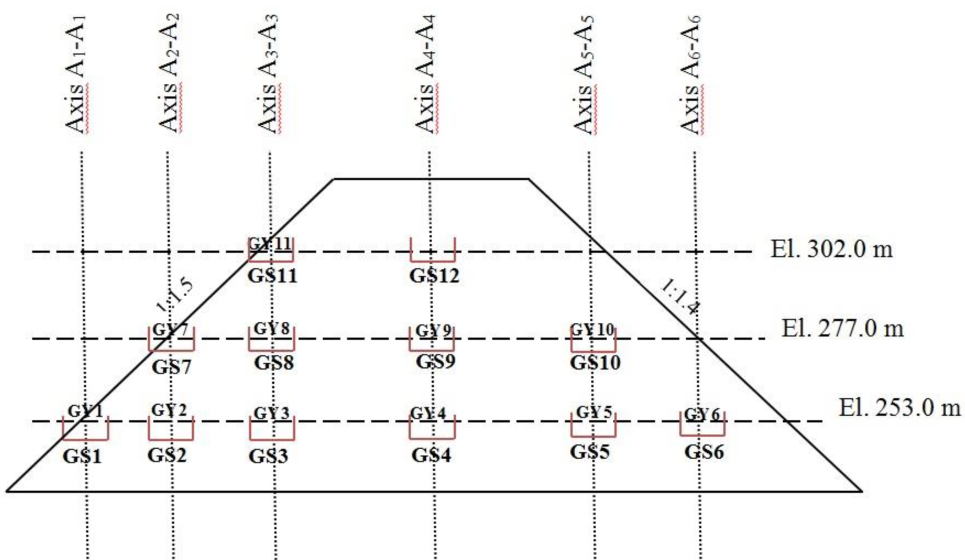

Figure 2.7 Profile diagram of body observation instrumentation of Gudongkou Dam

Gudongkou Dam has deformed for two years, starting from the beginning of the construction to reservoir full condition. Significant observation results of Gudongkou Dam are shown in *Table 2.1* and *Table 2.2*.

Table 2.1 Statistics of Gudongkou Dam settlement observation results in mm

Observation Time	Deformation at Measurement Points														
	GS$_1$	GS$_2$	GS$_3$	GS$_4$	GS$_5$	GS$_6$	Mark$_1$	GS$_7$	GS$_8$	GS$_9$	GS$_{10}$	Mark$_2$	GS$_{11}$	GS$_{12}$	Mark$_3$
17.11.1997	101.0	97.0	156.0	209.0	167.0	216.0	131.0	60.0	170.0	148.0	77.0	85.0	-	-	-
30.05.1998	181.0	126.0	275.0	235.0	358.0	227.0	141.0	100.0	204.0	185.0	188.0	96.0	49.0	67.0	12.0
20.06.1998	191.0	132.0	278.0	238.0	361.0	237.0	143.0	165.0	212.0	228.0	216.0	96.0	53.0	72.0	16.0
06.09.1998	204.0	139.0	281.0	246.0	368.0	245.0	144.0	-	-	-	-	110.0	127.0	146.0	89.0
19.07.1998	274.0	176.0	281.0	270.0	368.0	245.0	-	176.0	214.0	233.0	223.0	-	-	1480	-

Table 2.2 Statistics of Gudongkou Dam horizontal displacement in mm

Observation Time	Deformation at Measurement Points													
	GY$_1$	GY$_2$	GY$_3$	GY$_4$	GY$_5$	GY$_6$	Mark$_1$	GY$_7$	GY$_8$	GY$_9$	GY$_{10}$	Mark$_2$	GY$_{11}$	Mark$_3$
17.11.1997	39.0	15.0	63.0	42.0	26.0	56.0	46.0	-30.2	-31.7	-20.8	28.3	8.3	-	-
30.05.1998	79.1	57.5	63.9	51.5	40.8	76.9	58.0	-36.0	12.0	23.2	-16.1	23.8	-37.1	8.0
20.06.1998	73.8	52.5	62.9	64.1	54.3	74.1	58.0	-36.9	11.4	22.1	-16.5	23.8	45.1	8.0
06.09.1998	70.7	50.2	61.0	50.5	44.4	73.0	-	-	-	-	-	-	44.8	-
19.07.1998	62.0	3.2	67.0	51.9	40.3	80.9	58.0	53.9	11.5	-22.8	-10.5	23.8	48.2	8.0

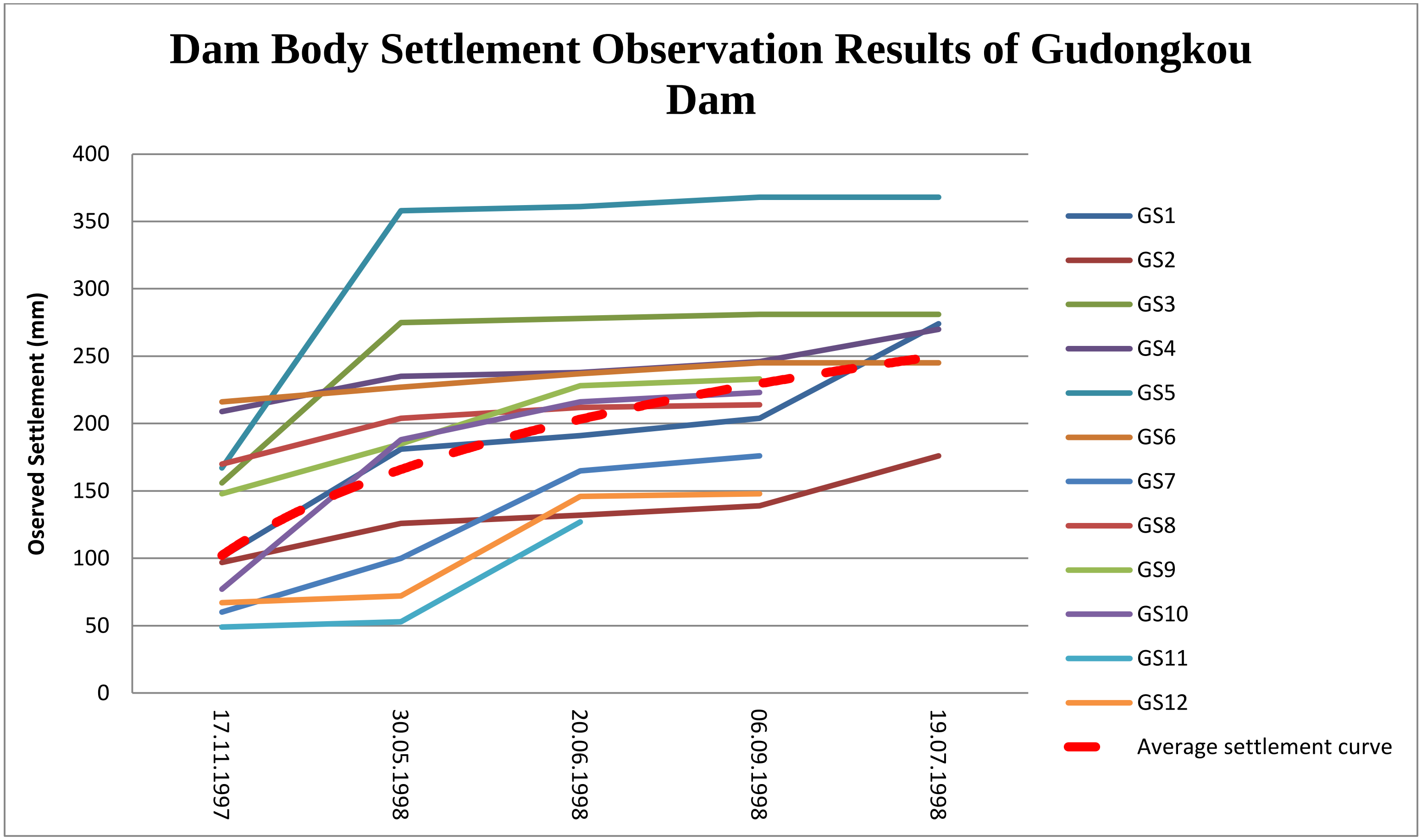

Figure 2.8 Observed settlement of Gudongkou Dam

Construction of the Gudongkou Dam was completed in August 1998, impoundment of reservoir water has begun to rise in May 1999. With respect to the results of observation instruments, except few abnormal observed measurements, dam settles within **10cm-28.1** cm during construction and impoundment periods. Maximum settlement was observed at nearly **0.24%** of the dam height. Observed settlements are much less than calculated value (54.7 cm) and other similar dam projects. One year after dam construction was completed, according to the observed settlements during construction and water impoundment periods, settlement of the upstream face of the dam body rises because of water loads. On the other hand, at the same time, downstream face of the dam body provides stability (Fanlie, 2000).

It is seen that observed horizontal displacements are generally within 3.2 mm – 67 mm and the maximum horizontal observed displacement is 80.9 mm. In the light of analysis of calculated and observed horizontal displacements, observed values are higher than calculated values (-33 mm, +20 mm)

Hence, sand-gravel fill has high shear strength and shows low compressibility under high stress levels. As a result, settlement of the dam body is minimized (Fanlie, 2000). Sand-gravel fill has disadvantages when compared with rock fill such as low permeability coefficient, poor erosion-resisting features, and small repose angle. However, sand-gravel is safe with high strength, economical, high quality building material. Thus, construction of concrete face sand-gravel dam is reliable (Fanlie, 2000).

Another case study of CFSGD is Çankırı-Koyunbaba Dam. By using 'GeoStudio' two dimensional finite element software, settlement analysis of Koyunbaba Dam was analyzed (General Directorate of State Hydraulic Works, DSİ, 2008). The height of the Koyunbaba Dam is 48 m. Dry density of fill material that was used in construction of Koyunbaba Dam is 19~20.5 kN/m^2. Average grain diameter is between 7 mm and 20 mm and the coefficient of the permeability is between $2.0x10^{-4}$ and $8.0x10^{-4}$ cm/s. Elasticity modulus is taken as 75 MPa. Other parameters are taken as c=1 kPa, ν= 0.25

and $\varnothing=38^o$. As a result of two dimensional finite element analyses, vertical and horizontal displacements were calculated as **55 cm**, **8 cm** for the end of construction. With respect to the case study of Çankırı-Koyunbaba Dam, dam settled vertically within a range of **1.14%** of dam height at the end of construction. Also, vertical and horizontal displacements were calculated as 20 cm and 14 cm during impoundment periods. Çankırı-Koyunbaba Dam settled within a range of **0.41%** of dam height for the end of construction (General Directorate of State Hydraulic Works, DSİ).

Finally, deformation behavior of Golillas Dam, also mentioned in the Section 2.4. of this study, will be explained.

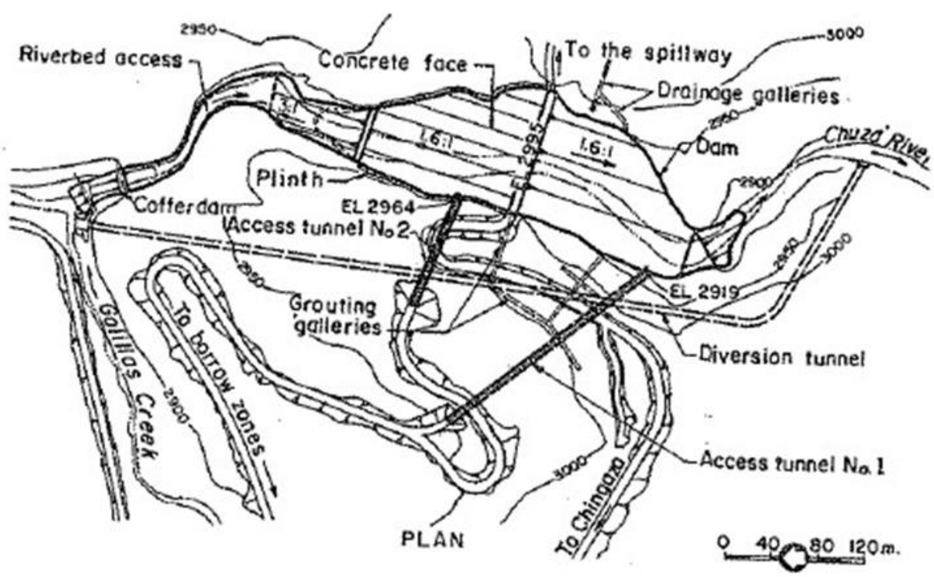

Figure 2.9 General layout of Golillas Dam (Cooke and Sherard, 1985)

Golillas Dam, which is a concrete faced gravel fill dam, was built in Colombia. The height of the dam is 125 m. The view of general layout of the dam is shown in the *Figure 2.9* and the maximum section and description of dam zones are shown in the *Figure 2.10.*

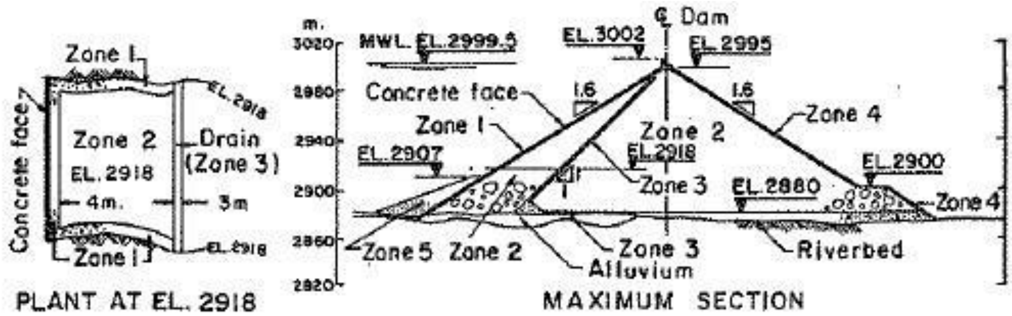

ZONE	FUNCTION	DESCRIPTION	MAXI-MUM SIZE m.	LAYER THICK-NESS m.	COMPACTION	PLACED VOLUME m³
1	Support of the concrete face	Processed dirty gravels	0.15	0.60	Layer: 4 passes of Vib roller (10 ton) Face: 4 passes of Vib. roller (Upslope)	66.000
2	Shoulders	Unprocessed dirty gravels	0.60	0.60	Four passes of Vib. roller (10 ton)	1'142.000
3	Drain	Processed clean gravels	0.30	0.60	Two passes of Vib. roller (10 ton)	52.000
4	Downstream slope protection	Oversize from zone 2	1.20	–	–	18.000
5	Impervious zone	Silty clays	–	0.30	Bulldozer	22.000
					TOTAL	1'300.000

Figure 2.10 Maximum section and zoning of Golillas Dam (Cooke and Sherard, 1985)

39 Hydraulic settlement devices were installed at El. 2903m, El. 2935m, El. 2961m in order to measure total settlements of the fill. 110 reference monuments along the joints on the concrete slab and parapet are placed so as to establish the movements of the slab and relative displacements between the joints. The results of the instrumentation records showed that larger deformations occurred in the lower half of the fill with a maximum value of 39 cm within a range of **0.31%** of dam height for the end of construction. According to the observed results, settlement value was practically the same in the center of the canyon and close to the abutments as a result of steepness of the abutments. The compressibility modulus was taken as a19608 kPa for the vertical stresses less than 588 kPa and 225500 kPa for the vertical stresses between 588 kPa and 980 kPa. Just

until the first filling of the reservoir, horizontal deformations were almost negligible. For the end of construction, larger settlements of the concrete slab occurred near the crest of the dam. Settlements near to the abutments were almost negligible. Total movements of the concrete slab are shown in the *Figure 2.11*.

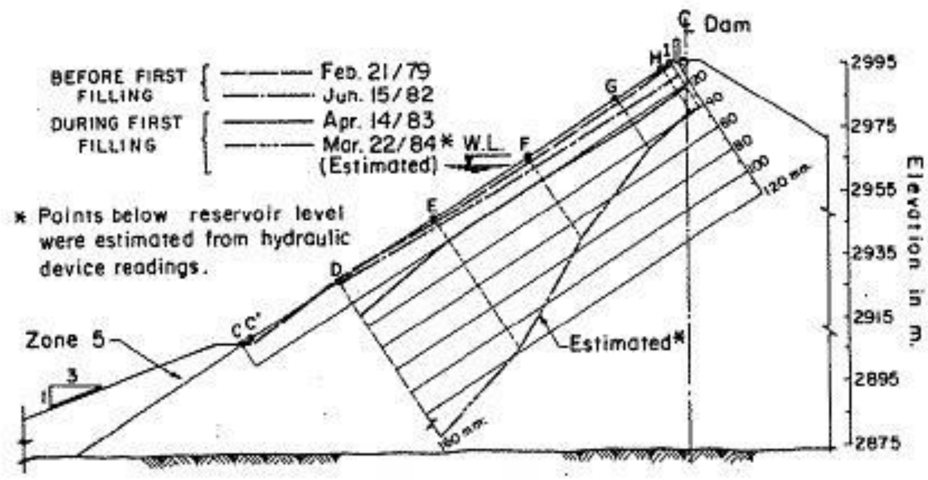

Figure 2.11 Total movements of the concrete slab, normal to the face (Cooke and Sherard, 1985)

During first reservoir filling, the largest movements occurred close to the concrete slab with a maximum value of 13 cm. These movements reduced to negligible values at the axis of the dam. Maximum settlements occurred all cross the canyon in the longitudinal direction (Cooke and Sherard, 1985).

In conclusion, as it has been claimed by Cooke (1984), the design and construction of CFDRs has been a process, governed by improvement based on the analyses of previous works.

CHAPTER 3

CONCRETE FACED AYDIN KARACASU DAM

In this chapter of the study, general characteristics of concrete faced Aydın Karacasu Dam are presented and the features of instrumentation devices are given. Finally, recorded instrumentation data, taken from General Directorate of State Hydraulic Works, is outlined.

3.1. General Characteristics of Aydın Karacasu Dam

There are 25 basins in Turkey. Kuzey Ege Basin, Gediz Basin, Küçük Menderes Basin and Büyük Menderes Basin are located within the border of Aegean Region. Karacasu Dam, which is the first concrete faced sand-gravel fill dam of Turkey, is built on Dandalaz River located in the Aydın province. Karacasu Dam came into operation within the borders of Büyük Menderes Basin in 2012. The main purposes of construction of Karacasu Dam are irrigation and drinking water procurement. By this means, water can be supplied in order to irrigate 1.125 ha/year land and produce 10.725hm^3/year drinking water for the habitants. . In the *Figure 3.1*and *Figure 3.2*, a view of the concrete faced Aydın Karacasu Dam during construction is given.

In the preliminary project, Karacasu Dam was designed as an earth fill embankment dam with clay core with 3-zone filling type in 1998 and total fill volume used in a construction was 3.212.000 m^3. Geologic features of the region and economic factors specified the construction of Karacasu Dam.

Figure 3.1 View of concrete faced Aydın Karacasu Dam (DSİ, 2011)

Figure 3.2 View of concrete faced Aydın Karacasu Dam during construction (DSİ, 2011)

With the concerns stated above, Karacasu Dam was designed as a concrete faced sand-gravel fill dam (CFSGD) and construction of the Karacasu Dam was completed in 2012. (DSİ, 2011) Catchment area of the dam is 537 km^2. Reservoir area is 1,07 km^2 with 17,20 hm^3 total reservoir capacity and active storage volume of the dam is 13,70 hm^3.Total fill volume used in the new design is 2.320.000 m^3 and it is explicitly seen that this amount is smaller than the first design. Hence, new design of Karacasu provides an economic advantage. A view of the general layout of Karacasu Dam is shown in *Figure 3.3*.

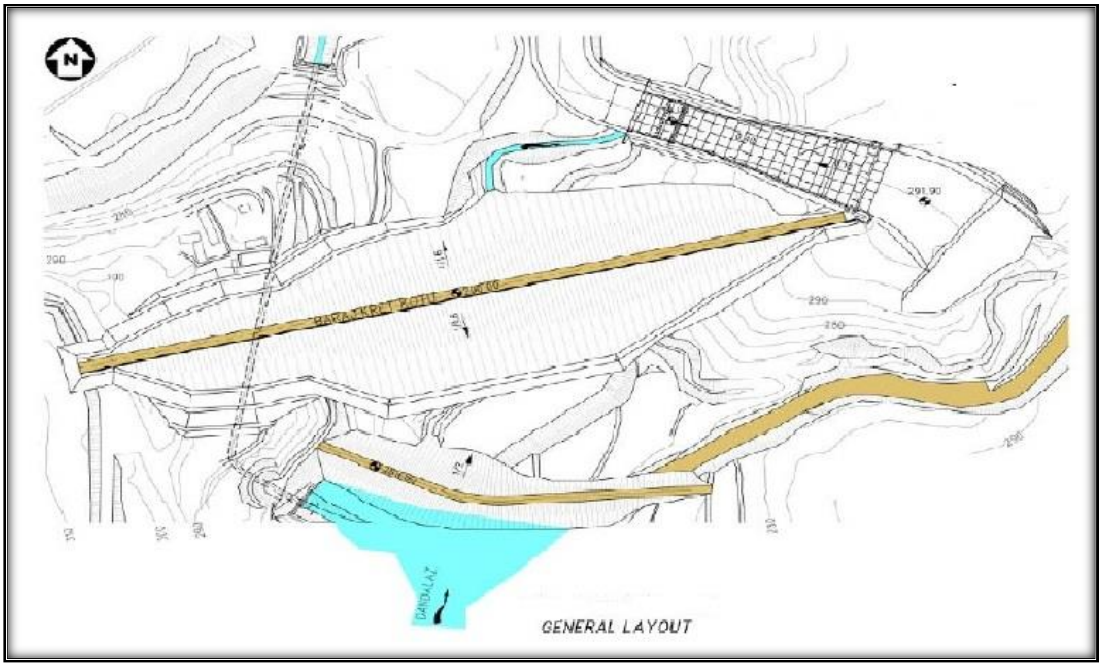

Figure 3.3 A general layout of Karacasu Dam (DSİ, 2011)

Crest level of the dam is 298.50 m and crest length is 649.4 m. Height of the dam is 60 m from foundation and 53.5 m from the river bed. Normal water level of the dam is 293.50 m. Spillway of Karacasu Dam is uncontrolled. Discharge capacity of the spillway is 1.389 m^3/s. A view of the maximum cross section and material zoning of Karacasu Dam are given in the *Figure 3.4*.

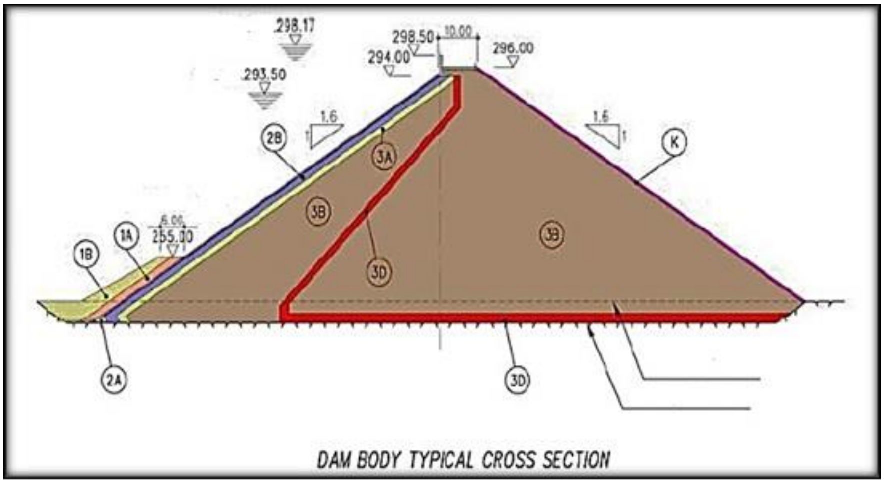

Figure 3.4 The cross-section of Karacasu Dam (DSİ, 2011)

In *Figure 3.4*,“Zone 1A” represents the cohesionless fill; “Zone1B” shows the random fill, perimetric joint filter zone is shown by the symbol; “2A” and “Zone2B” represents the cushion zone under concrete slab; “Zone3A” shows the filter zone; “Zone3B” displays the permeable sand-gravel fill; “Zone3D” shows the drainage zone or filter zone (clear gravel) and “K” represents surface protection material. As can be seen in the Figure 3.4 above, the main construction material of Karacasu is sand-gravel (Zone3B).

Favorable borrow areas are determined during exploration stage of the project to acquire the necessary quantities of fill materials for the different zones of the dam (Singh et al., 1995). Investigations to provide permeable and impermeable construction material are conducted on A, B, C, D, E, F, G, H, I, K, M borrow areas which are around the dam region. According to the data gathered by DSİ, ‘A, B, C, E, F, G, H, I, K, M’ borrow areas involve impermeable construction material; on the other hand, ‘D’ zone includes permeable construction material and near the construction site. Transportation of fill materials are economical. Thus, ‘Zone D’ is selected as a borrow area for concrete faced Aydın Karacasu Dam project. Borrow area ‘D’ is located 13 km north of the dam region. A view of borrow area ‘D’ is seen in the *Figure 3.5* (DSİ, 2011).

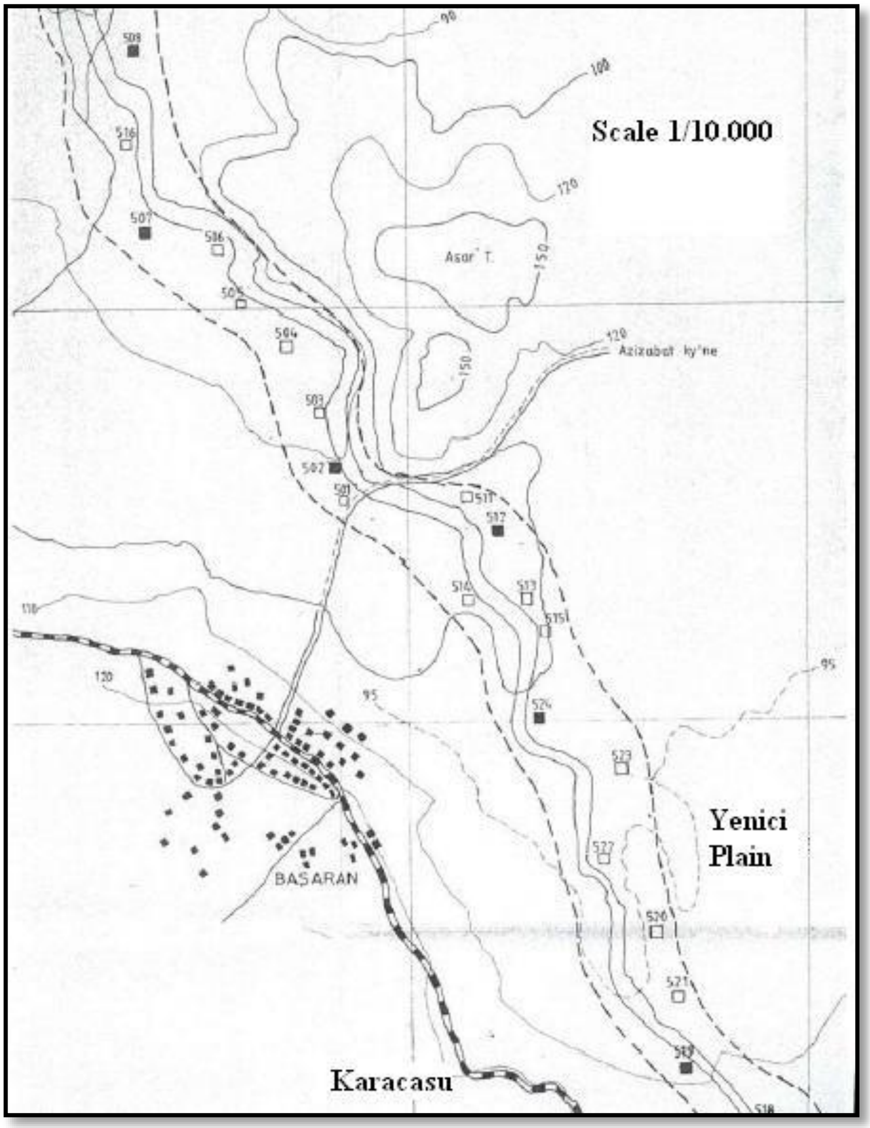

Figure 3.5 A View of Borrow Area 'D' (DSİ, 2011)

24 trial holes are drilled in the borrow area ‘D’ to obtain test samples as used in determining soil properties. According to the investigation results, average material gradation of borrow area ‘D’ is in the form of 55% sand and %45 gravel. A laboratory test result is seen in the *Table 3.1*.

Table 3.1 Laboratory experiment results of material of borrow area 'D' (DSİ, 2011)

Sample No	Unit Weight gr/cm^3		Water Absorption Specific Gravity gr/cm^3		Passing from 200 No Sieve %		Clay Soil %		Experiment of Na_2SO_4 %		Los Angeles Abrasion Loss	
	S	**G**	**S**	**G**	**S**	**G**	**S**	**G**	**S**	**G**	**S**	**G**
D-502	1.655	1.702	1.5 2.630	0.6 2.650	0.4	0.1	0.2	0.1	3.3	2.1		
D-507	1.753	1.752	1.6 2.630	0.7 2.610	0.8	0.1	0.4	0.1	2.6	2.7	9.8	44.7
D-508	1.655	1.759	1.7 2.690	1.6 2.560	1	0.1	0.2	0.1	5.3	3.7		
D-510	1.656	1.760	1.7 2.620	1.5 2.580	1	0.1	0.2	0.1	2.6	1.3		
D-512	1.753	1.752	1.6 2.630	0.6 2.600	0.6	0.2	0.4	0.1	3.6	1.8	8.8	42.1
D-517	1.758	1.784	0.6 2.784	1.1 2.600	4.4	0.2	2.6	0.3				
D-519	1.796	1.771	1.4 2.582	0.7 2.640	4.8	0.1	2	0.2				
D-524	1.717	1.772	1.9 2.682	0.5 2.630	4.8	0.1	2.2	0.2				

(*) 'S' represents 'sand' and 'G' represents 'gravel'

Figure 3.6 View of concrete faced Aydın Karacasu Dam end of the construction (DSİ, 2011)

Karacasu Dam is a moderate-sized dam. After the completion of main dam body, construction of concrete slab started. Concrete slab provides the impermeability and helps to decrease the leakage (Singh et al., 1995).Thickness of the concrete slab of Karacasu Dam is 30 cm and constant throughout the dam body. In recent years, the thickness of the concrete face has been decreasing for small or moderate-sized dams.

Cogoti Dam is a 85 m high concrete face rockfill dam. The concrete membrane of Cogoti varies in thickness from a maximum 80 cm at the dam foundation to 20 cm at the dam crest. New Exchequer Dam is a 150 m high concrete face rockfill dam. Concrete face slab of New Exchequer varies in thickness from 46 cm at the crest to 86 cm at the upstream toe. Foz do Areia Dam is a 160 m high concrete face rockfill dam. The face slab of the dam is 80 cm thick, at the base, and decreases linearly to 30 cm at the top (Cooke and Sherard, 1985). Kürtün Dam is a 133 m high concrete face rockfill dam. The concrete membrane of Kürtün Dam varies in thickness from a maximum 70 cm at the upstream toe foundation to 30 cm at the dam crest (Özkuzukıran, et. al., 2005).

3.1.1. General Geology

Geological formation of Karacasu region was studied in 1990 and 1994 by General Directorate of State Hydraulic Works (DSİ). Within the scope of Karacasu-Dandalaz Project, preliminary geological studies started and geological report was presented. In the light of these studies, 19 boreholes with 865 m total length were drilled. Then, 6 more boreholes with 357 m total length were drilled in an advanced stage. Drilled boreholes are listed in the *Table 3.2* and shown in *Figure 3.7.*Soil samples were obtained by boreholes and petrographic studies were conducted.

According to results of petrographic analysis, the basic geologic formations at the Karacasu Dam site are denominated as marl, calcareous marl, limestone, clayey-sandy lignite, clayey lignite. Among these geologic formations, limestone has spongy configuration due to de-liquation voids and it is formed from microcrystalline, little clay and feldspar fragments. Few amounts of Clayey-sandy lignite, quartz, feldspar fragments, calcium carbonate and gypsum are seen in the sample. Base rock of the Aydın Karacasu Dam comprises of old neogene sediments.

Table 3.2 Foundation Boreholes of Aydın Karacasu Dam (DSİ, 2011)

The Number of Borehole	Place of the Borehole	Depth of the Borehole (m)	Elevation of the Borehole (m)	The Experiments Conducted
SK-1	Left Side	55	269.2	Hydraulic Unpressure-Pressure Test + Penetration
SK-2	Left Side	40	252.3	Hydraulic Unpressure-Pressure Test
SK-3	Right Side	40	254.5	Hydraulic Unpressure-Pressure Test
SK-4	Right Side	60	270.9	Hydraulic Unpressure-Pressure Test
SK-5	Right Side	50	298.6	Hydraulic Unpressure-Pressure Test
SK-6	Left Side	70	291	Hydraulic Unpressure-Pressure Test
SK-7	Left Side	50	270.7	Hydraulic Unpressure-Pressure Test + Penetration
SK-8	River Bed	30	247	Hydraulic Unpressure-Pressure Test + Penetration
SK-9	Upstream (Left Side)	50	255.8	Hydraulic Unpressure-Pressure Test + Penetration
SK-10	Right Side	40	253.1	Hydraulic Unpressure-Pressure Test
SK-11	Right Side	50	264.8	Hydraulic Unpressure-Pressure Test
SK-12	Upstream (River Bed)	40	248.8	Hydraulic Unpressure-Pressure Test
SK-13	Upstream (River Bed)	100	254.81	Hydraulic Unpressure-Pressure Test
SK-14	Upstream (River Bed)	94	253.08	Hydraulic Unpressure-Pressure Test
ASK-12	River Bed	30	245.7	Hydraulic Unpressure-Pressure Test
DSK-1	Spillway (Left Side)	40	301.6	Hydraulic Unpressure-Pressure Test
DSK-2	Spillway (Left Side)	30	292.7	Hydraulic Unpressure-Pressure Test
DSK-3	Spillway (Right Side)	30	301.68	Hydraulic Unpressure-Pressure Test
DSK-4	Spillway (Right Side)	33	290.99	Hydraulic Unpressure-Pressure Test
DSK-5	Spillway (Right Side)	30	251.36	Hydraulic Unpressure-Pressure Test
TSK-1	Diversion Tunnel	55	293.5	Hydraulic Unpressure-Pressure Test + Penetration
TSK-2	Diversion Tunnel	40	284	Hydraulic Unpressure-Pressure Test
TSK-3	Diversion Tunnel	40	271.3	Hydraulic Unpressure-Pressure Test + Penetration
TSK-4	Diversion Tunnel	55	271.3	Hydraulic Unpressure-Pressure Test
TSK-5	Diversion Tunnel	70	291.96	Hydraulic Unpressure-Pressure Test
	Total	1222		

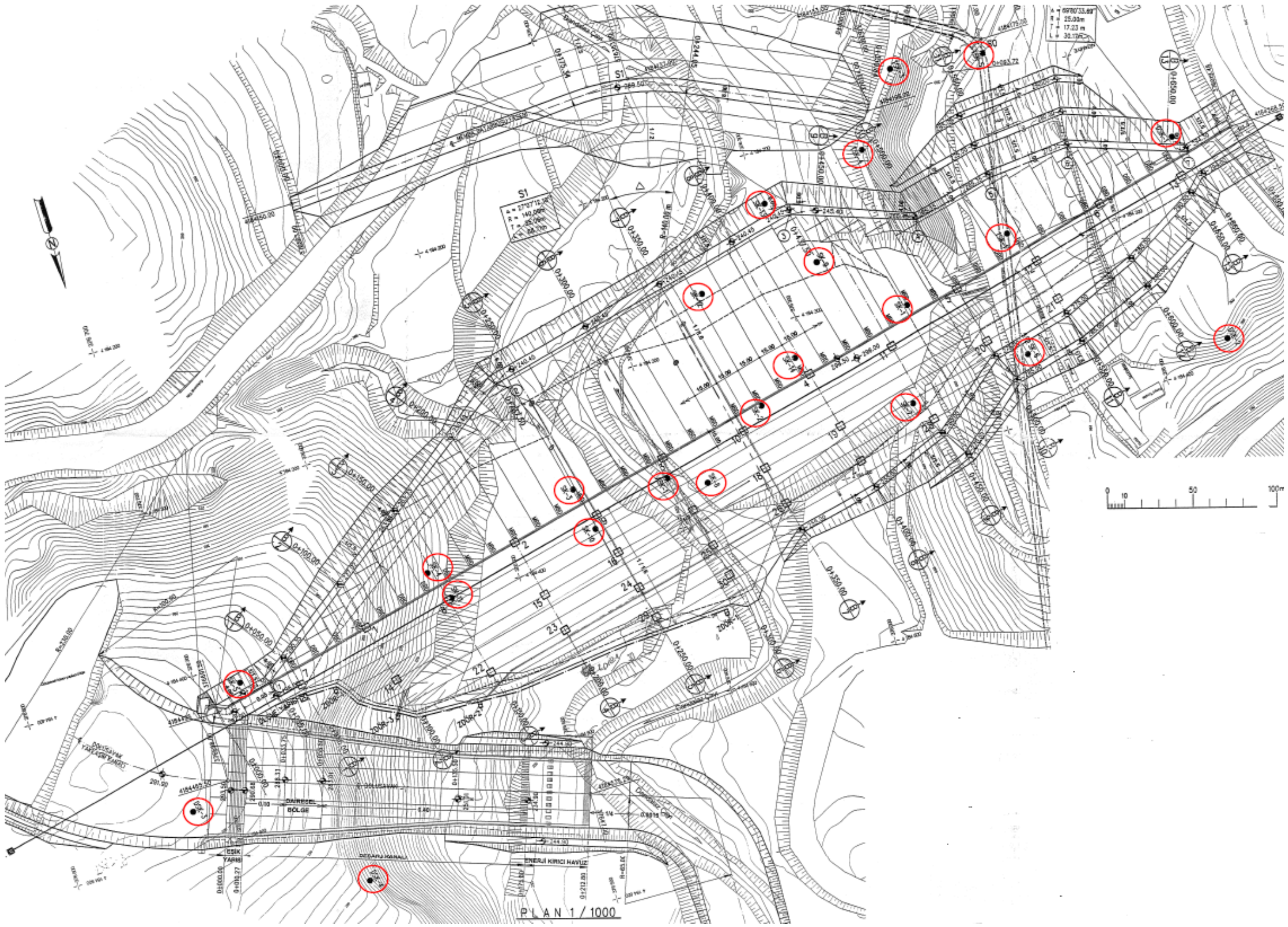

Figure 3.7 Location of boreholes installed in Aydın Karacasu Dam (DSİ, 2011)

Neogene sediments, located near the investigation area, substantially contained lignite. Economic value of lignite is highly significant. There has not been observed any landslide or fracture at investigation area.

3.2. Instrumentation of Aydın Karacasu Dam

The main purposes of instrumentation are to observe its safety, develop a better understanding of its behavior and to control the design concepts (Singh, 1995). An instrumentation system is designed at Aydın Karacasu Dam to observe the behavior of the dam. The instruments used in Aydın Karacasu Dam body are listed in *Table 3.3*

Table 3.3 Instrumentation Devices of Karacasu Dam (DSİ, 2011)

Parameters to Follow	Device Type	Symbol	Number
Pore pressure	Piezometer	T	21
Deformations	Hydraulic Settlement Gauge-	ZDÖ	30
Total Stress and Load	Total Pressure Gauge	BÖ	18
Concrete Stress	Strain Meter	GÖ	-
Joint Movements	Joint meter	DDÖ	15

As seen in the *Table 3.3*, 21 piezometer (T), 18 total pressure gauge (BÖ), 30 hydraulic settlement gauge (ZDÖ) and 15 joint meter (DDÖ) were installed in the Karacasu Dam body. Instruments were located at three different cross-sections Km 0+250.00 m, Km 0+300.00 m, Km 0+350.00 m, respectively. The maximum cross-section of the dam body is the section located at Km 0+300.00 m. Thus, instruments of Km 0+300.00 m are examined.

3.2.1. Vibrating Wire Piezometer

Piezometers are the instrumentation devices that are used for measuring pore-water pressure. They are utilized in both embankments and foundations. Embankment piezometers are generally placed in the fill while it is being constructed, whereas foundation piezometers are installed in drill holes. Piezometers show an increment in the construction pore pressure with increasing dam height or show their dispersion with time after end of the dam construction. After reservoir impoundment, the piezometers display the pattern of seepage flow throughout the dam (Singhet al., 1995).

During the construction and the operation period of Karacasu, pore water pressure at dam foundation and in the fill is thought to be followed by vibrating wire piezometer. By this way, zones, where excess pore pressures affect the stability of embankment, are thought to be determined. A view of vibrating wire piezometer is seen in the *Figure 3.8.*

Figure 3.8 Vibrating Wire Piezometer (DSİ, 2011)

3.2.2. Hydraulic Settlement Gauge

The main purpose of installing hydraulic settlement devices is to monitor settlement behavior of dam body. These devices comprise of measuring sensors. Measuring sensors includes temperature compensated pressure transducers. Pressure transducers are connected to each other by a data line and liquid line. There is a pressure difference in the between the column of liquid in tubes. Settlements are measured by using this pressure difference. Then, pressures are converted into settlements by the equation of '1 bar=10 m' (Özkuzukıran et. al., 2006). An outside profile of the hydraulic settlement device is seen in the *Figure 3.9.*

Figure 3.9 Outside Profile of Hydraulic Settlement Gauge (DSİ, 2011)

3.2.3. Total Pressure Gauge

Earth pressure is measured for two significant purposes. First one is to follow the loading on the structure. This purpose helps to verify the system and correct the prospective designs. Second purpose on measuring the earth pressure is to follow the earth stress. Total Pressure Gauges are utilized to observe the total of effective stresses and pore pressures. The total pressure gauges are composed from two circular plates that are made of stainless steel. Plates are welded each other with their edges in order to create a sealed cavity, which is filled with fluid. After filling with fluid, a pressure transducer is connected to the cell. When the cell is placed, its surface directly gets in touch with soil. Total pressure that acts on the surface is transmitted to the fluid that is inside the cell. Finally, the fluid is measured by the pressure transducer. In the *Figure 3.10*total pressure gauge and hydraulic settlement gauge are shown.

Figure 3.10 Total pressure gauge and hydraulic settlement gauge of Aydın Karacasu Dam (DSİ, 2011)

3.2.4. Joint Meter

Vibrating wire joint meter is designed to monitor deformations and cracks at joints. Joint meter consists of a body on which there is a vibrating wire mechanism and a bar that detects the deformation. Joint meter can be placed as one-directional, bi-directional and trilateral. The jointmeters installed in Aydın Karacasu Dam measure deformations in three directions (trilateral) (DSİ, 2011). A view of trilateral joint meter is seen in the *Figure 3.11*.

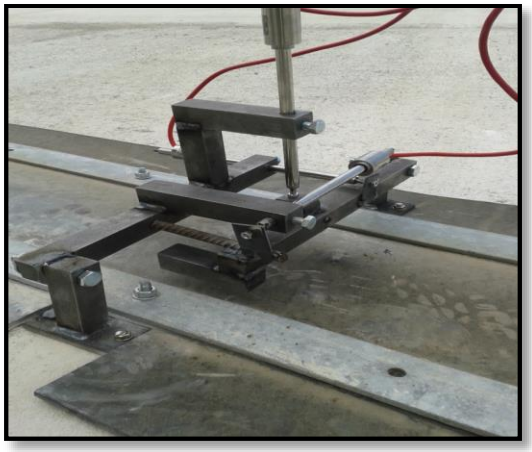

Figure 3.11 View of trilateral joint meter of Aydın Karacasu Dam (DSİ, 2011)

3.2.5. Strain Meter

Strains in any direction are observed by strain meters. These devices are basically operated by gauging unit in order to measure extension or compression within the gauge length (Singh et al., 1995). It comprises of one body in which there is a vibrating wire mechanism and legs that exist from two different sides of the body. Legs detect the tension (DSİ, 2011). A view of strain meter is shown in the *Figure 3.12*

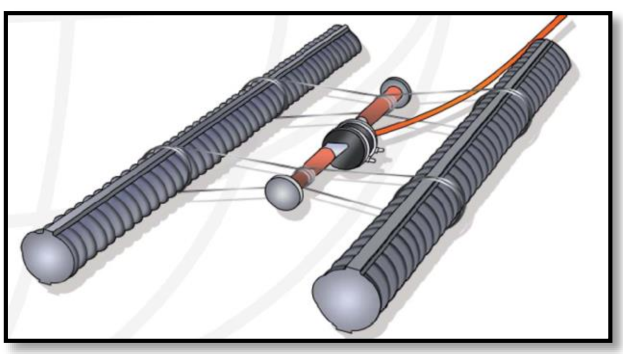

Figure 3.12 Strain Meter

3.3. Observed Settlement Behavior of Aydın Karacasu Dam

According to the general schedule of the Aydın Karacasu Project, dam construction has started in December 2009 and the main body has filled to El. 296m in February 2012 (20.02.2012). Reservoir impounding has officially started in September 2012; however, it is said that the reservoir has begun to rise two months after official impounding date. During these periods, the performance of the dam has been observed by instrumentation devices located at different elevations and cross-sections. The settlements and stresses, which occur in the foundation and occur in the dam body, have been recorded respectively by hydraulic settlement devices and pressure gauges. Hydraulic settlement devices and pressure gauges are installed in three different cross-section of the dam body (Km 0+250.00m, Km 0+300.00m, Km 0+350.00m). As mentioned in the section *3.2*, settlement devices are represented with a symbol of “ZDÖ” and pressure gauges are represented with a symbol of “BÖ” in this study. Location of these devices can be seen from *Table 3.4* and *Table 3.5.*

Table 3.4 Coordinate of pressure gauges installed in Aydın Karacasu Dam (DSİ, 2011)

BÖ				
Pressure Gauge				
Elevation (m)	No	Cross Section (Km)	Distance From the Dam Axis	
			Upstream (m)	Downstream (m)
260.00	BÖ-1	0+250.00	25.00	-
	BÖ -2		-	5.00
	BÖ -3		-	27.50
	BÖ -4		-	50.00
	BÖ -5	0+300.00	25.00	-
	BÖ -6		-	5.00
	BÖ -7		-	27.50
	BÖ -8		-	50.00
	BÖ -9	0+350.00	25.00	-
	BÖ -10		-	5.00
	BÖ -11		-	27.50
	BÖ -12		-	50.00
275.00	BÖ -13	0+250.00	5.00	5.00
	BÖ -14		-	30.00
	BÖ -15	0+300.00	-	5.00
	BÖ -16		-	30.00
	BÖ -17	0+350.00	-	5.00
	BÖ -18		-	30.00

Table 3.5 Coordinate of hydraulic settlement devices installed in Aydın Karacasu Dam (DSİ, 2011)

ZDÖ				
Hydraulic Settlement Gauge				
Elevation (m)	No	Cross Section (Km)	Distance From the Dam Axis	
			Upstream (m)	Downstream (m)
245.00	ZDÖ-1	0+250.00	75.50	-
	ZDÖ -2	0+300.00	75.50	-
	ZDÖ -3	0+350.00	75.50	-
260.00	ZDÖ -4	0+250.00	52.00	-
	ZDÖ -5		25.00	-
	ZDÖ -6		-	5.00
	ZDÖ -7		-	27.50
	ZDÖ -8		-	50.00
	ZDÖ -9	0+300.00	52.00	-
	ZDÖ -10		25.00	-
	ZDÖ -11		-	5.00
	ZDÖ -12		-	27.50
	ZDÖ -13		-	50.00
	ZDÖ -14	0+350.00	52.00	-
	ZDÖ -15		25.00	-
	ZDÖ -16		-	5.00
	ZDÖ -17		-	27.50
	ZDÖ -18		-	50.00
275.00	ZDÖ -19	0+250.00	28.00	-
	ZDÖ -20		-	5.00
	ZDÖ -21		-	30.00
	ZDÖ -22	0+300.00	28.00	-
	ZDÖ -23		-	5.00
	ZDÖ -24		-	30.00
	ZDÖ -25	0+350.00	28.00	-
	ZDÖ -26		-	5.00
	ZDÖ -27		-	30.00
290.00	ZDÖ -28	0+250.00	-	7.00
	ZDÖ -29	0+300.00	-	7.00
	ZDÖ-30	0+350.00	-	7.00

The maximum cross-section of the dam body is Km 0+300.00m. Maximum settlements occur at the maximum cross-section of the dam body, as expected (Özkuzukıran et. al., 2006). According to the data taken from DSİ, recorded values of hydraulic settlement devices located at Km 0+300.00m are higher than the settlements values recorded on other cross-sections as expected. Hence, in this study, instrumentation devices installed in Km 0+300.00m are taken into account. Figure 3.13 shows the location of the hydraulic settlement device sand pressure gauges installed in Km 0+300.00m.Hydraulic settlement devices are installed in four different elevation El 245, El 260, El 275, El 290 at Km 0+300.00m.

Concrete Faced Aydın Karacasu Dam has been observed for two condition, end of construction (EOC) and reservoir impoundment (RI). Observed settlement values, which have been recorded by DSİ, are displayed in the *Table 3.6.*

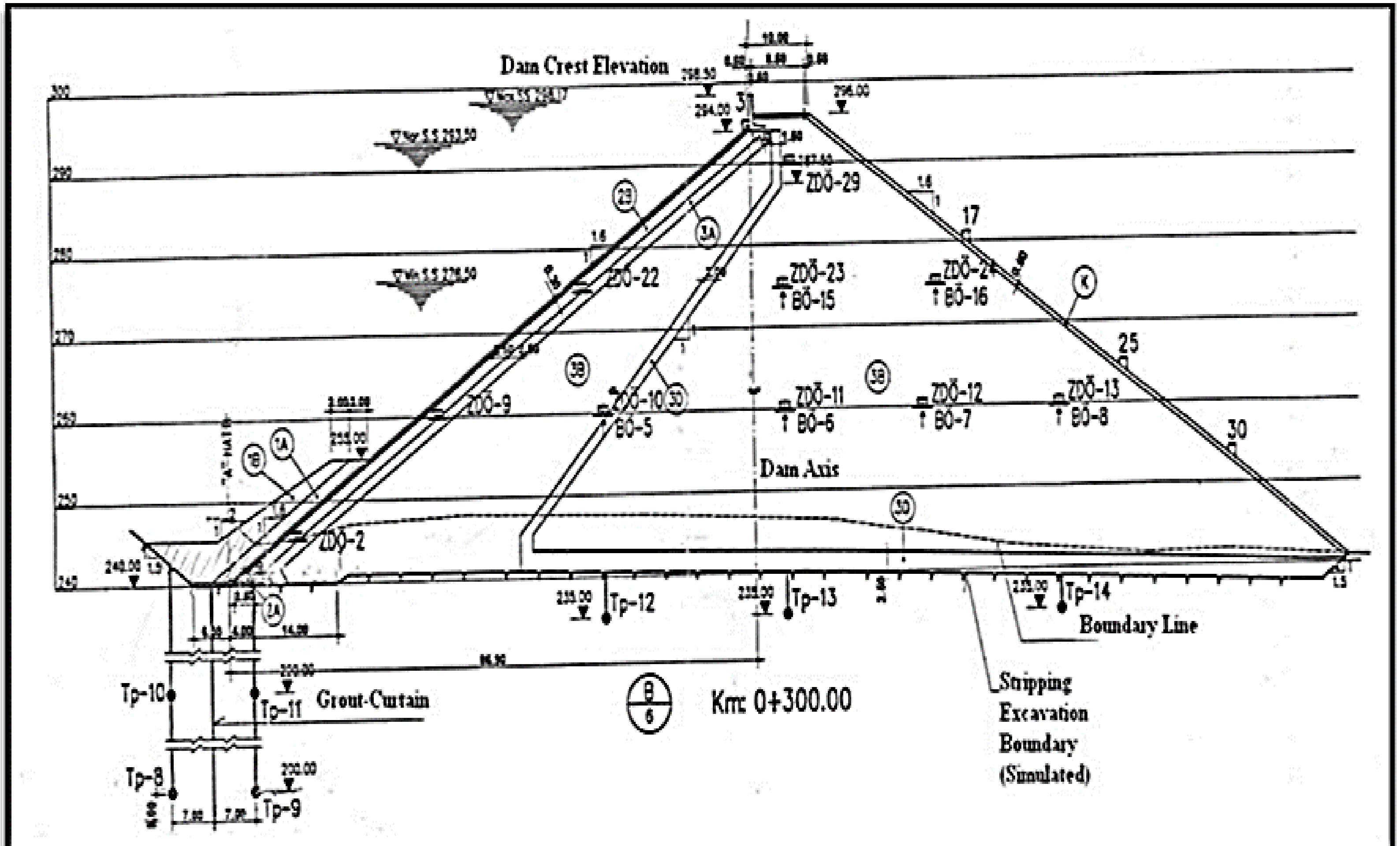

Figure 3.13 Location of the hydraulic settlement devices of Aydın Karacasu Dam at Km 0+300.00m (DSİ, 2011)

Table 3.6 Observed Settlements for End of Construction Condition Period of Aydın Karacasu Dam (DSİ, 2011)

OBSERVED VERTICAL SETTLEMENTS AT MAX. CROSS SECTİON OF KARACASU DAM (Km 0+300.00m)				
Settlement Features				
Hydraulic Settlement Gauge	**Elevation (m)**	**Horizontal Distance From Upstream Toe (m)**	**Max. Settlement Observed by General Directorate of State Hydraulic Works EOC (cm)**	**Max. Settlement Observed by General Directorate of State Hydraulic Works RI (cm)**
ZDÖ2	245.00	19.50	-32.00	-42.00
ZDÖ9	260.00	43.00	-36.00	-44.00
ZDÖ10	260.00	70.00	-22.00	-32.00
ZDÖ11	260.00	100.00	-23.00	-27.50
ZDÖ12	260.00	132.50	-27.00	-40.00
ZDÖ13	260.00	155.00	-28.00	-41.00
ZDÖ22	275.00	67.00	-28.00	-41.00
ZDÖ23	275.00	100.00	-37.50	-45.50
ZDÖ24	275.00	135.00	-32.00	-42.00
ZDÖ29	290.00	102.00	-32.00	-44.00

3.3.1. Observed Settlements for End of Construction Period (EOC)

The CFSGDs deform under their own weight during the end of construction period. As seen in the *Table 3.6,* maximum settlement value is recorded as 37.50 cm by the hydraulic settlement device "ZDÖ23" for the end of construction condition. ZDÖ 23 is installed at El 275.When recorded settlement values of Aydın Karacasu dam are analyzed, maximum settlement value, which is recorded by "ZDÖ 22" at El 290, is 28 cm and maximum settlement value is 32 cm recorded by "ZDÖ 24" which is located at

El 290. Settlement value reduces in the downstream and upstream direction at the same cross-section of the embankment, as seen in the Figure xxx. It reaches the maximum value at the dam centerline. Maximum settlement value is 32cm recorded by “ZDÖ 11” which is located at El 290. Maximum settlement value is 23cm recorded by “ZDÖ 29” which is located at El 260. Settlement values decrease towards upper and lower elevations (towards the foundation and dam crest) along the dam centerline. This condition is a result of decreasing compressibility of the fill material. While the construction of CFSGD goes on, compressibility of sand-gravel fill material at lower elevations decreases as compared with newly filled upper layers. Upper layers continue to deform with a decreasing rate.

3.3.2. Observed Settlements for Reservoir Impoundment Period (RI)

Water loads act on an upstream slab of the embankment during reservoir impoundment period, so hydraulic settlement devices, which are installed near the upstream slab, are affected more than others. When compared to two hydraulic settlement devices (ZDÖ22 and ZDÖ24), located at the same elevation and same cross-section, the effect of the water load decreases towards the downstream. Hence, important settlements are recorded at “ZDÖ2, ZDÖ9, ZDÖ22” during reservoir impoundment, as expected. The effect of the water load reduces with the increment in the elevation. Observed settlements are larger at hydraulic settlement devices installed in lower elevations.

CHAPTER 4

SETTLEMENT ANALYSIS OF CONCRETE FACED AYDIN KARACASU DAM

In this chapter of the study, material models used in the analyses of concrete faced Aydın Karacasu Dam are presented and preliminary analysis of Aydın Karacasu Dam is comprehensively explained.

4.1. Constitutive Law

A constitutive law reflects the stress-strain relationship of materials. It depends on constitutional factors and environmental factors. Constitutional factors comprise the characteristics of the soil. Environmental factors include the loading features (Singh et al., 1995). The constitutive laws can be divided into groups as followings:

4.1.1. Linear-Elastic Analysis

Stress-strain curve is taken as linear in this analysis. So that, the elastic modulus is constant at all stress levels. This is not realistic since soils and rocks show non-linear stress-strain relationship.

.Penman and Charles used a linear stress-strain relationship for the analysis of Llyn Brianne Dam by developing equivalent values of the Young Modulus, which is based on the equivalent compressibility approach for rockfill. In this analysis, one-dimensional compression test, which is applied on the embankment material, is used (Singh et al., 1995).

4.1.2. Non-linear Stress-Strain Behavior

Stress-strain relationship of soils is examined more complicated than the simple linear-elastic analysis described in the previous section. The non-linear model can be subdivided as followings:

4.1.2.1. Duncan and Chang's Hyperbolic Model

Konder (1963) has shown that the nonlinear stress- strain behavior of soils can be approximated reasonably by hyperbolic stress-strain models. Since the model is simple and multi-directional, this model has been commonly in use for modeling behavior of soils. Konder (1963) expressed the soil stress-strain response with hyperbolic relation by Equation *4.1*,

$$\frac{\varepsilon}{\sigma_1 - \sigma_3} = \left[\frac{1}{E_i} + \frac{\varepsilon}{(\sigma_1 - \sigma_3)_u}\right] \qquad \boldsymbol{Eq\ (4.1)}$$

Where E_i is the initial tangent modulus or initial slope of the stress-strain curve, and $(\sigma_1 - \sigma_3)_u$ is the asymptotic value of stress difference which is related to the strength of the soil; σ_1 and σ_3 are major and minor principal stresses; and ε is axial strain. The ultimate stress difference is proportional to the compressive strength, or stress difference at failure $(\sigma_1 - \sigma_3)_f$, by the failure ratio, R_f which is defined by Equation *4.2* (Anochie et al., 2007).

$$R_f = \frac{(\sigma_1 - \sigma_3)_f}{(\sigma_1 - \sigma_3)_u} \qquad \boldsymbol{Eq\ (4.2)}$$

The variation of $(\sigma_1 - \sigma_3)_f$ can be expressed in terms of the Mohr Coulomb criterion as in Equation *4.3*,

$$(\sigma_1 - \sigma_3)_f = \left[\frac{2c\ cos\phi}{1 - sin\phi} + \frac{2sin\phi}{1 - sin\phi}\sigma_3\right] \qquad \boldsymbol{Eq\ (4.3)}$$

Duncan and Chang (1970) and Duncan (1980) later published that for most types of soils, the value of R_f is between 0,5 and 1,0. (Yoo, 2007)

Janbu (1963) recommended a stress- dependent hyperbolic model for soils in which E_i depends on $\sigma_3$as expressed in Equation *4.4*,

$$E_i = \mathrm{k}\, P_a \left(\frac{\sigma_3}{P_a}\right)^n \qquad \boldsymbol{Eq\ (4.4)}$$

Where P_a is atmospheric pressure; k is Young's modulus and n is Young's modulus exponent.

Duncan and Chang (1970) combined Kondner and Janbu models to develop a hyperbolic model which is pressure dependent. The Duncan and Chang hyperbolic model is obtained by substituting *Equations 4.3* and *4.4* into derivative of *Equation 4.2.* The model is expressed in terms of the tangent modulus E_t, of the soil material as in *Equation 4. 5,*

$$E_t = \left[1 - \frac{R_f(1 - sin\phi)(\sigma_1 - \sigma_3)}{2c\ cos\phi + 2\sigma_3\ sin\phi}\right]^2\ k\ P_a \left(\frac{\sigma_3}{P_a}\right)^n \qquad \boldsymbol{Eq\ (4.5)}$$

In addition, Duncan and Chang (1970) proposed another hyperbolic stress-strain model to show variation of modulus. In this model, the modulus of the material was related to confining pressure as in Equation *4.6*,

$$E_{ur} = \mathrm{k}_{ur} P_a \left(\frac{\sigma_3}{P_a}\right)^n \qquad \boldsymbol{Eq\ (4.6)}$$

Where $E_{ur}$is unloading/reloading Young's modulus, k_{ur} unloading/reloading Young's modulus number. Duncan (1980) reported that for stiff soils the value of k_{ur} 20.0% greater that the value of k in *Equation 4.5,*

Duncan (1980) also reported that for a conventional triaxial test, there was a nonlinear relationship between the bulk modulus, the deviator stress and the volumetric strain. The relation is as in *Equation 4.7*,

$$K = \left(\frac{\sigma_1 - \sigma_3}{3\varepsilon_v}\right) \qquad \boldsymbol{Eq\ (4.7)}$$

Where K is bulk modulus and $\boldsymbol{\varepsilon_v}$ is volumetric strain of soil material.

For modeling volumetric responses of soils, Duncan (1980) suggested a hyperbolic model for the variation of bulk modulus as a function of confining pressure. The model is as in Equation *4.8* (Anochie et al., 2007),

$$K = \mathrm{k}_b P_a \left(\frac{\sigma_3}{P_a}\right)^m \qquad \boldsymbol{Eq\ (4.8)}$$

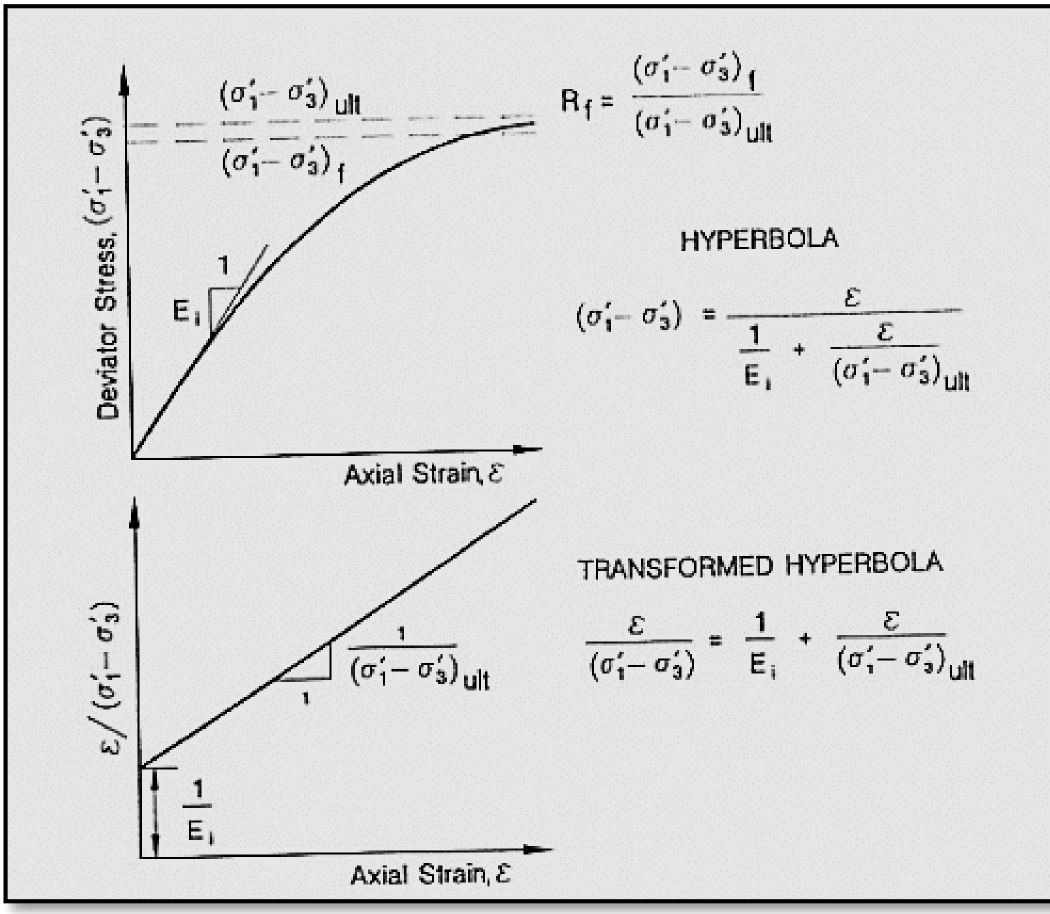

Figure 4.1 Hyperbolic representation of a stress-strain relationship (Duncan et al., 1980)

Hyperbolic model is easier to analyze the soil behavior than Mohr-Culoumb model. *Figure 4.1* shows the relation between stress and strain (Duncan et al.,1970) Hyperbolic equation is transformed as shown in *Figure 4.1*, it represents a linear relationship between [ε/ (σ1- σ3)] and ε. (Abdul et al., 2007)

4.1.2.2. Hardening Soil Model

The hardening soil model is derived from the hyperbolic model of Duncan and Chang (1970), with some improvement on the hyperbolic formulations (Schanz *et al.*, 1999).

The hardening soil model is the advanced version of the Duncan-Chang's hyperbolic model. It can be applied for any kind of the material (Brinkgreve, 2005).

Plastic shear strain under deviatoric loading is displayed by friction hardening and plastic volumetric strain under primary compression is modeled by cap hardening. Friction hardening differs from cap hardening. Friction hardening is utilized to obtain irreversible plastic strains. These strains occur as a result of primary deviatoric loading. Compression hardening is utilized to obtain irreversible plastic strains and these strains comprise as a result of primary compression under both isotropic loading and oedometer loading. However, present model includes both of the hardening types that are explained above (Ti et al., 2009). Model comprises of yield contours that is seen in 3D from the *Figure 4.2.*

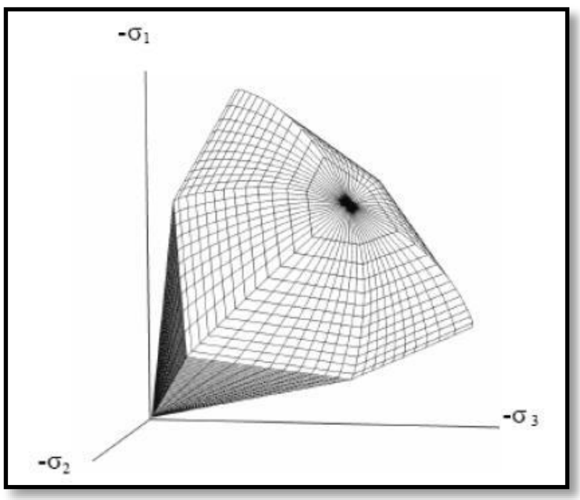

Figure 4.2 Total yield contours of hardening soil model under principal stresses for cohesionless soil (Ti et al., 2009).

Soil hardening model is similar to the Duncan and Chang's hyperbolic model. Hardening soil model depends more on hardening plasticity than non-linear elasticity. Constraints and instability problems of Duncan-Chang's hyperbolic model in terms of neutral loading and dilatancy are achieved. In addition to these features, the model also comprises of yield cap and dilatancy (Schanz et. al., 1999).

Some features of hardening model are stiffness that is based on stress respect to *m*, plastic straining as a result of E^{ref}_{50} and E^{ref}_{oed}, E^{ref}_{ur}, v_{ur} and failure criterion with respect to *c*, ϕ, ψ parameters of Mohr-Coulomb model, where,

m :power law

E^{ref}_{50} : primary deviator loading,

E^{ref}_{oed} : primary compression,

E^{ref}_{ur} : elastic unloading,

v_{ur}: elastic reloading.

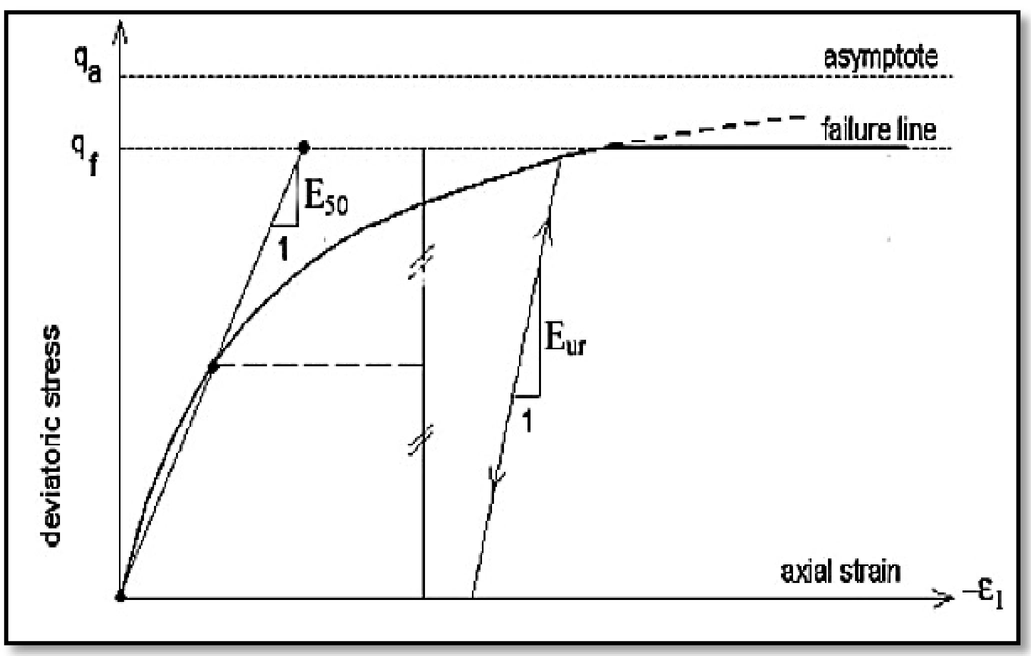

(*) Negative values mean compression in the graph

Figure 4.3 Hyperbolic stress-strain graph in hardening soil model (Schanz et., al., 1999)

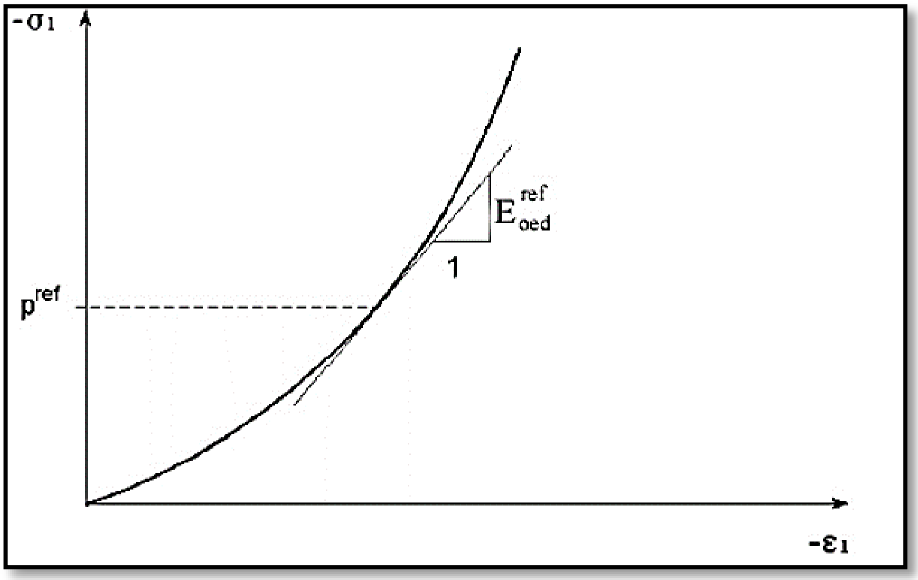

(*) Negative values mean compression in the graph

Figure 4.4 Definition of E_{oed}^{ref} from oedometer test results (Schanz et., al., 1999)

In *Figure 4.3*, hyperbolic stress-strain relationship is given as graphically. Kondner (1963) studied on hyperbolic formula for triaxial test and it was explained as,

For $q_x < q_f$,

$$\varepsilon_1 = \frac{q_a}{2E_{50}} \cdot \frac{q_x}{q_a - q_x} \qquad \textbf{\textit{(Eq 4.9)}}$$

$$q_a = (\sigma_1 - \sigma_3) \qquad \textbf{\textit{(Eq 4.10)}}$$

Where,

q_a : shear strength at asymptotic value,

q_f : ultimate deviator stress,

$$\varepsilon_1 = \frac{6sin\phi}{3 - sin\phi}.(\sigma_3 + \mathrm{c}\cot\phi) \qquad \textbf{(Eq 4.11)}$$

And

$$q_a = \frac{q_f}{R_f} \qquad \textbf{(Eq 4.12)}$$

When $q_{f=}$ q_a *(R_f=1)* the failure criterion is provided and perfectly plastic yielding happens. As seen from *Figure 4.3,* stress-strain curve tends to be non-linear for the primary loading. E_{50} represents the stiffness modulus that depends on confining stress at initial loading. Thus E_{50} is utilized on behalf of initial modulus E_i for smaller strain parameters. E_{50} can be determined as,

$$E_{50} = E_{50}^{ref}\left(\frac{c'cos\phi' - \sigma_3' sin\phi'}{c'cos\phi' + p^{ref} sin\phi'}\right)^m \qquad \textbf{(Eq 4.13)}$$

Where,

E_{50}^{ref}: Stiffness occuring with respect to the reference stress 'p^{ref}'

σ_3' : Effective confining pressure determined from triaxial test

In finite element software, Plaxis v8.2, reference stress value is taken as a 100 kN/m^2. Effective confining pressure determines the actual stiffness and it takes negative value in compression.

It can be seen from *Figure 4.3*, there is two loading condition, unloading condition and reloading condition. Stiffness modulus for these loading conditions is determined as,

$$E_{ur} = E_{ur}^{ref}\left(\frac{c'cos\phi' - \sigma_3' sin\phi'}{c'cos\phi' + p^{ref} sin\phi'}\right)^m \qquad \textbf{(Eq 4.14)}$$

Where,

E_{ur}^{ref}: Stiffness occuring with respect to the reference stress 'p^{ref}' for unloading case and reloading case.

Finite element software, Plaxis v8.2 takes E_{ur}^{ref} as three times of E_{50}^{ref}. In contrast to the Mohr-Coulomb Model, curve of stress and strain under primary loading tends to be hyperbolic in soil hardening model.

4.2 Preliminary Analysis of Aydın Karacasu Dam

4.2.1. Material Model

Finite element method is executed to compute the settlements analysis of Karacasu Dam. Firstly, appropriate material model is determined to examine the stress-strain behavior of the fill materials in the correct way for the finite element analysis. Sand-gravel is non-linear, inelastic and stress dependent. As mentioned in the section 4.1.2, when literature is examined, soil behavior is represented by utilizing frequently hyperbolic model that was improved by Duncan and Chang (1970) and updated by Kulhawy et al. (1972).

The soil hardening model is formulated in a system of complicated theory based on plasticity rather than elasticity (Schanz et. al., 1999). By virtue of the plastic shear and strain properties, soil hardening model is thought to be isotropic. Finite element software Plaxis v8.2 is utilized with the hardening soil model and also, Phase2 is utilized with the Mohr-Coulomb model to compute the finite element analysis more realistically.

4.2.2. Material Model Parameters

4.2.2.1. Shear Strength of Sand- Gravel Fill Material

The greater part of the performed tests, which is conducted to determine shear strength of sand-gravel, ejects the oversize particles due to constraints of laboratory devices. Shear strength of the sand-gravel mixtures including the oversize particles are affected by many parameters such as gravel ratio in the mixture, relative density, particle size and shape and surcharge (Salimi et al, 2008). In a study handled by Fragaszy et al. (1990, 92), ‘far-field matrix density’ was used to put on the impact of oversize particles on strength parameters since oversize particles affect the deformation behavior of sand-gravel soil. According to this study, oversize particles reduce the soil density. As a result of the increment in the gravel content, strength of sand-gravel soil decreases.

On the other hand, other studies conducted by Yagiz (2001), Kokusho et al. (2004), Simoni and Houlsby (2006) emphasized that the shear strength of the sand-gravel soil increase with the increment in the gravel content. In addition to these studies, research conducted by Vallejo (2001) claimed that gravel particles mainly affected the shear strength of the soil when its ratio in the soil is more than 70%.

On the other side, shear strength of the soil is controlled by the sand particles, if the ratio of gravel particles in the soil is less than 40%. As a consequence, if the ratio of gravel particles in the soil is between 40% and 70%, gravel particles partially affect the shear strength of the soil mixture.

In a study carried on by Seyed Nima Salimi et al. (Tehran, 2008), sand and gravel grains were used as a testing material. According to the results, gravel ratio that was not more than 60%, did not affect the shear strength of the mixture as much as the mixture whose gravel ratio is more than 60%. Minimum and maximum dry densities reduced, if the gravel ratio of the mixture exceeded 60%. In addition, shear strength of the mixture is affected by the contact between gravel particles. The results of this study are compatible with the studies conducted by Yagiz (2001), Kokusho et al. (2004), Simoni and Houlsby (2006) and Vallejo (2001).

The average gradation of Aydın Karacasu Dam is in the form of 55% sand and %45 gravel (DSİ, 2014). Hence, the gravel ratio that was not more than 60%, so gravel particles did not affect as much as the shear strength of sand-gravel mixture whose gravel ratio is more than 60%.

4.2.2.2. Material Model Parameters of Sand-Gravel

As seen in the *Table 4.6*, maximum settlement observed as 37.5 cm at ZDÖ 23 for the end of construction period (EOC). As mentioned in the Section *2.3.1.*, Çankırı Koyunbaba Dam is the CFSGD in Turkey. Maximum calculated settlement for the Koyunbaba Dam was 55 cm for the EOC period. Thus, material model parameters of Koyunbaba Dam are chosen to give the idea for the determination of material model parameters, which will be used in the preliminary analysis of Aydın Karacasu Dam. In the settlement analysis of Çankırı Koyunbaba Dam, hyperbolic material model parameters were determined from the similar studies in the literature such as Gudongkou Dam in China. Hyperbolic parameters, which were used in the preliminary analysis of Çankırı Koyunbaba Dam is shown in the *Table4.1.*

Table 4.1 Material model parameters used in hyperbolic models of Çankırı Koyunbaba Dam

Elasticity Modulus	Unit weight γ	*c* (kN/m^2)	ϕ	v
75 MPa	19~20.5 kN/m^3	1	38^o	0.25

There are not sufficient material parameters for hardening soil model or Mohr- Coulomb Model. Thus parameters are determined by utilizing similar range of parameters for Aydın Karacasu dam as the ones utilized in Çankırı Koyunbaba Dam. In addition to these parameters, which are taken from study of Çankırı Koyunbaba Dam, material parameters of Karacasu Dam are also selected with respect to the *Table 4.2, 4.3 and 4.4.*

Table 4.2 Values or value ranges for Poisson's ratio (Bowles et al., 1997)

μ	Soil type
0.4-0.5	Most clay soils
0.45-0.50	Saturated clay soils
0.3-0.4	Cohesionless—medium and dense
0.2-0.35	Cohesionless—loose to medium

Table 4.3 Values or value ranges for Poisson's ratio(Bowles et al., 1997)

Values or value ranges for Poisson's ratio /μ	
Type of soil	μ
Clay, saturated	0.4-0.5
Clay, unsaturated	0.1-0.3
Sandy clay	0.2-0.3
Silt	0.3-0.35
Sand, gravelly sand	- 0.1-1.00
commonly used	0.3-0.4
Rock	0.1-0.4 (depends somewhat on type of rock)
Loess	0.1-0.3
Ice	0.36
Concrete	0.15
Steel	0.33

Table 4.4 Value range for the static stress-strain modulus E_s for selected soils (Bowles et al., 1997)

Field values depend on stress history, water content, density, and age of deposit	
Soil	**E_s, MPa**
Clay	
Very soft	2-15
Soft	5-25
Medium	15-50
Hard	50-100
Sandy	25-250
Glacial till	
Loose	10-150
Dense	150-720
Very dense	500-1440
Loess	15-60
Sand	
Silty	5-20
Loose	10-25
Dense	50-81
Sand and gravel	
Loose	50-150
Dense	100-200
Shale	150-5000
Silt	2-20

** Value range is too large to use an "average" value for design.*

Moreover, studies on concrete faced rock fill dam are beneficial to predict correct parameter for the hyperbolic model. Özkuzukıran et. al., (2006), in the study of settlement analysis of Kürtün Dam, was assumed E_{50}^{ref} as fifty times more than Modulus Number 'K_E'. The hyperbolic model parameters, which are utilized in preliminary analysis of Aydın Karacasu Dam, are shown in the *Table 4.5.*

Table 4.5 Parameters used in hyperbolic models for sand-gravel fill material of Aydın Karacasu Dam

Alternative	Triaxial Stiffness E_{50}^{ref} (kPa)	Triaxial Unloading Stiffness E_{ur}^{ref} (kPa)	Oedometer Loading Stiffness E_{oed}^{ref} (kPa)	Unit weight (γ) (kN/m^3)	*c* (kN/m^2)	ϕ
1	39000	117000	39000	17.2	2	38^o
2	30000	90000	30000	17.2	2	38^o
3	25000	75000	25000	17.2	2	38^o

(*) Detailed information about hyperbolic model and its parameters are given in the section 4.1.

Sand and gravel are the noncohesive materials; so, "c" value is taken equal to zero. However, in the software programs (Plaxis v8.2 and Phase2), "c" is taken as "2 kPa" to carry out stability analysis realistically. From geological test results obtained from DSİ (1994), unit weight of the fill is taken as "17.2 kN/m^3" and strength parameters "*c*" and "ϕ" are chosen respectively "2" and "38^o". Besides, "R_{inter}" is taken 0.70.

Bedrock of the Karacasu Dam is assumed as a rigid body and hyperbolic model parameters, which are chosen for bedrock, are indicated in *Table 4.6.*

Table 4.6 Parameters used in hyperbolic models for bedrock material of Aydın Karacasu Dam

Elasticity Modulus	Unit weight γ	*c* (kN/m^2)	ϕ
600000 KPa	22 kN/m^3	25	40^o

The thickness of the concrete slab of Aydın Karacasu dam is constant throughout the dam body. Its thickness is 0.30 m from top to bottom of the dam body. Concrete slab of Aydın Karacasu Dam displays the elastic behavior and its material properties are chosen according to TS 500. Also, elasticity modulus of the concrete slab is taken 28500 MPa. Hyperbolic model parameters, which are chosen for concrete slab, are indicated in *Table 4.7*.

Parapet wall is also designed behind of the concrete face (Between elevation 294.00 m and 298.50 m) and it is built after the construction of concrete membrane.

Table 4.7 Parameters used in hyperbolic models for concrete slab of Aydın Karacasu Dam

EA (kN/m)	**EI (kNm^2/m)**	***d (m)***	***v***
8550000	64125	0.30	0.20

4.2.3. Elements and Mesh Model used in Finite Element Analyses

As mentioned in the previous section, finite element analyses of Aydın Karacasu Dam are conducted by using two program, Plaxis v8.2 and Phase2.

4.2.3.1. Mesh Model used in Plaxis v8.2

In Plaxis v8.2 program, settlements are calculated at nodes and stresses are calculated at Gauss integration points. Finite element system is formed with 6-node triangle mesh elements or 15-node triangle mesh elements in Plaxis v8.2. In this study, 15-node triangle element model is used to design and carry out finite element analyses of Aydın Karacasu Dam. Node types used in Plaxis v8.2 program are displayed in the *Figure 4.5.*

Mesh Model of Karacasu Dam, used in preliminary analysis, comprises of 8125 nodes, 990 Soil Elements, 11880 Global Stress Points. The model is shown in the *Figure4*

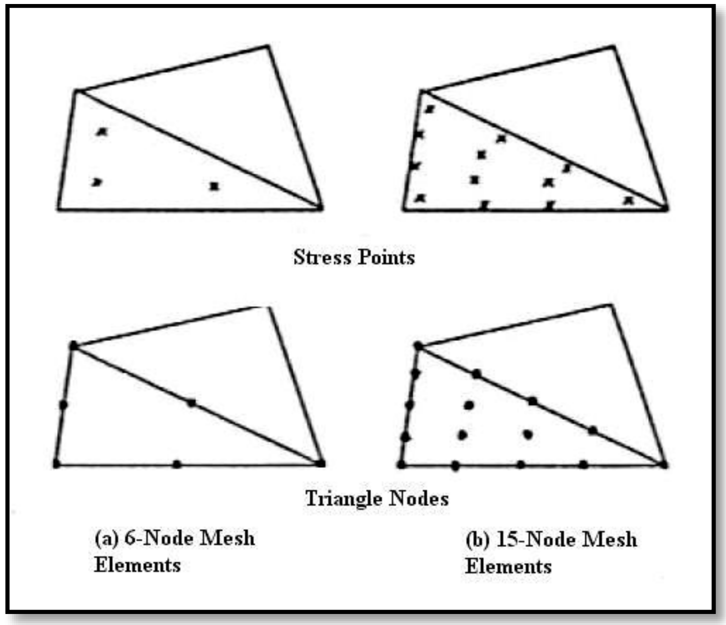

Figure 4.5 Node types in Plaxis v8.2

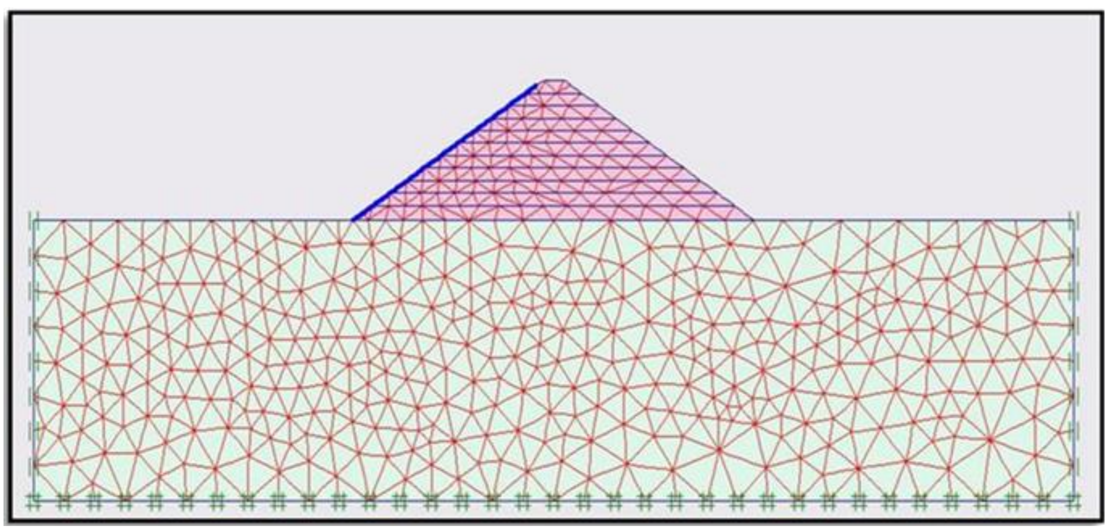

Figure 4.6 Connectivity in mesh analysis of Aydın Karacasu Dam (Plaxis v8.2)

4.2.3.2. Mesh Model used in Phase2

In Phase2 Program, settlements are calculated at nodes. Finite element system is formed with 3-noded triangle mesh elements, 6-noded triangle mesh elements, 4-noded quadrilaterals or 8-noded quadrilaterals. In this study, 6-noded triangle elements are used to design and carry out finite element analyses of Aydın Karacasu Dam. Approximate number of mesh elements used in the analysis is 1500. Analysis type is Plane Strain and solver type of the finite element analysis is Gaussian Elimination. Meshed and discretized model used in Phase2 Software are displayed *in Figure 4.7.*

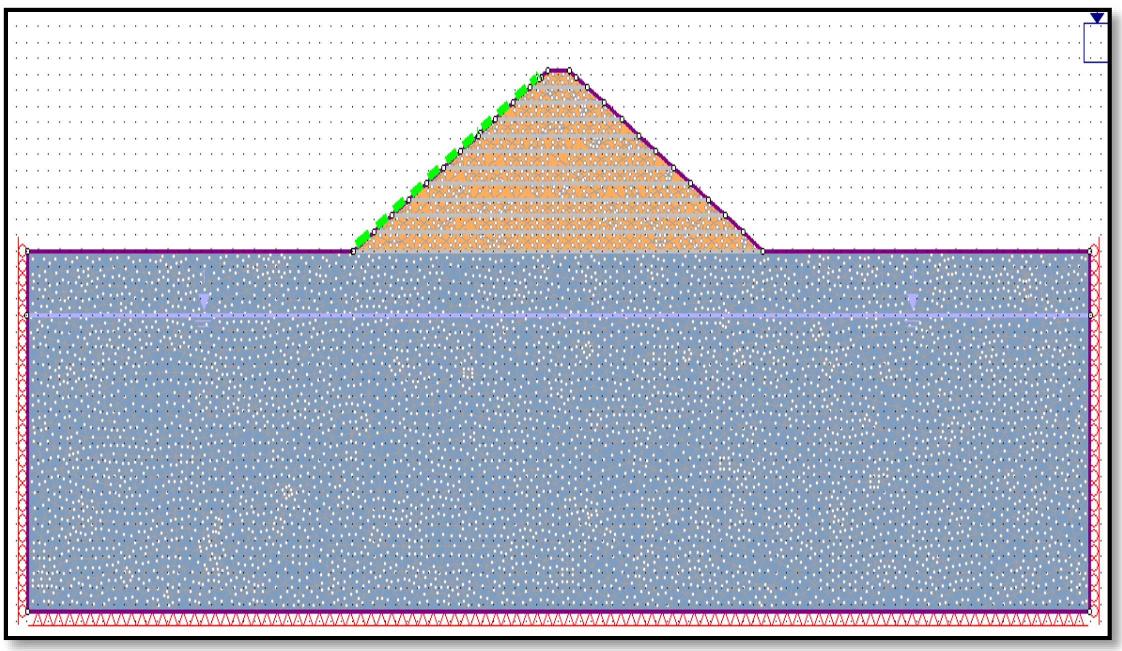

Figure 4.7 Meshed and discretized model of Aydın Karacasu Dam (Phase2)

4.2.4. Analysis Method

Analysis of the dam is carried out by stage construction method, recalling that embankment is formed in layers. Stage construction affects stress dispersion and settlements occurred in vertical or horizontal direction (Clough et. al., 1967). Layer thickness affects the analysis results. Analyses conducted by smaller layer thicknesses, is more accurate. However, it takes too much computation time (Özkuzukıran et. al., 2006).

In this study, imaginary axes are determined at the maximum cross-section of Aydın Karacasu Dam to show locations of instrumentation devices. Imaginary axes are shown in the *Figure 4.8.* Hydraulic settlement devices are assumed to be located in six different axes of the dam body. As seen in the *Figure 4.8,* ZDÖ2 is located in axis X_1-X_1, ZDÖ9 is located in axis X_2-X_2, ZDÖ10 and ZDÖ22 are located in axis X_3-X_3, ZDÖ11, ZDÖ23 and ZDÖ29 are located in axis X_4-X_4, ZDÖ12 and ZDÖ24 are located in axis X_5-X_5 and ZDÖ13 is located in axis X_6-X_6.

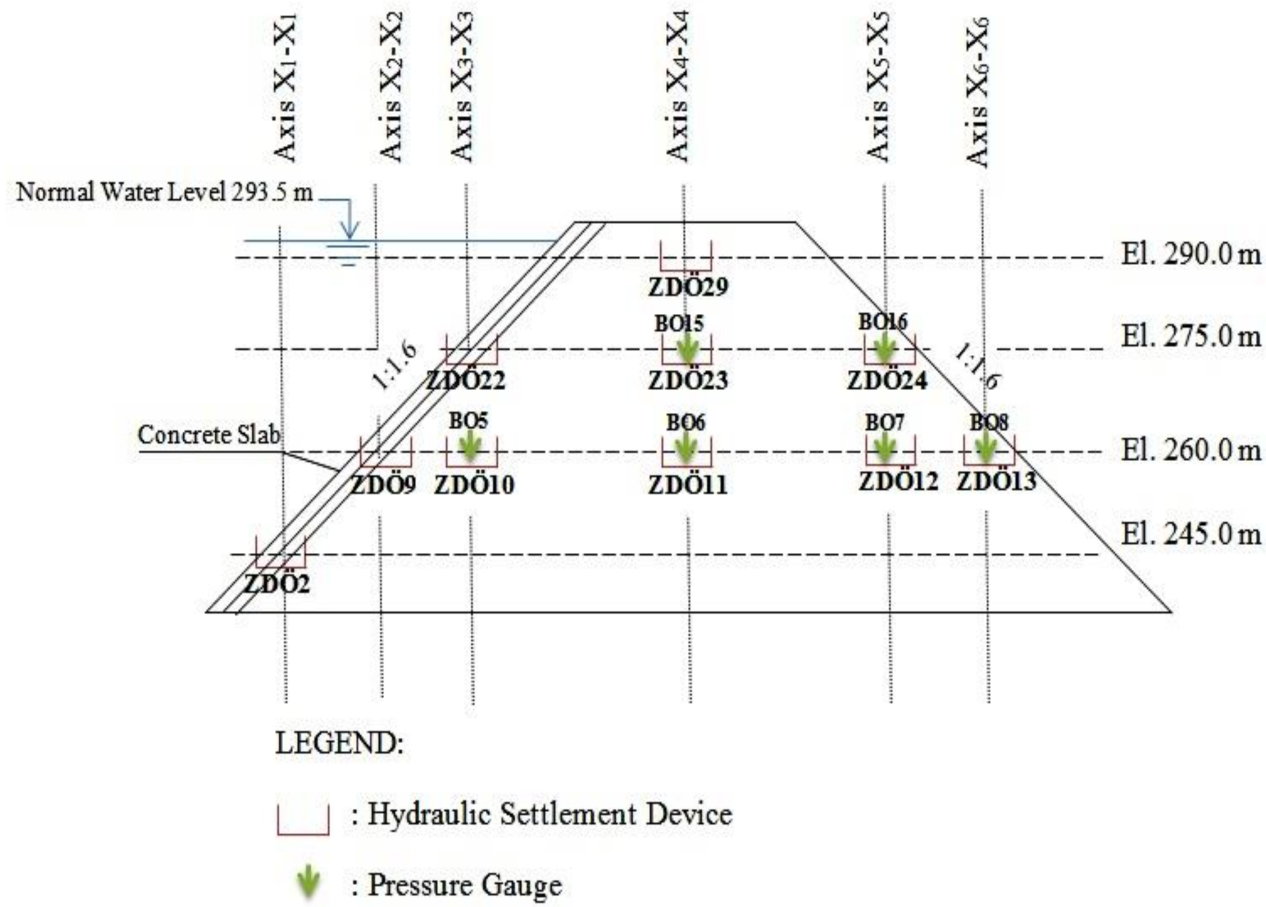

Figure 4.8 Location of imaginary axes and instrumentation devices at maximum cross-section (Km: 0+300.00 m) of Aydın Karacasu Dam

Deformation analyses are carried out for two important conditions such as end of construction (EOC) and reservoir impoundment (RI). Sand-gravel fill material deforms under only its own weight for end of construction condition. However, water load causes additional deformation in the embankment for reservoir impoundment condition (RI). Two dimensional finite element analyses are conducted for the maximum cross-section Km 0+300.00 m of Aydın Karacasu Dam.

As mentioned in *section 4.2.1*, Finite element softwares Plaxis v8.2 and Phase2 are used to compute deformations. In Plaxis v8.2 Software, embankment is designed in layers and deformation calculations start with foundation excavation at the dam site and continue layer by layer forming the embankment body. For each layer settlements are calculated at specific points where hydraulic settlement devices are located. At the end of each layer, recorded settlements are resetted to zero and intermediate steps are deleted. Then, calculated settlements are superposed to find the total settlements at specific points for EOC and RI conditions. In Phase2 Software, embankment is also designed in layers and deformation analyses are also computed step by step. After the computation, program gives the maximum stresses and deformations.

The rock foundation of the Aydın Karacasu Dam is thought to be infinitely rigid. It is also assumed that there is a perfect bond between concrete slab and sand-gravel fill.

4.2.4.1. Effect of Layer Thickness

Settlement calculations of Karacasu Dam are made in layers as explained above, by using 5 m thick layers in finite element programs, Plaxis v8.2 and Phase2. However, the embankment is also analyzed by using 3m thick layers to assess the effect of layer thickness on the analyses results. As mentioned in *section 3.3.1*, maximum observed settlement is recorded as 37.50 cm for end of construction condition from hydraulic settlement device "ZDÖ23", located on axis X_4-X_4(shown in the *Figure 4.8*). Settlements, along axis X_4-X_4 of maximum cross-section of Aydın Karacasu Dam, are analyzed by utilizing 5m thick layers and 3m thick layers to depict the impact of layer thicknesses. In the *Figure 4.9*, results of both analyses are shown.

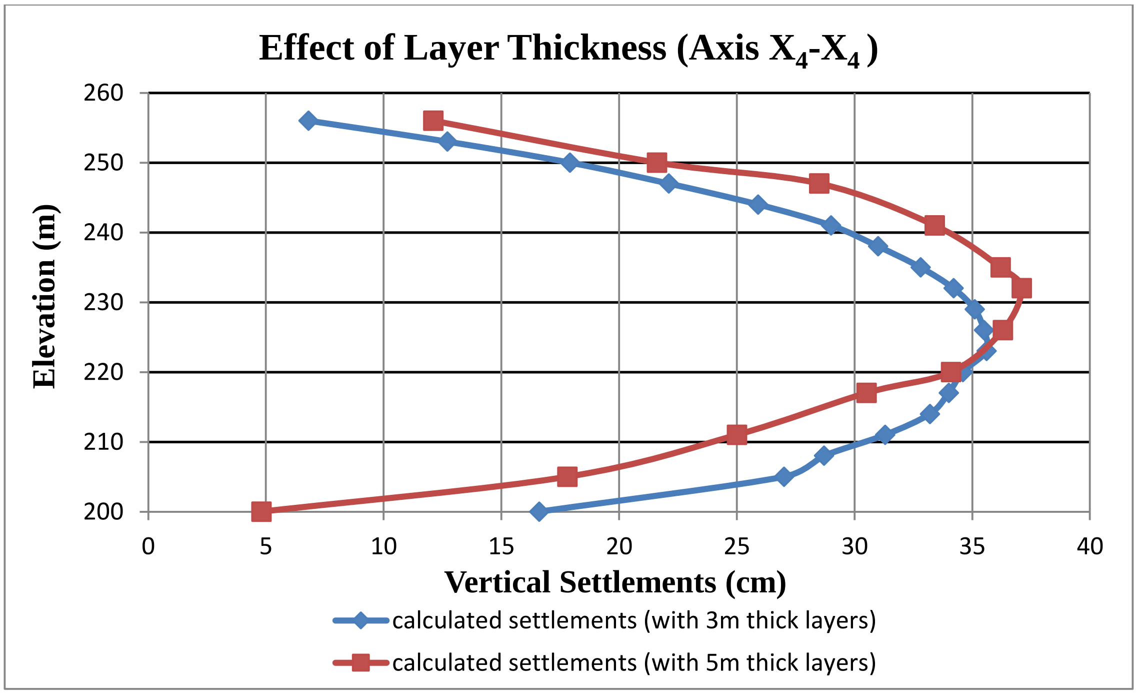

(*) Settlement values are calculated by Plaxis v8.2.

(*) El. 200.00 m is taken as the reference elevation for base of the dam.

Figure 4.9 Comparison of calculated settlements by utilizing 5 m layers and 3 m layers at axis X_4-X_4

As seen in the *Figure 4.9*, there is not remarkable difference between two analyses. Maximum settlement is calculated as 35.6 cm by using 3 m thick layers and as 36.2 cm by using 5 m thick layers for axis X_4-X_4 for the end of construction condition. It is seen that using 5 m layers gives the close results with the maximum observed settlement for axis X_4-X_4, recorded by DSİ. Therefore, it is decided to utilize 5 m layers in the following analyses.

CHAPTER 5

RESULTS OF ANALYSES

In this chapter, results of analyses for end of the construction condition and reservoir impoundment are presented by using both Plaxis v8.2 and Phase2 Software and calculated deformations and stresses are compared with observed values recorded by DSİ. Finally, deformation and stress contours are shown so as to depict the deformation behavior of the embankment.

5.1. End of Construction Analyses (EOC)

Embankment is formed by sand-gravel material prior to impounding. Material model parameters, used in finite element calculations by both Plaxis v8.2 and Phase2, are shown in *Table 4.5* (Comprehensive data about material model parameters is explained in *Section 4.2.2.1*).

Results of analyses are conducted by using each loading condition, which are shown in the *Table 4.5*, are close to each other. However, loading condition 2 gives the closest results to observed ones recorded by DSİ. Hence, parameters, shown in the loading condition 2, are used as an input for both programs. Results of analyses for end of construction condition are presented in *Table 5.1*.

Figures 5.1-5.5 give the comparison of observed vertical settlement values (recorded by DSİ) with analyses results, which are conducted by using Plaxis v8.2 and Phase2.

Table 5.1 Results of Analyses of Aydın Karacasu Dam at Max. Cross-Section (Km 0+300.00 m) for EOC

Axes	X_2-X_2	X_3-X_3		X_4-X_4			X_5-X_5		X_6-X_6
Instrument	**ZDÖ9**	**ZDÖ10**	**ZDÖ22**	**ZDÖ11**	**ZDÖ23**	**ZDÖ29**	**ZDÖ12**	**ZDÖ24**	**ZDÖ13**
Elevation (m)	260.00	260.00	275.00	260.00	275.00	290.00	260.00	275.00	260.00
Vertical Settlement Observed by DSİ (cm)	-36.0	-22.0	-28.0	-23.0	-37.5	-32.0	-27.0	-32.0	-28.0
Calculated Vertical Settlement by Plaxis v8.2 (cm)	-15.0	-27.9	-23.0	-32.5	-35.5	-21.6	-26.2	-18.8	-16.5
Calculated Vertical Settlement by Phase2 (cm)	-10.3	-27.6	-16.0	-35.7	-35.5	-16.5	-24.6	-14.6	-11.9
Difference between Observed Settlement and Plaxis v8.2 Results (cm)	-21.0	5.9	-5.0	9.5	-2.0	-10.4	-0.8	-13.2	-11.5
% Difference between Observed Settlement and Plaxis v8.2 Results	58.4	26.6	17.7	41.4	5.3	32.4	2.9	41.1	41.1
Difference between Observed Settlement and Phase2 Results (cm)	-25.7	5.6	-12.0	12.7	-2.0	-15.5	-2.4	-17.4	-16.1
% Difference between Observed Settlement and Phase2 Results	71.3	25.6	43.0	-55.4	5.4	48.4	8.9	54.4	57.5
% Difference between Calculated Settlement by Plaxis v8.2 and Phase2	30.9	0.8	30.7	9.9	0.1	23.7	6.2	22.6	27.9

(*) In the Table "-" settlement value shows compression

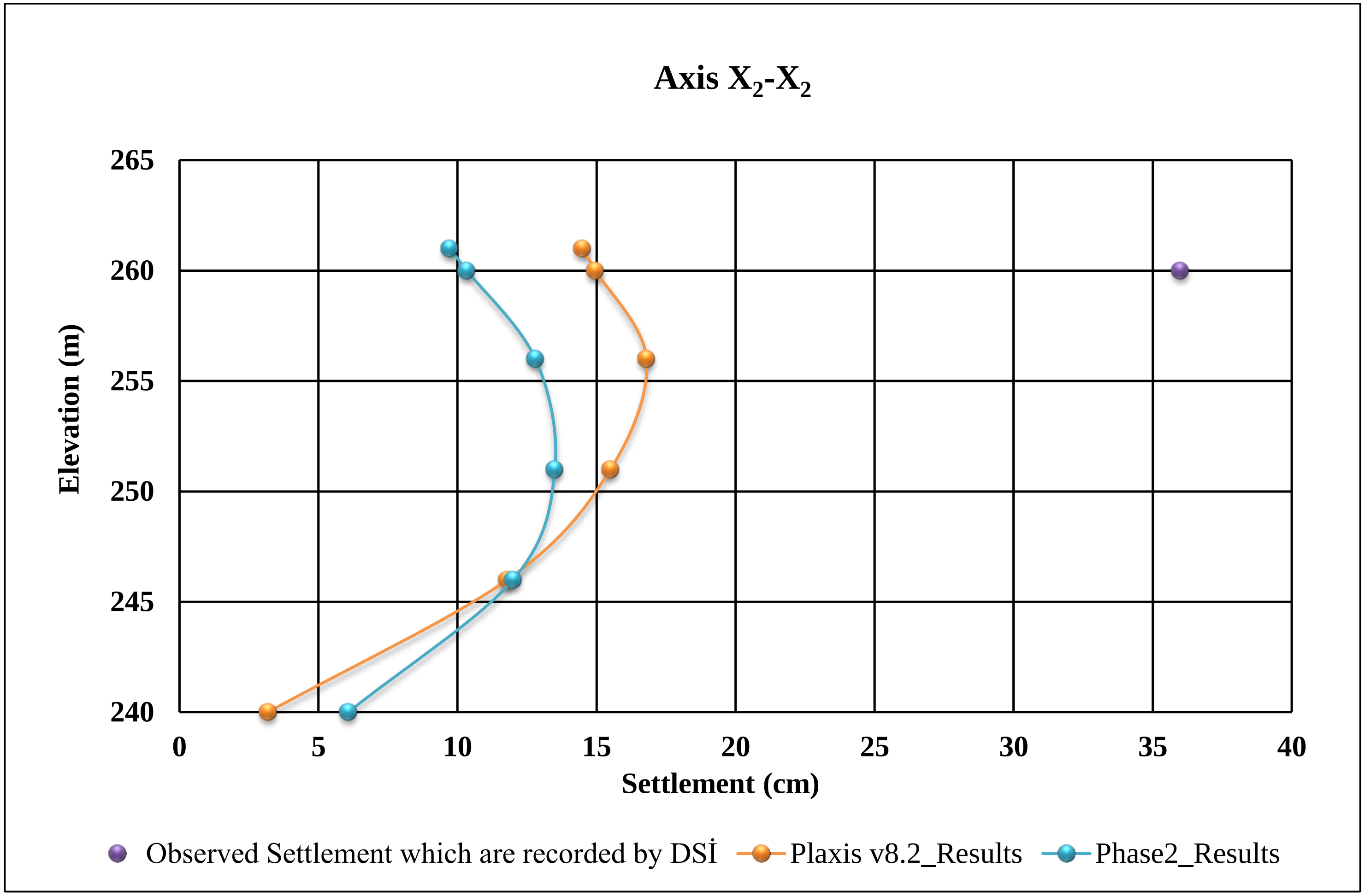

Figure 5.1 Comparison of analyses results with observed data that are recorded by DSİ in axis X_2-X_2 for EOC

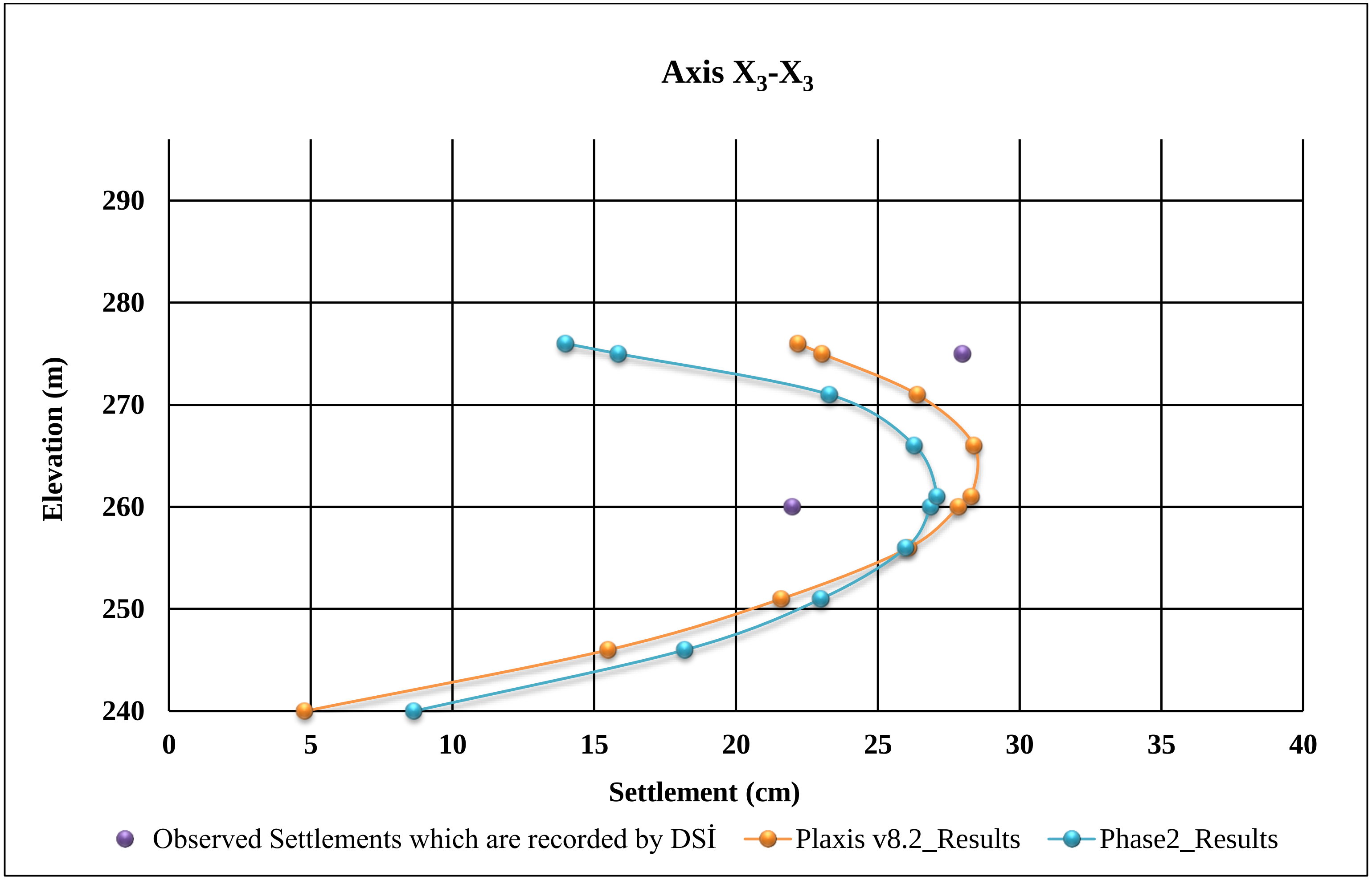

Figure 5.2 Comparison of analyses results with observed data that are recorded by DSİ in axis X_3-X_3 for EOC

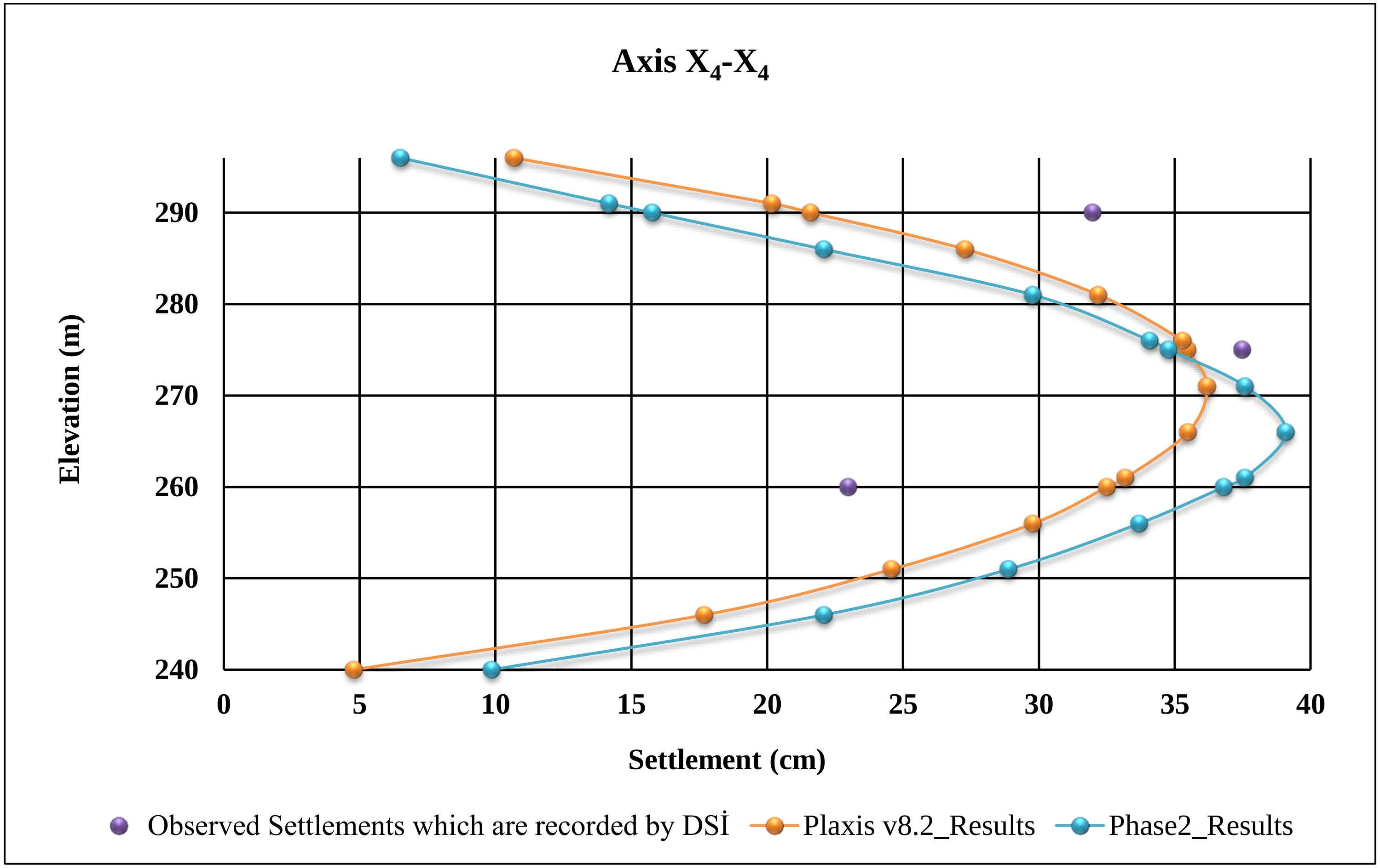

Figure 5.3 Comparison of analyses results with observed data that are recorded by DSİ in axis X_4-X_4 for EOC

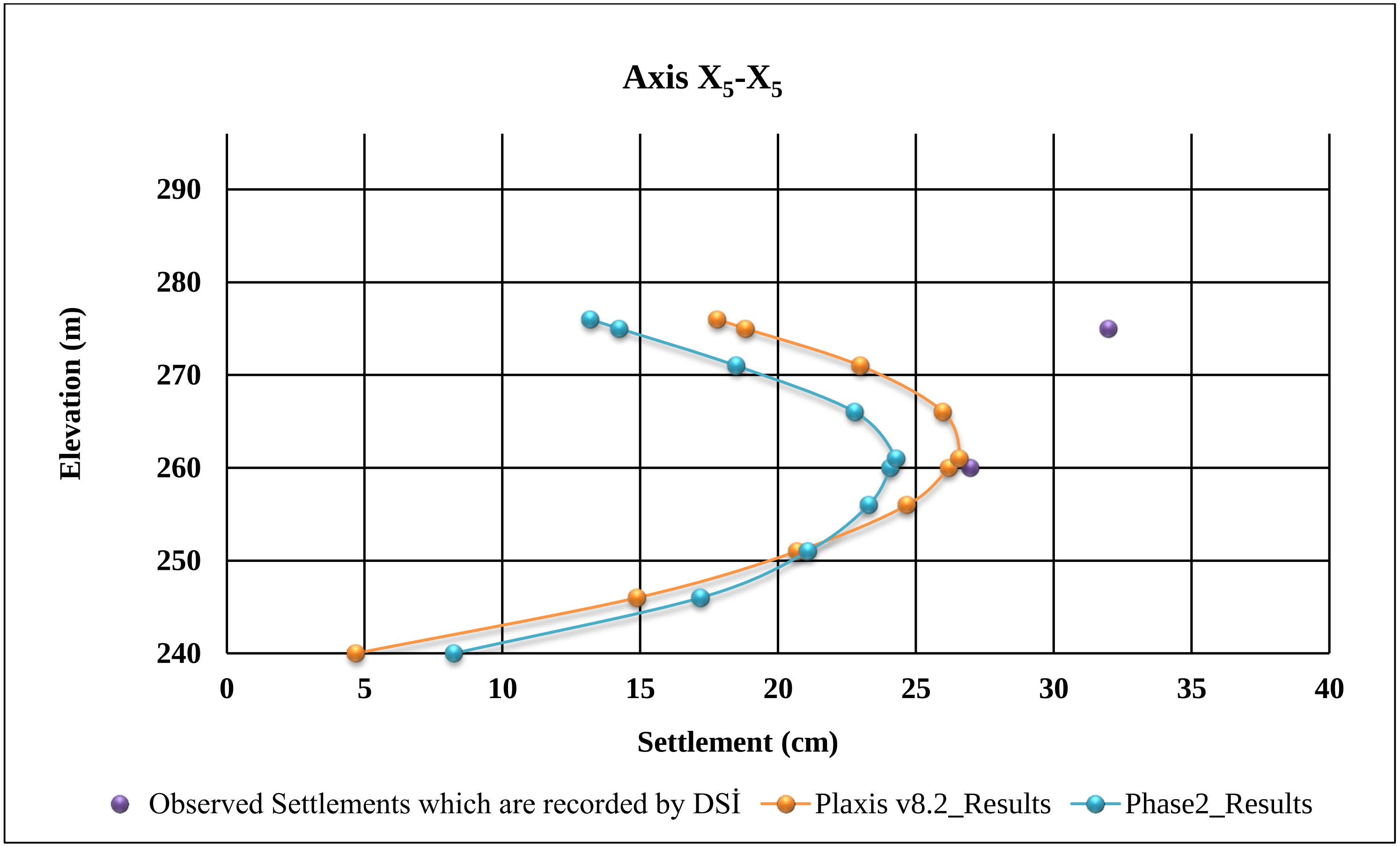

Figure 5.4 Comparison of analyses results with observed data that are recorded by DSİ in axis X_5-X_5 for EOC

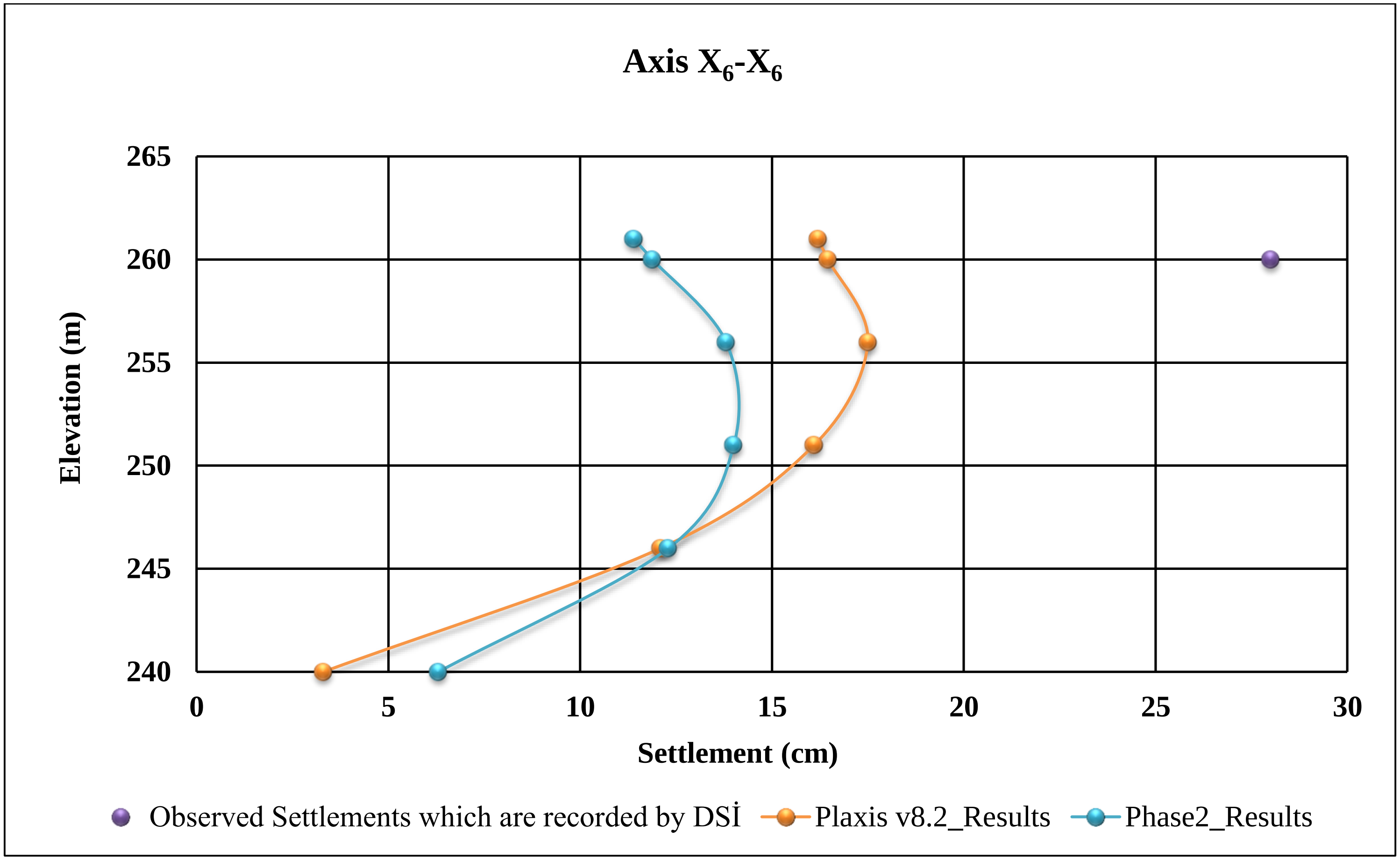

Figure 5.5 Comparison of analyses results with observed data that are recorded by DSİ in axis X_6-X_6 for EOC

As seen from the Figures 5.1-5.5, finite element analyses results are in agreement for the axes X_3-X_3, X_4-X_4 and X_5-X_5. Vertical settlement values, which are calculated by using Phase2 and Plaxis v8.2, are compatible with recorded vertical settlements obtained from DSİ. Difference between observed and calculated settlements increases through the upstream and downstream toe. As mentioned in *Section 3.3*, maximum observed settlement is recorded as 37.50 cm in the axis X_4-X_4 for EOC. This value is obtained from hydraulic settlement device "ZDÖ23" located corresponding to 62.50% of the dam height from the bottom. Therefore, "ZDÖ23" is the best chosen hydraulic settlement device in this study. Maximum vertical settlement is calculated as 36.20 cm at El. 271 m, corresponding to 55.36% of the dam height from the bottom by Plaxis v8.2. It is also calculated as 38.20 cm by Phase 2 and it is almost at 46.43% of the dam height from the bottom. Majority of the calculated values from both finite element program results are compatible with observed settlement values. Maximum settlement of the Aydın Karacasu Dam is expected to occur close the mid height of the dam body, since compressibility of the fill material decreases with increasing elevation.

5.2. Reservoir Impoundment (RI)

One of the significant conditions that should be analyzed to assess dam behavior is reservoir impoundment. Because a large part of post-construction deformations occur during this period. Settlements increase by rising water level. Large settlements may cause cracks in the concrete slab and leakage problems may emerge as a result of cracks in the concrete slab.

In Aydın Karacasu Dam, reservoir impounding started in 07.09.2012. Water level reached El. 293.50 m in a short time and then ultimately reached El. 298.17m. After end of construction of the dam body, majority of the deformations occur during first impounding so, first impounding is a critical condition that should be analyzed (Özkuzukıran et al., 2006). Thus, El. 293.50 m is considered as a critical condition to be considered in finite element calculations.

Concrete slab is presumed as uncracked and impervious in the finite element analyses and water load is assumed as acting in a perpendicular direction to the concrete slab and calculated as a uniformly distributed load as shown in the *Figure 5.6* below.

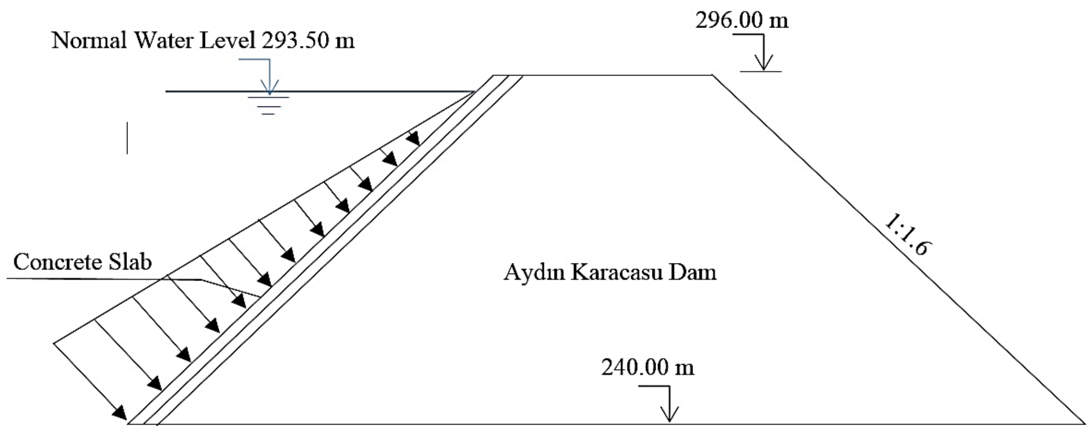

Figure 5.6 Uniformly distributed water load applied on concrete membrane of Aydın Karacasu Dam

The maximum water load (at El 240.00 m) is 524,835 kN/m^2. It decreases with increasing elevations. Reservoir impounding analyses are conducted for six imaginary axis, which are mentioned in *Section 4.2.4*, during finite element analyses by using Plaxis v8.2 and Phase2 programs. Results of the analyses for reservoir impounding condition are shown in *Table 5.2*.

In the *Figures 5.7-5.11*, observed vertical settlement values (recorded by DSİ) are compared with results of analyses, conducted by using Plaxis v8.2 and Phase2 for reservoir impounding condition.

Table 5.2 Results of analyses of Aydın Karacasu Dam at max. Cross-section (Km 0+300.00 m) for RI Condition

Axis	X_2-X_2	X_3-X_3		X_4-X_4			X_5-X_5		X_6-X_6
Instrument	**ZDÖ9**	**ZDÖ10**	**ZDÖ22**	**ZDÖ11**	**ZDÖ23**	**ZDÖ29**	**ZDÖ12**	**ZDÖ24**	**ZDÖ13**
Elevation (m)	260.00	260.00	275.00	260.00	275.00	290.00	260.00	275.00	260.00
Settlement Observed by DSİ (cm)	-44,0	-32,0	-41,0	-40,0	-45,5	-44,0	-40,0	-42,0	-41,0
Calculated Settlement by Plaxis v8.2 (cm)	-23,5	-31,6	-28,7	-35,1	-38,8	-25,3	-28,1	-21,4	-17,6
Calculated Settlement by Phase2 (cm)	-27,2	-35,1	-30,5	-37,8	-35,9	-17,7	-24,8	-15,3	-12,2
Difference between Settlement Observed by DSİ and Settlement Calculated by Plaxis v8.2 (cm)	-20,5	-0,4	-12,3	-4,9	-6,7	-18,7	-11,9	-20,6	-23,4
% Difference between Observed Settlement and Calculated Settlement by Plaxis v8.2	46,5	1,1	30,0	12,3	14,7	42,5	29,9	49,0	57,0
Difference between Settlement Observed by DSİ and Settlement Calculated by Phase2 (cm)	-16,8	3,1	-10,5	-2,2	-9,6	-26,3	-15,3	-26,7	-28,8
% Difference between Observed Settlement and Calculated Settlement by Phase2	38,2	9,7	25,7	5,5	21,2	59,7	38,1	63,6	70,3
% Difference between Calculated Settlement by Plaxis v8.2 and Phase2	15,6	11,0	6,1	7,8	7,6	30,0	11,8	28,6	31,0

(*) In the Table "-" settlement values shows compression

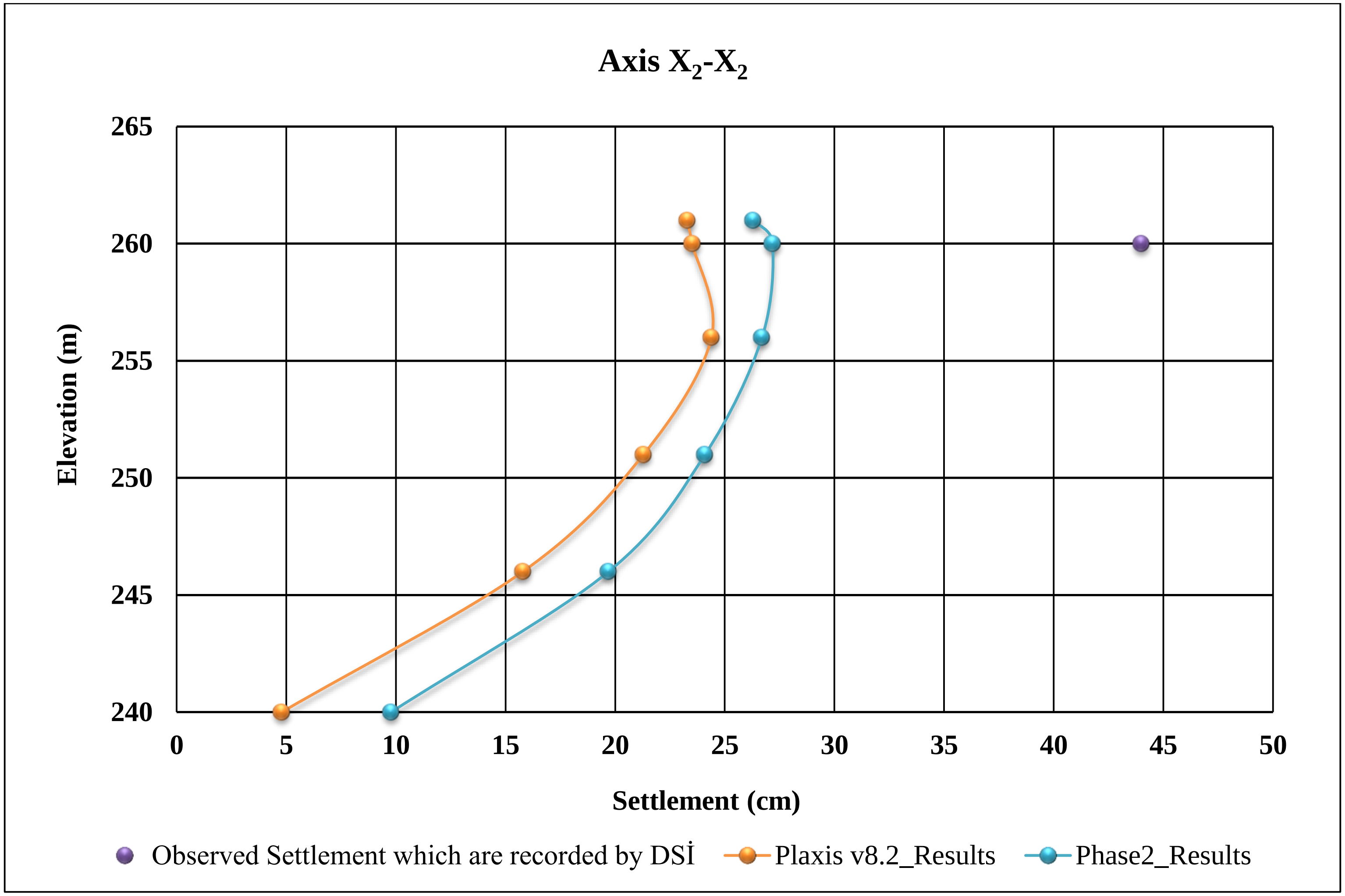

Figure 5.7 Comparison of analyses results with observed data that are recorded by DSİ in axis X_2-X_2 for RI

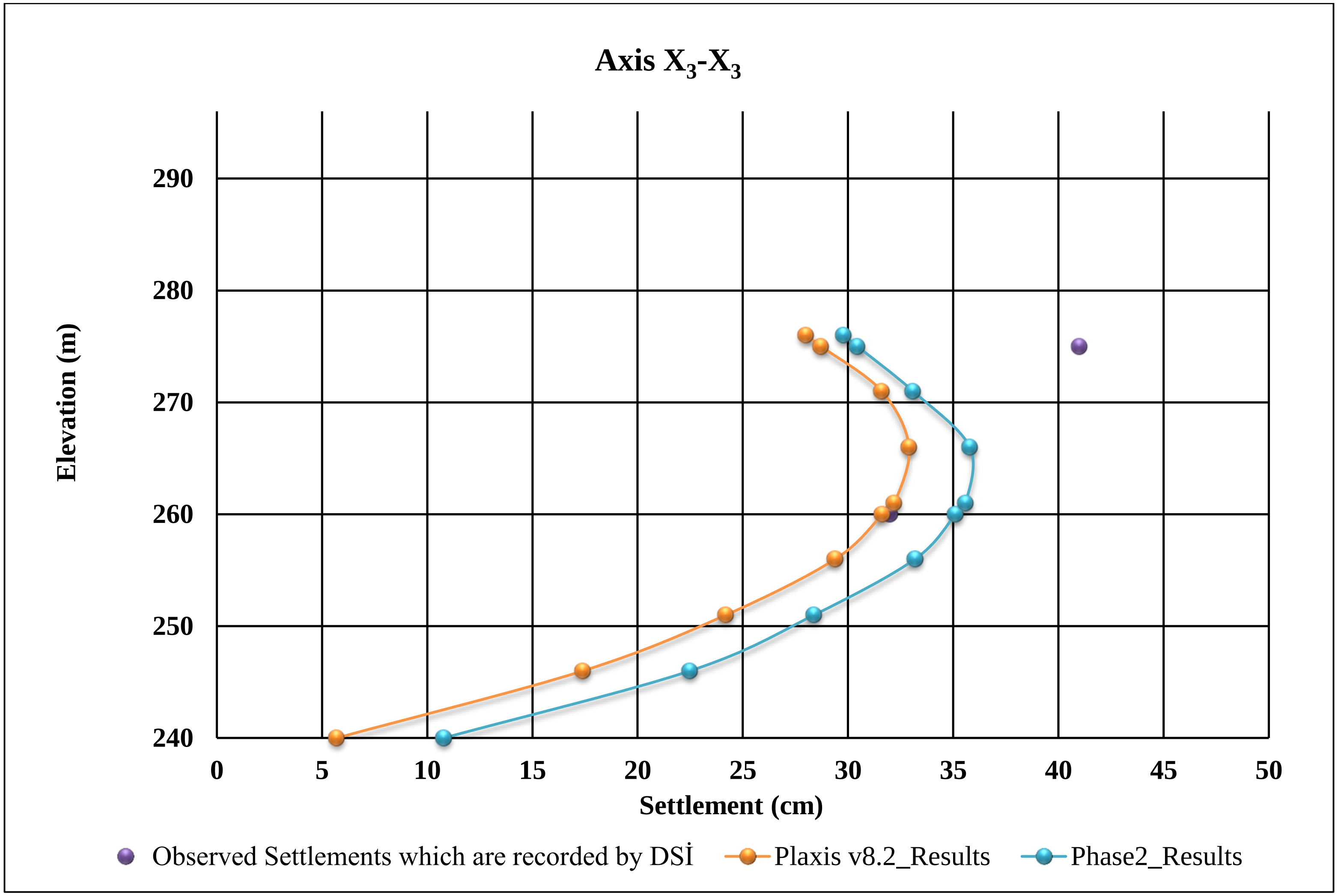

Figure 5.8 Comparison of analyses results with observed data that are recorded by DSİ in axis X_3-X_3 for RI

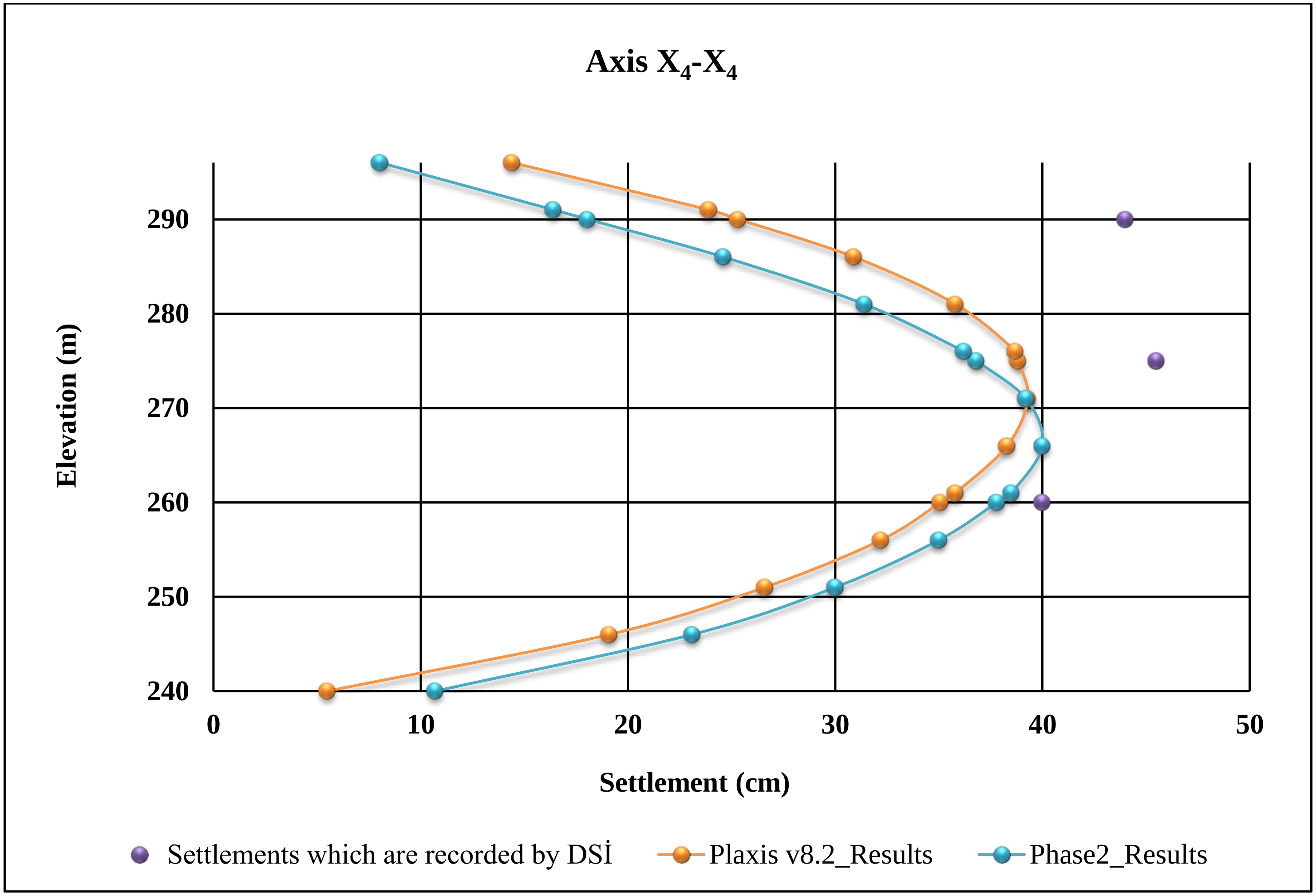

Figure 5.9 Comparison of analyses results with observed data that are recorded by DSİ in axis X_4-X_4 for RI

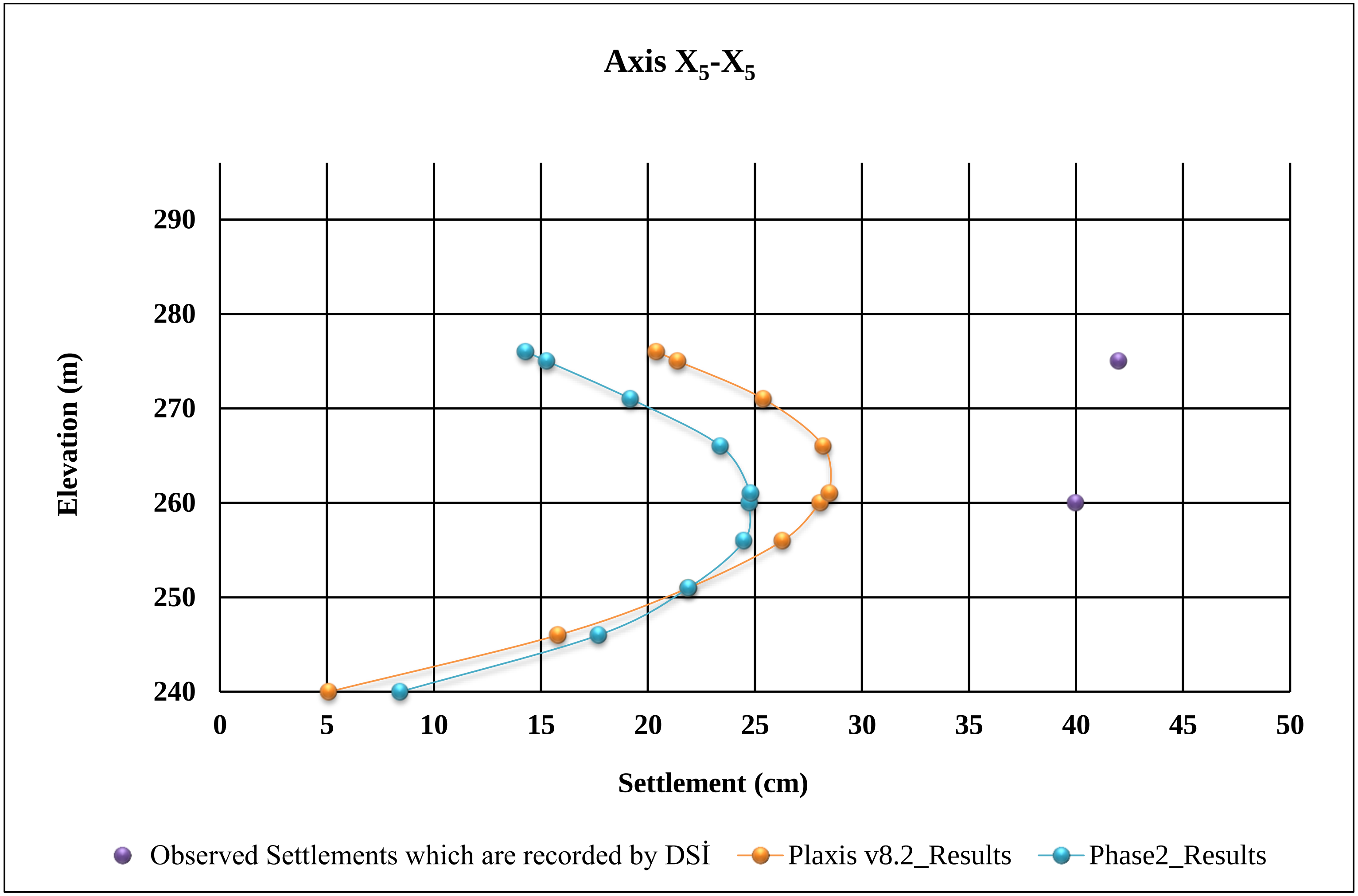

Figure 5.10 Comparison of analyses results with observed data that are recorded by DSİ in axis X_5-X_5 for RI

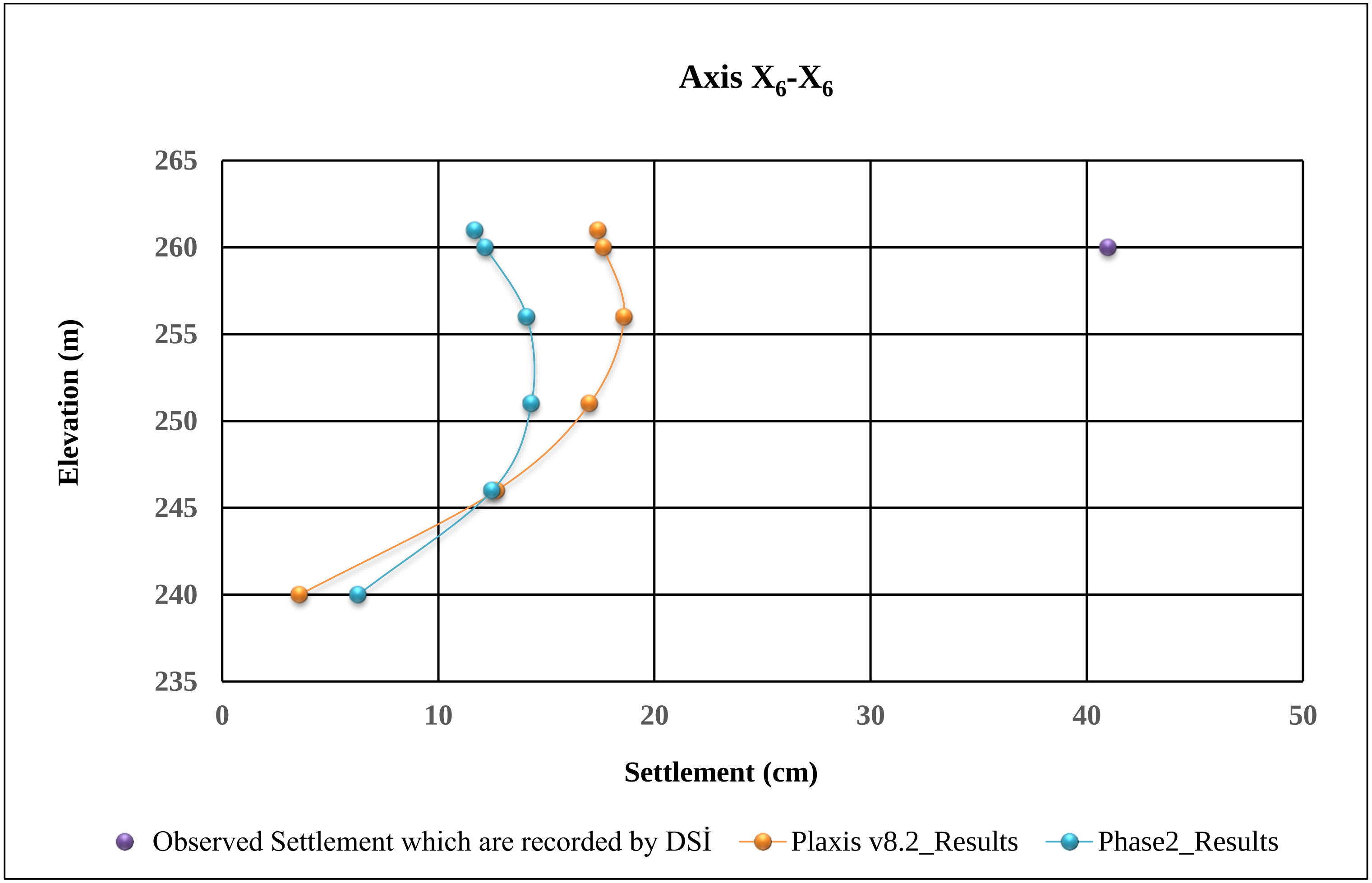

Figure 5.11 Comparison of analyses results with observed data that are recorded by DSİ in axis X_6-X_6 for RI

As seen in the Figures 5.7-5.11, results of analyses are quite compatible with the measured values for the axes X_3-X_3 and X_4-X_4. Vertical settlement values, which are calculated by using Phase2 and Plaxis v8.2, are compatible with recorded vertical settlements obtained from DSİ for these axes. As mentioned in *Section 3.3*, maximum observed settlement is recorded as 45,50 cm in the axis X_4-X_4 for RI. As obtained by hydraulic settlement device “ZDÖ23” and ZDÖ 23 located at 62,50% of the dam height from bottom. Maximum vertical settlement is calculated as 39,30 cm at El. 271 m at 55,00% of the dam height by Plaxis v8.2 for RI and as 40,00 cm by Phase 2 for RI and it is almost at 46,00% of the dam height measured from the bottom.

Table 5.3-5.5 show the impact of water loading on vertical settlements, recorded by DSİ and calculated by finite element analyses. EOC settlements are not included in these values, which are indicated in the following tables in order to show the reservoir impounding effect on the deformation behavior of the dam body. Therefore, vertical settlement values observed at the end of construction are subtracted from the ones observed when reservoir impounding reaches El 293,50 m.

Table 5.3 Effect of reservoir impounding on vertical settlements that are observed by DSİ

Axis	X_2-X_2	X_3-X_3		X_4-X_4			X_5-X_5		X_6-X_6
Instrument	**ZDÖ9**	**ZDÖ10**	**ZDÖ22**	**ZDÖ11**	**ZDÖ23**	**ZDÖ29**	**ZDÖ12**	**ZDÖ24**	**ZDÖ13**
Elevation (m)	260.00	260.00	275.00	260.00	275.00	290.00	260.00	275.00	260.00
Settlement Observed by DSİ for EOC (cm)	-36,0	-22,0	-28,0	-23,0	-37,5	-32,0	-27,0	-32,0	-28,0
Settlement Observed by DSİ for RI (cm)	-44,0	-32,0	-41,0	-40,0	-45,5	-44,0	-40,0	-42,0	-41,0
Effect of Reservoir İmpounding (cm)	-8,0	-10,0	-13,0	-17,0	-8,0	-12,0	-13,0	-10,0	-13,0

Table 5.4 Effect of reservoir impounding on vertical settlements that are calculated by Plaxis v8.2

Axis	X_2-X_2	X_3-X_3		X_4-X_4			X_5-X_5		X_6-X_6
Instrument	**ZDÖ9**	**ZDÖ10**	**ZDÖ22**	**ZDÖ11**	**ZDÖ23**	**ZDÖ29**	**ZDÖ12**	**ZDÖ24**	**ZDÖ13**
Elevation (m)	260.00	260.00	275.00	260.00	275.00	290.00	260.00	275.00	260.00
Settlements Calculated by Plaxis v8.2 for EOC (cm)	-15,0	-27,9	-23,0	-32,5	-35,5	-21,6	-26,2	-18,8	-16,5
Settlements Calculated by Plaxis v8.2 for RI (cm)	-23,5	-31,6	-28,7	-35,1	-38,8	-25,3	-28,1	-21,4	-17,6
Effect of Reservoir İmpounding (cm)	-8,5	-3,7	-5,7	-2,6	-3,3	-3,7	-1,9	-2,6	-1,1

Table 5.5 Effect of reservoir impounding on vertical settlements that are calculated by Phase2

Axis	**X_2-X_2**	**X_3-X_3**		**X_4-X_4**			**X_5-X_5**		**X_6-X_6**
Instrument	**ZDÖ9**	**ZDÖ10**	**ZDÖ22**	**ZDÖ11**	**ZDÖ23**	**ZDÖ29**	**ZDÖ12**	**ZDÖ24**	**ZDÖ13**
Elevation (m)	260.00	260.00	275.00	260.00	275.00	290.00	260.00	275.00	260.00
Settlements Calculated by Phase2 for EOC (cm)	-10,3	-27,6	-16,0	-35,7	-35,5	-16,5	-24,6	-14,6	-11,9
Settlements Calculated by Phase2 for RI (cm)	-27,2	-35,1	-30,5	-37,8	-35,9	-17,7	-24,8	-15,3	-12,2
Effect of Reservoir İmpounding (cm)	-16,9	-7,5	-14,5	-2,1	-0,4	-1,2	-0,1	-0,7	-0,3

When *Tables 5.4-5.5* are examined, it is seen that reservoir impounding effect decreases from upstream membrane to downstream part of the dam body due to water loading, as expected. Larger settlements are seen in the region close to upstream face. Throughout axis X_3-X_3, calculated settlement increase with a significant amount from El 260 m to El 275 m. In other axes, X_4-X_4, X_5-X_5 there is a negligible increment in the vertical settlement.

5.3. Evaluation of Total Stresses

In Aydın Karacasu Dam, total pressure gauges are utilized to record stresses. Location of total pressure gauges are shown in *Figure 4.8* (see *Section 4.2.4*). Total stresses are calculated by using Plaxis v8.2 and Phase2 both for EOC and RI. The results of the analyses are indicated in *Tables 5.6-5.7* and in *Figures 5.12-5.13*. Also, *Table 5.8* shows the stress increment both for EOC and RI conditions.

When *Table 5.6* is examined, it is exactly seen that stress values calculated by Plaxis v8.2 are lower than observed ones except total pressure gauge “BÖ15” where the total stresses are higher than the calculated ones for EOC. It is also seen that stress values calculated by Phase2 are lower than observed ones except in total pressure gauges “BÖ6, BÖ15, BÖ7” where the total stresses are higher than the calculated ones for EOC. The maximum observed total stress is recorded by the instrumentation device “BÖ 5”, located closest to upstream membrane. The maximum stress is calculated as 388,8 kPa for the location of the instrumentation device “BÖ 5” by Phase2. This is in agreement with maximum observed stress. However, the maximum stress is calculated as 298,7 kPa for the location of instrumentation device “BÖ 6” by Plaxis v8.2.

When *Table 5.7* is examined, it is exactly seen that stress values calculated by Plaxis v8.2 are lower than observed ones except for the location of total pressure gauge “BÖ 6” where the total stress is higher than the calculated ones for RI condition. It is also seen that stress values calculated by Phase2 are higher than observed ones except for the location of total pressure gauge “BÖ16” where the observed total stress is slightly lower than the calculated ones for RI condition. The maximum observed total stress is recorded by the instrumentation device “BÖ 5” which is located closest to upstream membrane, as expected. The maximum stress is calculated as 461,2 kPa for the location of total pressure gauge “BÖ 5” by Phase2 and calculated as 330,9 kPa for the location of total pressure gauge “BÖ 5” by Plaxis v8.2. Phase 2 results are more compatible with observed ones for RI condition. Comparison of calculated and observed stresses is shown in Figures 5.12-5.13.

When *Table 5.8* is examined, it is seen that stress increment is generally higher for the total pressure gauges located at El. 260 m than for the total pressure gauges located at El. 275 m and it generally decreases with increasing elevation. However, there is a significant difference between calculated and observed stresses both for EOC and RI conditions at the location of total pressure gauge “BÖ 15”. This situation is also a result of reservoir impounding.

Table 5.6 Comparison of Calculated and Observed Stresses of Aydın Karacasu Dam for EOC

Total Pressure Gauge	Elevation (m)	Axis	Results of Plaxis v8.2 (kPa)	Results of Phase2 (kPa)	Observed Values (kPa)	Difference of the Results of Plaxis v8.2 and Observed Values	Difference of the Results of Phase2 and Observed Values	% Difference of Plaxis v8.2 Calculations and Observations	% Difference of Phase2 Calculations and Observations
BÖ-5	260,00	X3-X3	235,74	388,79	405,54	169,80	16,75	41,87	4,13
BÖ-6	260,00	X4-X4	298,69	356,22	323,86	25,17	-32,36	7,77	9,99
BÖ-15	275,00		170,62	229,07	123,16	-47,47	-105,91	38,54	86,00
BÖ-7	260,00	X5-X5	206,11	307,63	257,12	51,01	-50,51	19,84	19,65
BÖ-16	275,00		86,51	97,33	144,50	57,99	47,17	40,13	32,64
BÖ-8	260,00	X6-X6	100,96	132,82	133,83	32,87	1,01	24,56	0,75

(*) Observed Stress Values are recorded by DSİ

(*) Imaginary axes are shown in *Figure 4.8* (see *Section 4.2.4*)

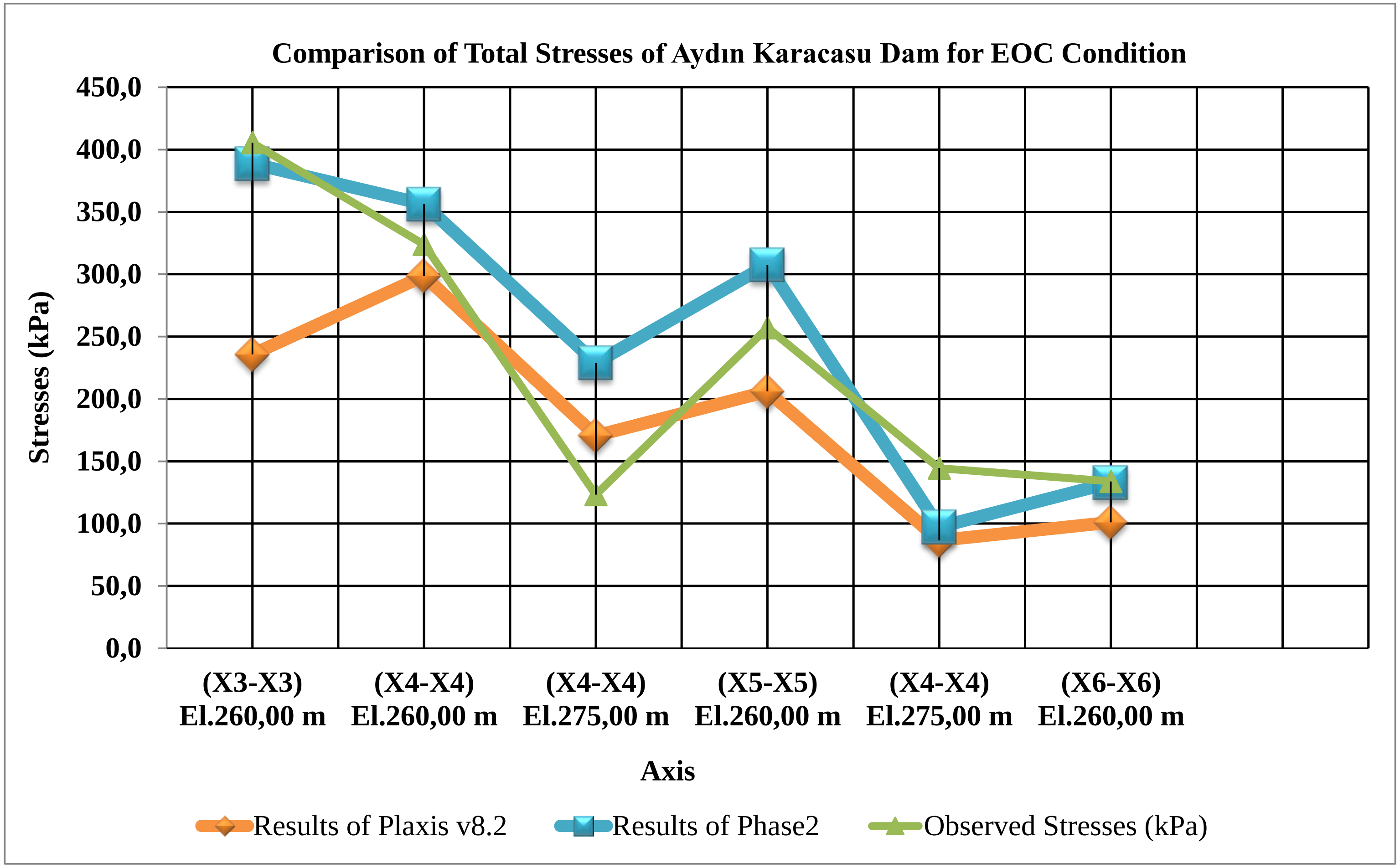

(*) Observed Stress Values are recorded by DSİ

(*) Imaginary axes are shown in *Figure 4.8* (see *Section 4.2.4*)

Figure 5.12 Comparison of Calculated Stresses with Observed Ones for EOC condition

Table 5.7 Comparison of Calculated and Observed Stresses of Aydın Karacasu Dam for RI

Total Pressure Gauge	Elevation (m)	Axis	Results of Plaxis v8.2 (kPa)	Results of Phase2 (kPa)	Observed Values (kPa)	Difference of the Results of Plaxis v8.2 and Observed Values	Difference of the Results of Phase2 and Observed Values	% Difference of Plaxis v8.2 Calculations and Observations	% Difference of Phase2 Calculations and Observations
BÖ-5	260,0	X_3-X_3	330,9	461,2	455,8	124,9	-5,4	27,4	1,2
BÖ-6	260,0	X_4-X_4	330,2	385,7	328,8	-1,4	-56,9	0,4	17,3
BÖ-15	275,0		243,8	265,7	258,6	14,8	-7,1	5,7	2,8
BÖ-7	260,0	X_5-X_5	181,7	314,0	258,1	76,4	-55,9	29,6	21,6
BÖ-16	275,0		87,3	105,8	145,1	57,8	39,3	39,8	27,1
BÖ-8	260,0	X_6-X_6	133,3	145,1	135,4	2,1	-9,7	1,6	7,2

(*) Observed Stress Values are recorded by DSİ

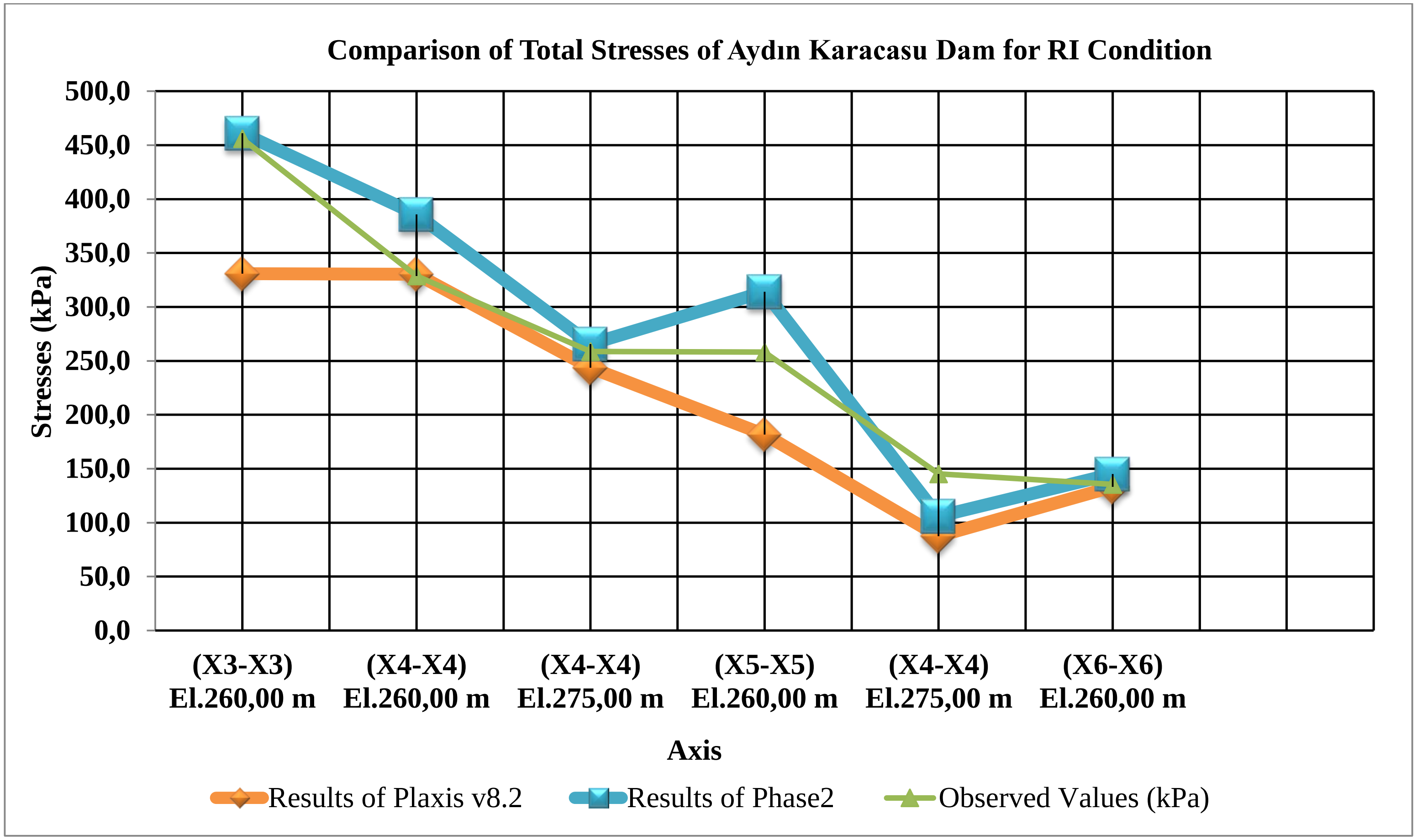

(*) Observed Stress Values are recorded by DSİ

(*) Imaginary axes are shown in *Figure 4.8* (see *Section* 4.2.4)

Figure 5.13 Comparison of Calculated Stresses with Observed Ones for RI

Table 5.8 Calculated and observed Stress increments

Total Pressure Gauge	Elevation (m)	Axis	Results of Plaxis v8.2 (kPa)		Results of Phase2 (kPa)		Observed Values (kPa)		Stress Increment (kPa)		
			EOC	**RI**	**EOC**	**RI**	**EOC**	**RI**	**Observed**	**Plaxis v8.2**	**Phase2**
BÖ-5	260	X_3-X_3	235,7	330,9	388,8	461,2	405,5	455,8	50,3	95,2	72,4
BÖ-6	260	X_4-X_4	298,6	330,2	356,2	385,7	323,9	328,8	4,9	31,6	29,5
BÖ-15	275		170,6	243,8	229,1	265,7	123,2	258,6	135,4	73,2	36,6
BÖ-7	260	X_5-X_5	206,1	181,6	307,6	314,0	257,1	258,1	0,9	-24,4	6,3
BÖ-16	275		86,5	87,3	97,3	105,8	144,5	145,1	0,6	0,8	8,5
BÖ-8	260	X_6-X_6	100,9	133,3	132,8	145,1	133,8	135,4	1,6	32,3	12,3

(*) Observed Stress Values are recorded by DSİ

5.4. Evaluation of Horizontal Deformations

In Aydın Karacasu Dam, no instrumentation is provided to observe horizontal deformation of embankment by DSİ. However, in this study, horizontal deformations are calculated and are given in Figures 5.14-5.19 both for EOC and RI conditions to depict deformation behavior of dam. Imaginary axes examined in the following Figures are shown in *Figure 4.8* (see *Section 4.2.4*). Horizontal deformations are calculated for the axes X_3-X_3, X_4-X_4, X_5-X_5 in both Plaxis v8.2 and Phase2. Figures 5.14-5.19 show the results of analyses.

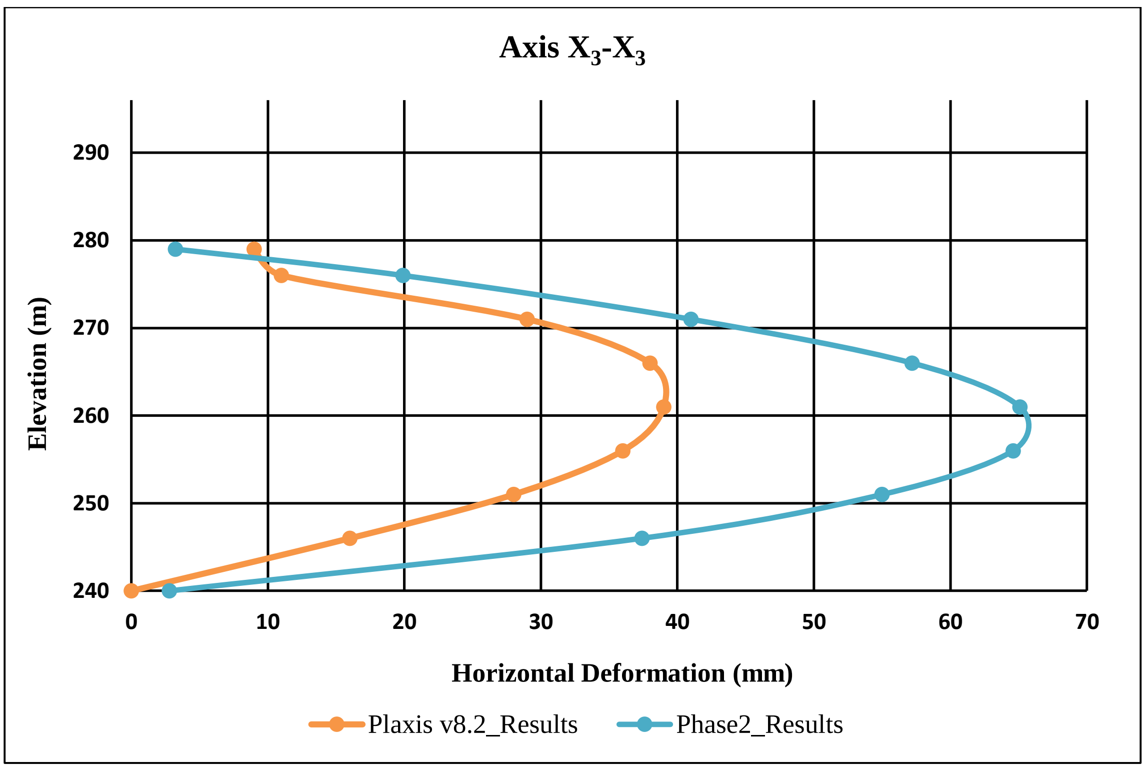

Figure 5.14 Comparison of calculated horizontal deformations for EOC

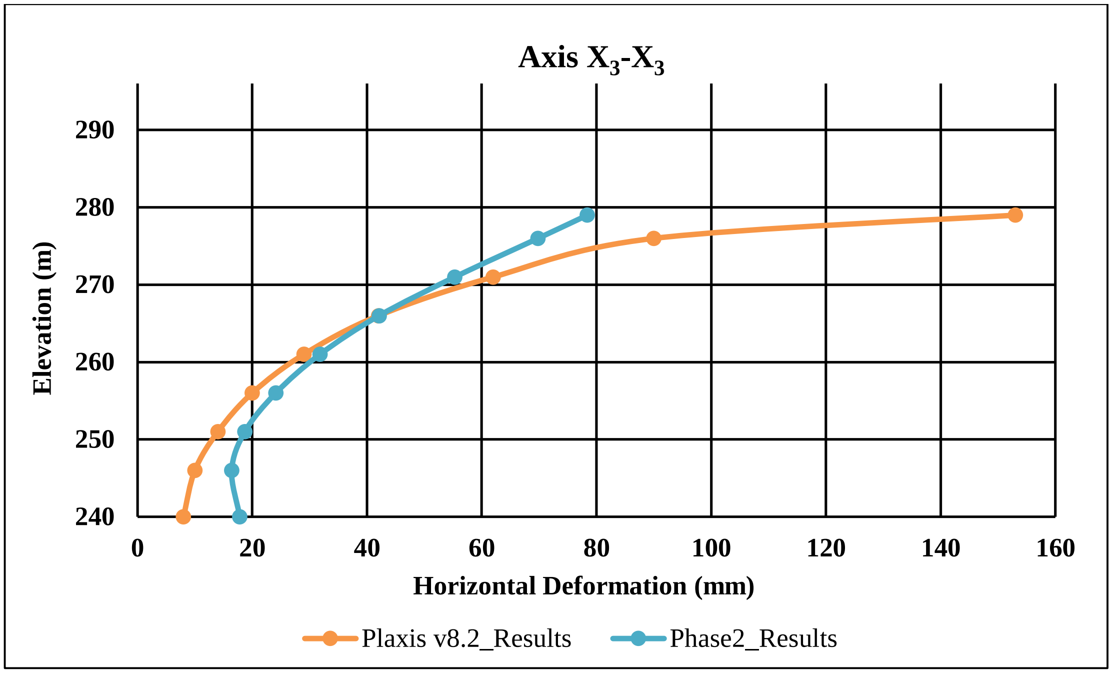

Figure 5.15 Comparison of calculated horizontal deformations for RI

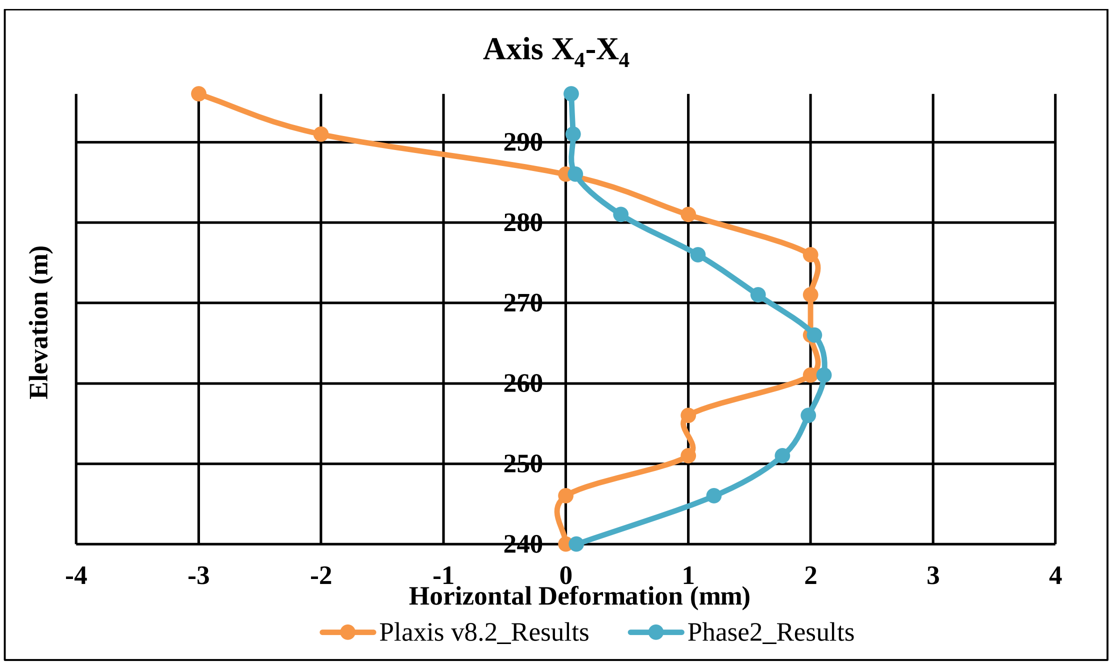

Figure 5.16 Comparison of calculated horizontal deformations for EOC

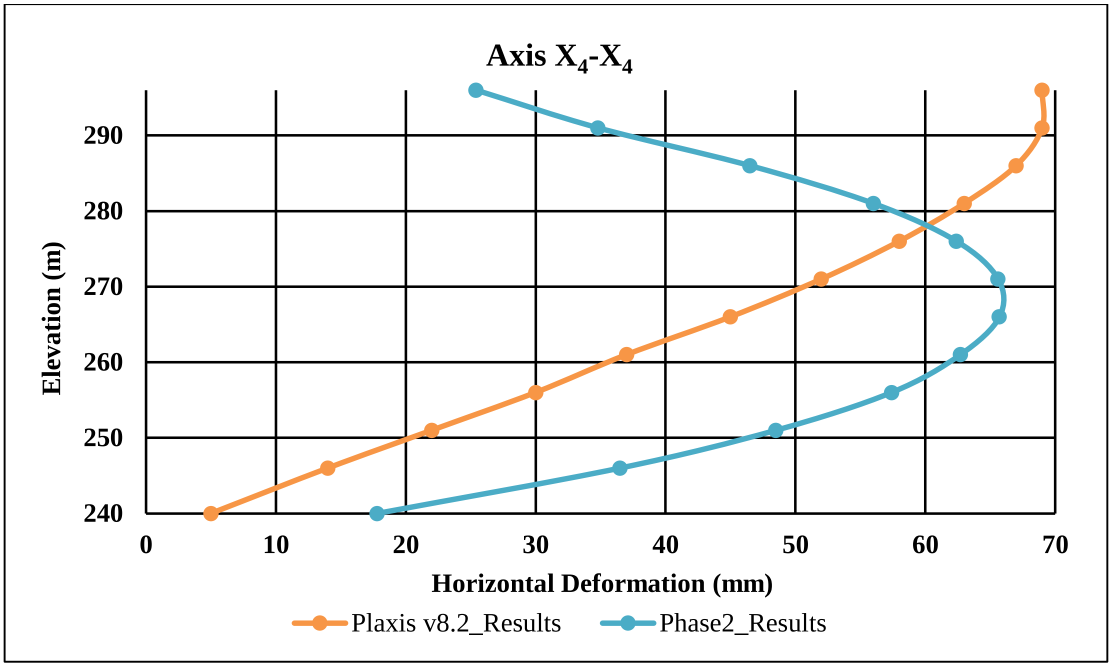

Figure 5.17 Comparison of calculated horizontal deformations for RI

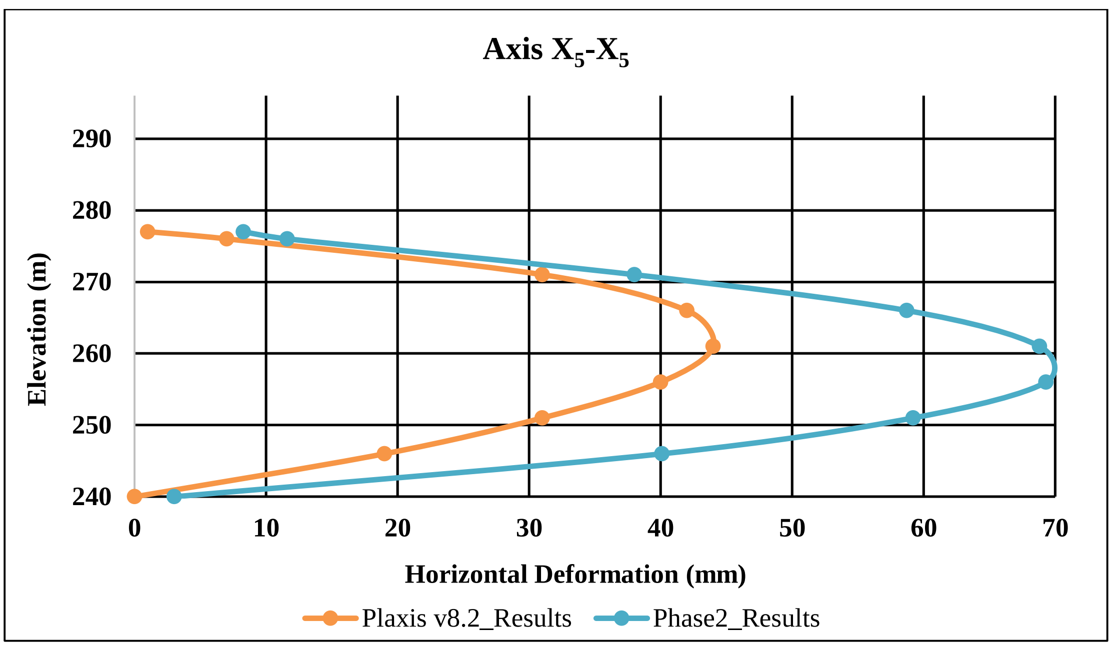

Figure 5.18 Comparison of calculated horizontal deformations for EOC

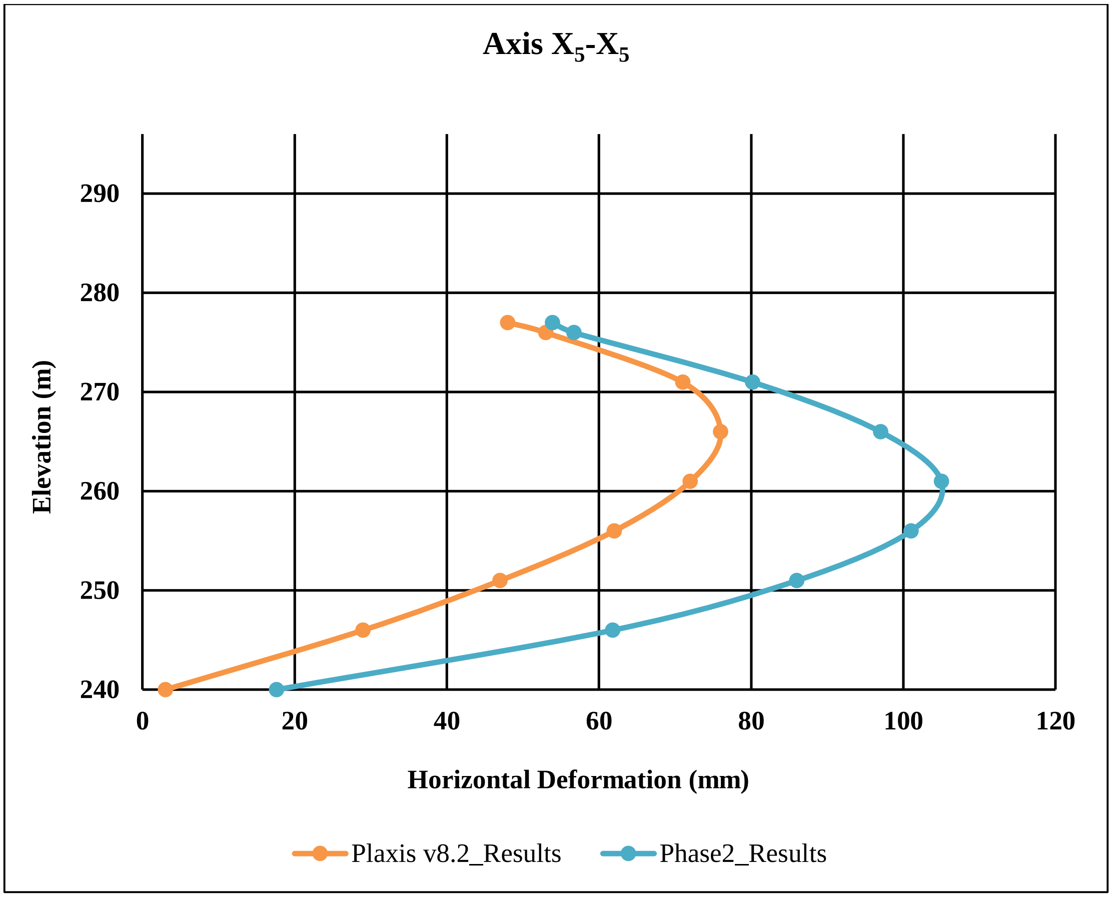

Figure 5.19 Comparison of calculated horizontal deformations for RI

5.5. Effect of Reservoir Impounding on Concrete Membrane

In this study, axial strains of concrete slab are calculated by finite element analyses (Plaxis v8.2) in order to assess the deformation behavior. Using of Plaxis v8.2, results of axial forces and axial strains of concrete slab are found. Axial rigidity of concrete slab (EA) is given in the *Table 4.7* (see *Section 4.2.2.1*). In *Table 5.8*, calculated axial strains are indicated for both EOC and RI conditions. In this Table, positive strain values represent tensile strains and negative strain values represent compressive strains.

Table 5.9 Axial Strains of Concrete Slab of Aydın Karacasu Dam for both EOC and RI Conditions

Elevation (m)	EOC Condition			RI Condition		
	Axial Force Calculated by Plaxis v8.2 (kN/m)	EA (kN/m)	Axial Strains Calculated by Plaxis v8.2 (10^{-6} m/m)	Axial Force Calculated by Plaxis v8.2 (kN/m)	EA (kN/m)	Axial Strains Calculated by Plaxis v8.2 (10^{-6} m/m)
240,0	-177,2	8550000,0	-20,7	1229,2	8550000,0	143,8
246,0	-191,8	8550000,0	-22,4	484,6	8550000,0	56,7
251,0	-178,9	8550000,0	-20,9	22,1	8550000,0	2,6
256,0	-167,0	8550000,0	-19,5	-463,6	8550000,0	-54,2
261,0	-161,6	8550000,0	-18,9	-913,1	8550000,0	-106,8
266,0	-144,3	8550000,0	-16,9	-1066,2	8550000,0	-124,7
271,0	-126,5	8550000,0	-14,8	-1072,7	8550000,0	-125,5
276,0	-106,2	8550000,0	-12,4	-925,0	8550000,0	-108,2
281,0	-81,8	8550000,0	-9,6	-683,3	8550000,0	-79,9
286,0	-53,9	8550000,0	-6,3	-470,6	8550000,0	-55,0
291,0	-23,0	8550000,0	-2,7	-185,1	8550000,0	-21,6
294,0	-0,9	8550000,0	-0,1	-12,2	8550000,0	-1,4

When Table 5.8 is examined, it is seen that compressive axial strains occur for EOC condition and axial strains decreases with increasing elevations. However, tensile axial strains are recorded at lower elevations for RI condition. This condition is attributed to first reservoir impounding. “First reservoir impounding” means that reservoir level reaches normal water level (El. 293.50 m). It is seen from Table 5.8, reservoir impounding creates a remarkable increments in axial strains. Axial strain diagrams of concrete membrane for both EOC and RI conditions are shown in the Figures 5.20-5.21.

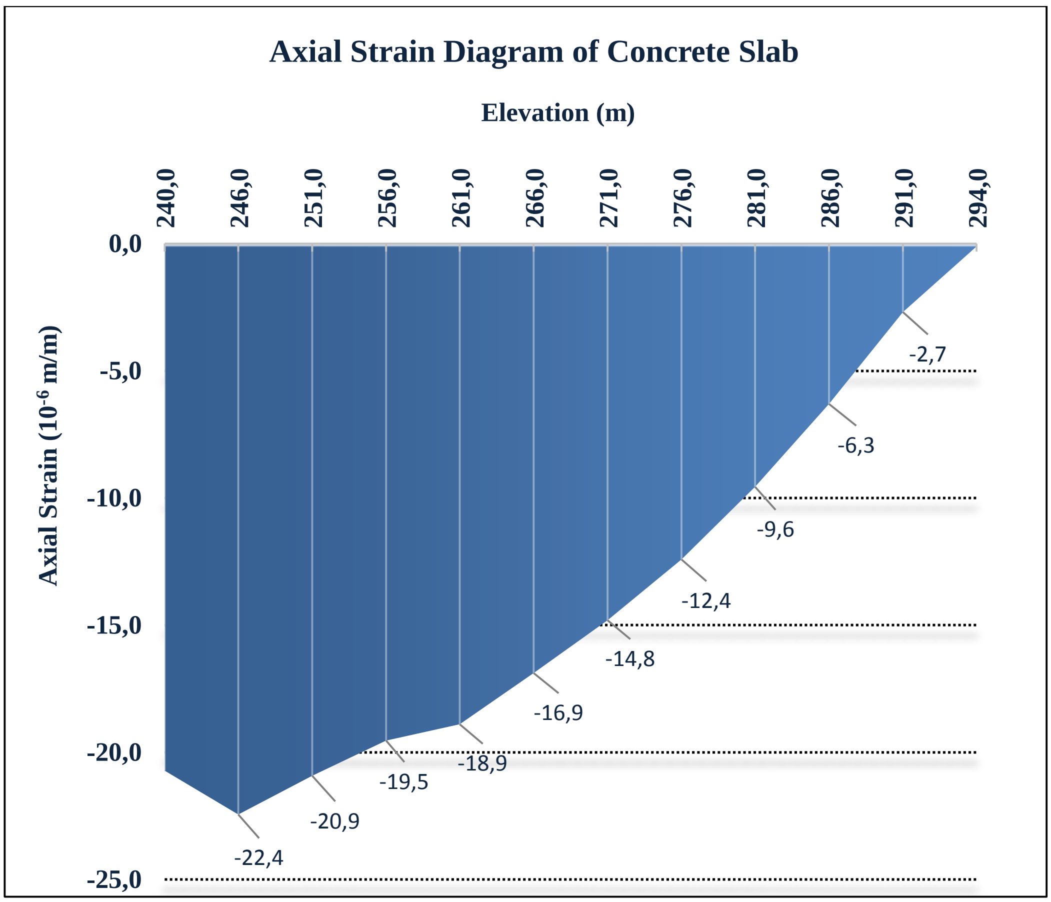

Figure 5.20 Axial strains calculated by Plaxis v8.2 for EOC condition (10^{-6} m/m)

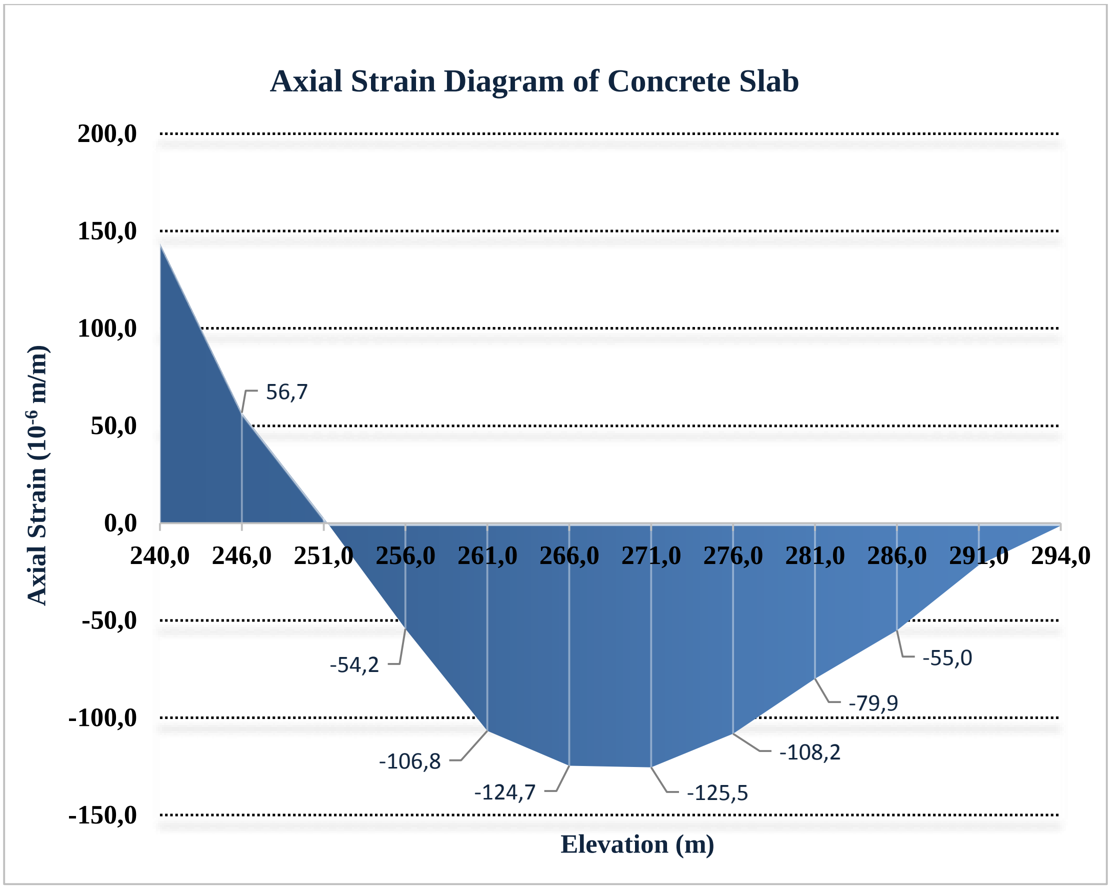

Figure 5.21 Axial strains calculated by Plaxis v8.2 for RI condition (10^{-6} m/m)

Axial forces, shear forces and bending moments diagram of concrete slab are shown for both EOC and RI conditions in Figures 5.22-5.27.

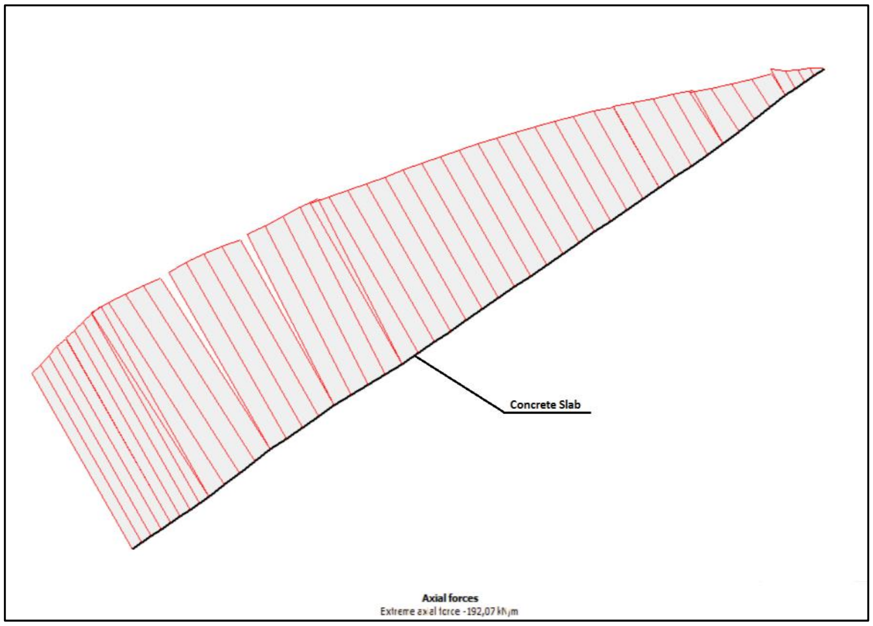

Figure 5.22 Axial force diagram of concrete slab for EOC condition (Plaxis v8.2)

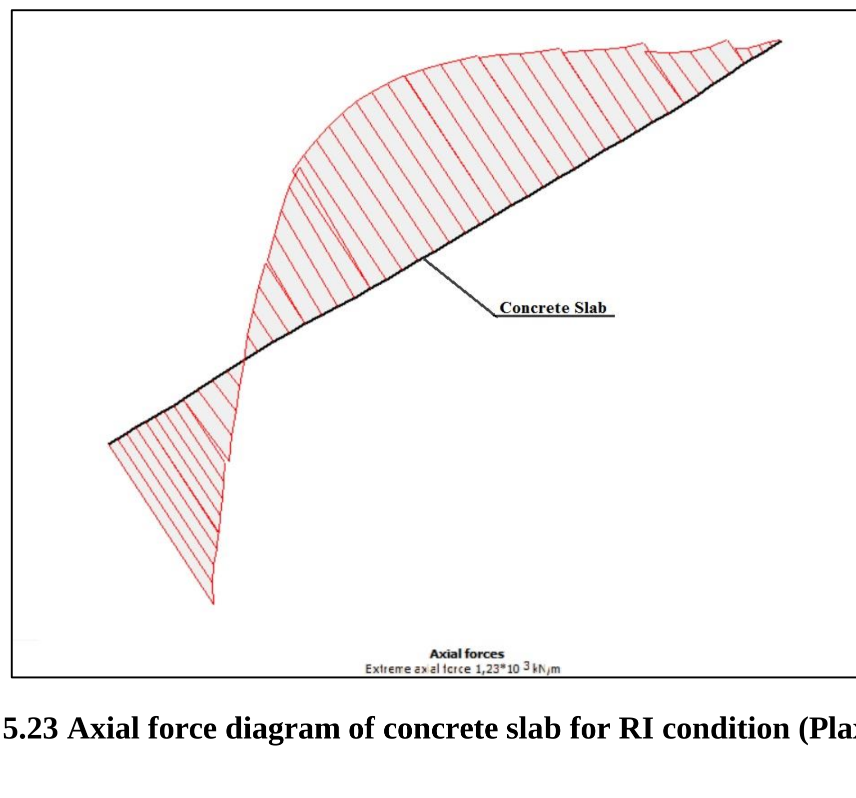

Figure 5.23 Axial force diagram of concrete slab for RI condition (Plaxis v8.2)

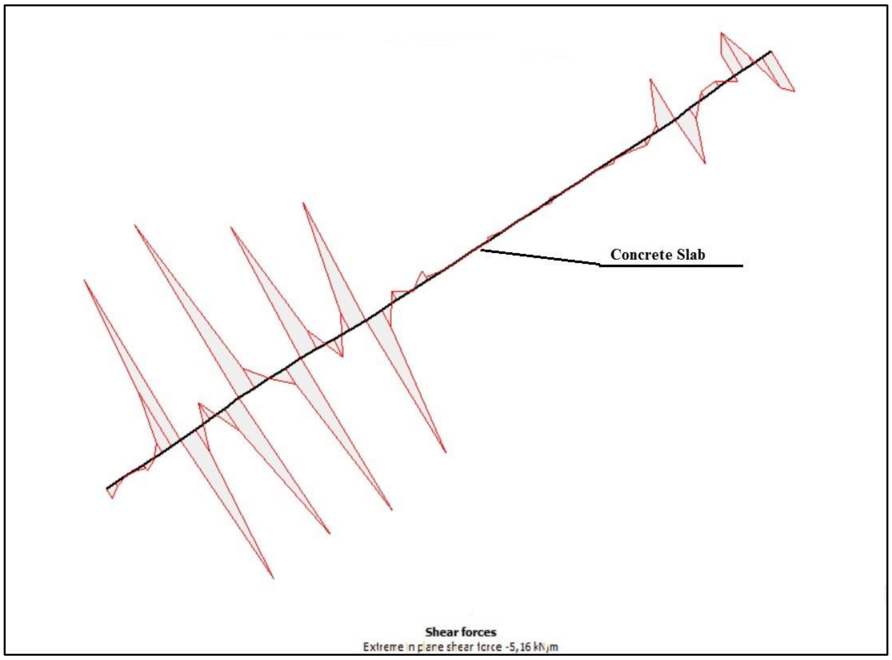

Figure 5.24 Shear force diagram of concrete slab for EOC condition (Plaxis v8.2)

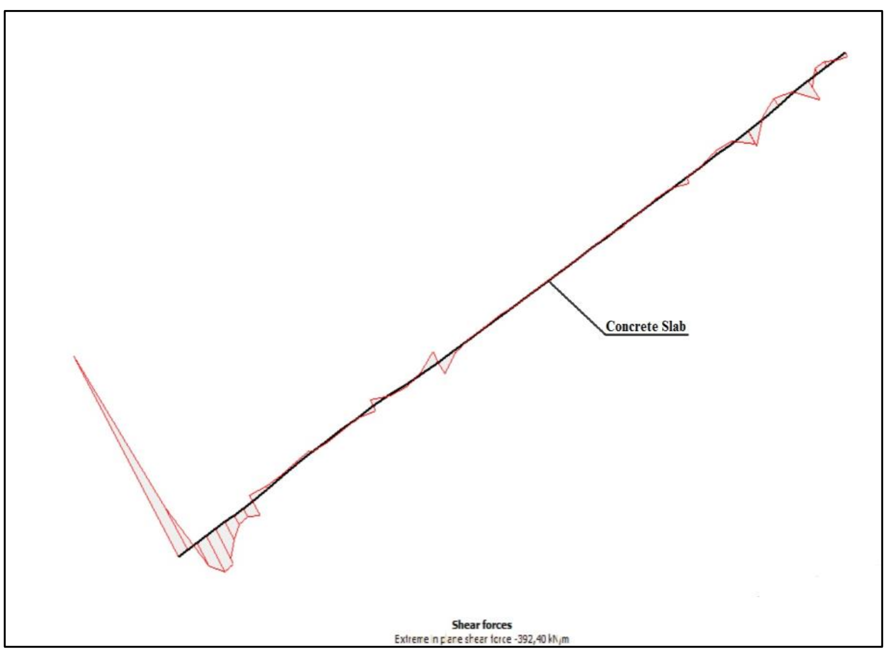

Figure 5.25 Shear force diagram of concrete slab for RI condition (Plaxis v8.2)

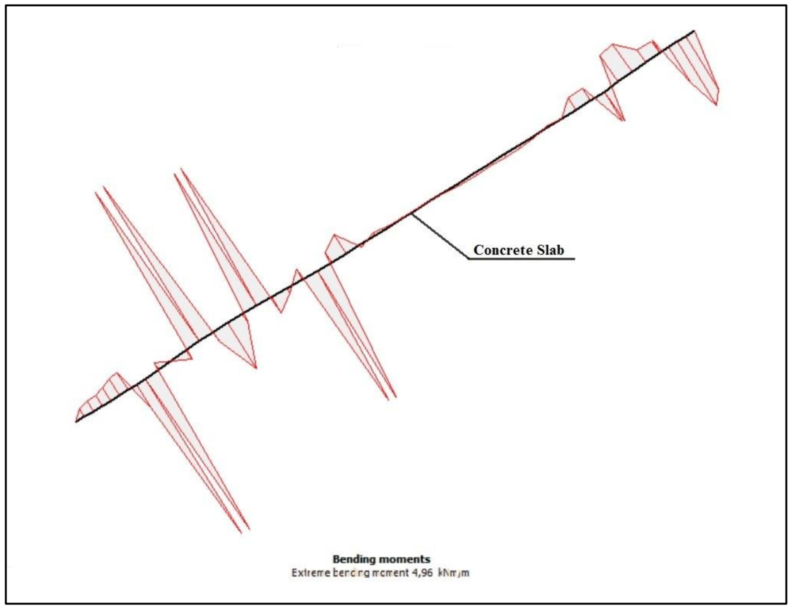

Figure 5.26 Bending moment diagram of concrete slab for EOC condition (Plaxis v8.2)

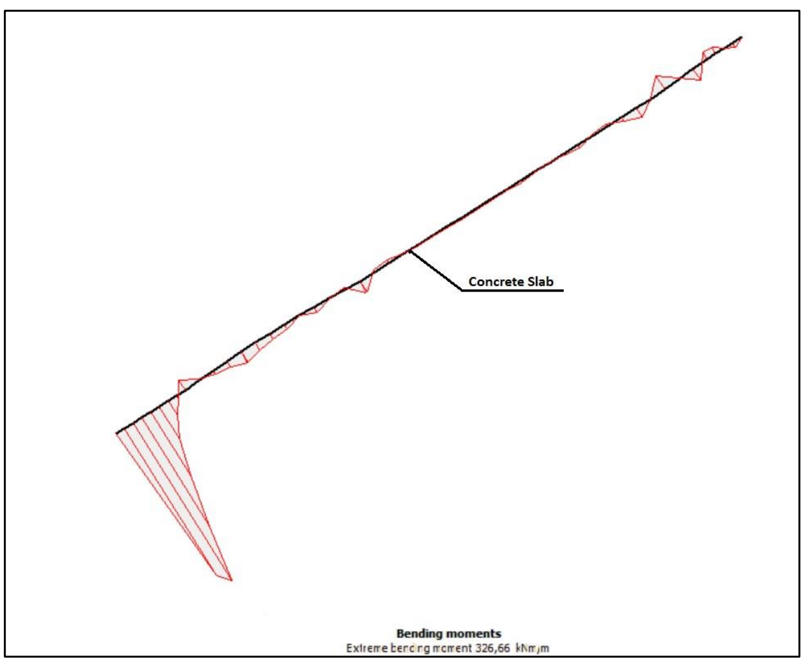

Figure 5.27 Bending moment diagram of concrete slab for RI condition (Plaxis v8.2)

5.6. Total Stress Contours

Stress contours are determined by Plaxis v8.2 both for EOC and RI conditions. In *Figures 5.28-5.33*, vertical, horizontal and shear stress contours, calculated in finite element analyses, are shown. In these Figures, "EOC" and "RI" are respectively represent "end of construction" and "reservoir impoundment" conditions.

Upstream and downstream slopes of Aydın Karacasu Dam are the same. Hence, stress contours tend to behave symmetrical with respect to the dam axis for the end of construction condition. In the following figures, positive stress values show tension and negative stress values show compression.

When *Figures 5.28-5.33* are analyzed, it is obviously seen that reservoir impounding causes significant increments in both vertical and horizontal stresses in the regions closer to upstream membrane where, reservoir loading causes rather smaller increments in the stresses of downstream region.

As it is seen from the *Figure 5.28 and 5.29*, maximum total horizontal stress is measured respectively as 303.2 kN/m^2 for EOC and 345,2 kN/m^2 for RI near the dam foundation. As it is seen from the *Figure 5.30 and 5.31*, maximum total vertical stress is respectively measured as 999,9 kN/m^2 for EOC and 1093,8 kN/m^2 for RI near the dam foundation.

In *Figure 5.32*, shear stress contours show that shear stress values are close to the zero at the dam centerline for EOC. Shear stresses increase through the upstream and downstream region. Upstream and downstream slopes of Karacasu are the same; so, shear stress values increased with a similar rate from the centerline of the dam to the upstream and downstream regions for EOC. Positive shear stresses occur in the upstream region and negative shear stresses occur in the downstream region of the dam body for EOC. Maximum positive shear stress calculated in the downstream region for the end of construction condition is 125,5 kN/m^2. Maximum negative shear stress found in the upstream region for the end of construction condition is 125,6 kN/m^2. As it is seen in *Figure 5.33*, maximum positive shear stress is 145,2 kN/m^2 for RI condition.

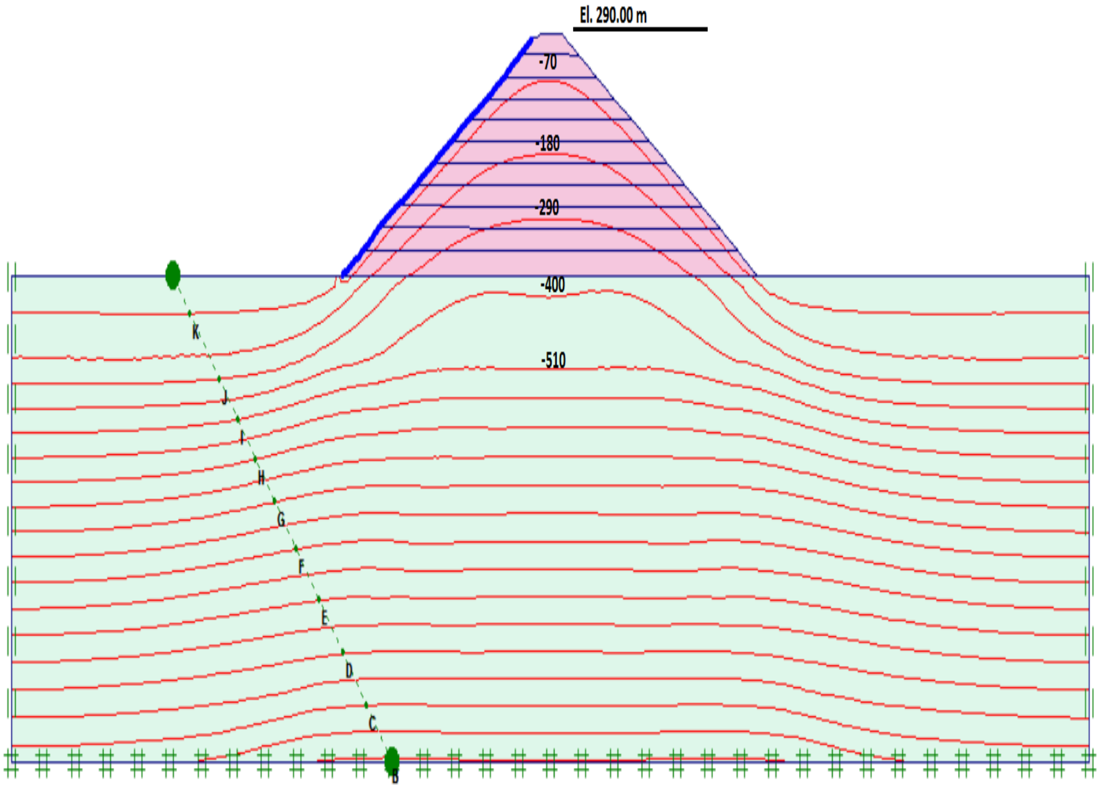

(*) Stress contours are calculated in Plaxis v8.2.

Figure 5.28 Horizontal stress contours for EOC condition (kPa)

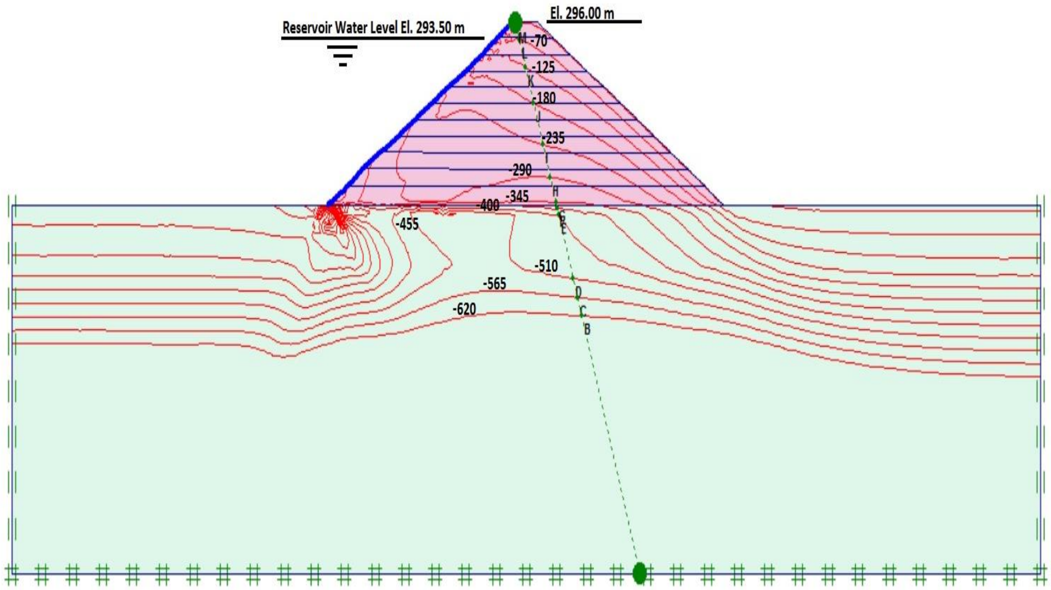

(*)Stress contours are calculated in Plaxis v8.2.

Figure 5.29 Horizontal stress contours for RI condition (kPa)

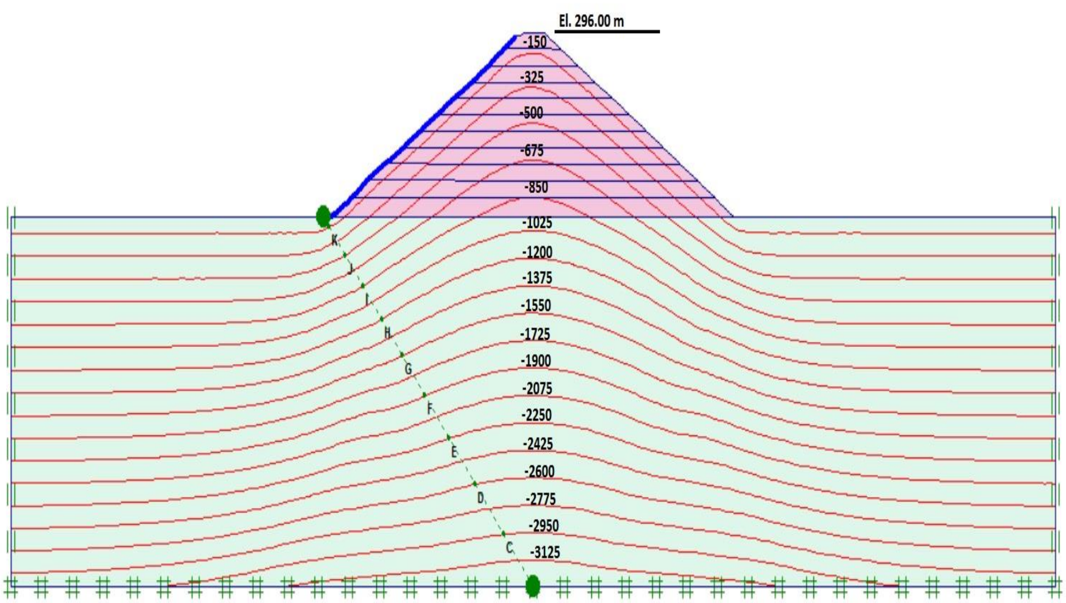

(*)Stress contours are calculated in Plaxis v8.2.

Figure 5.30 Vertical stress contours for EOC condition (kPa)

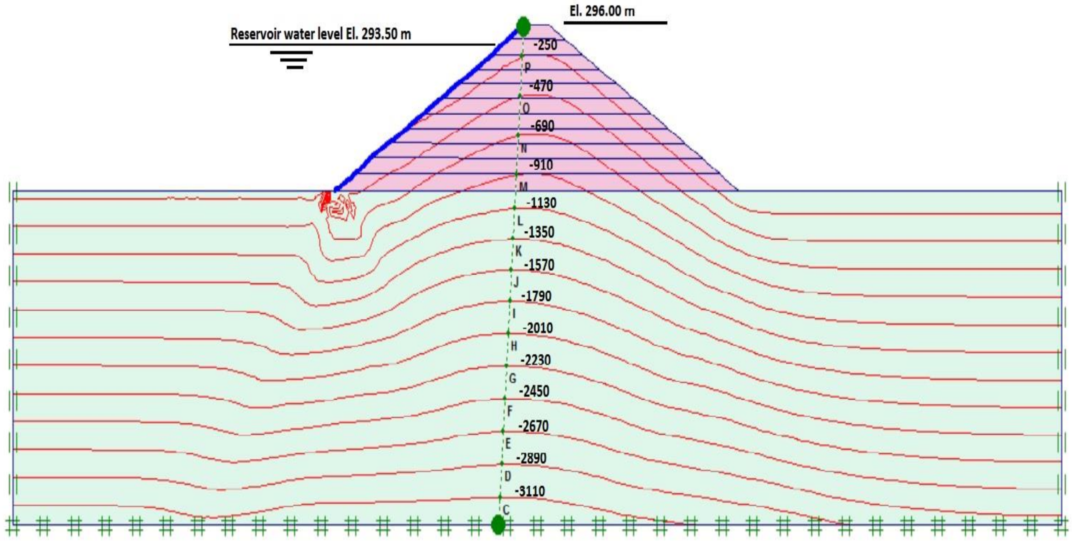

(*)Stress contours are calculated in Plaxis v8.2.

Figure 5.31 Vertical stress contours for RI condition (kPa)

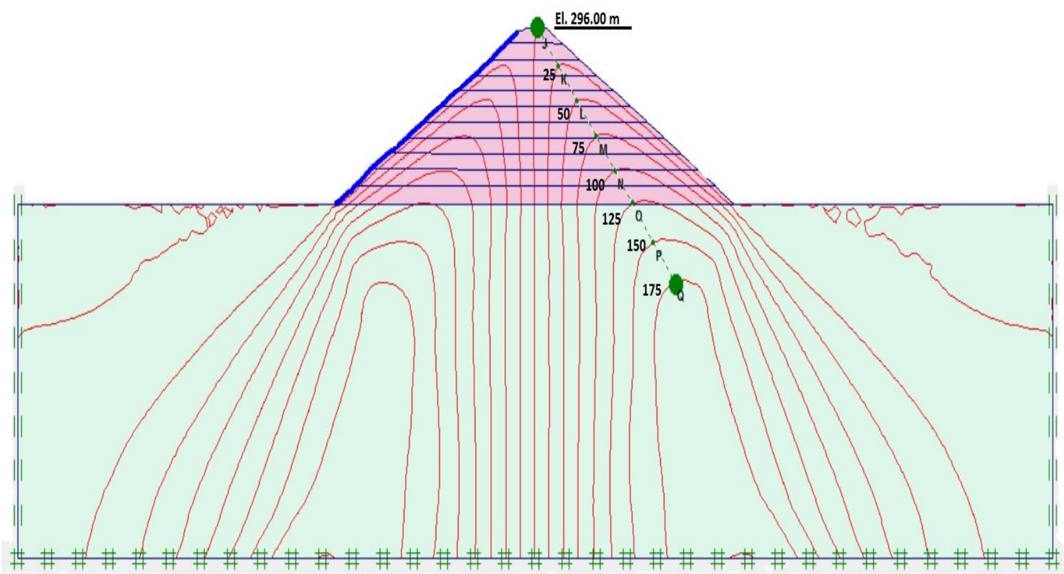

(*)Stress contours are calculated in Plaxis v8.2.

Figure 5.32 Shear Stress Contours for EOC Condition (kPa)

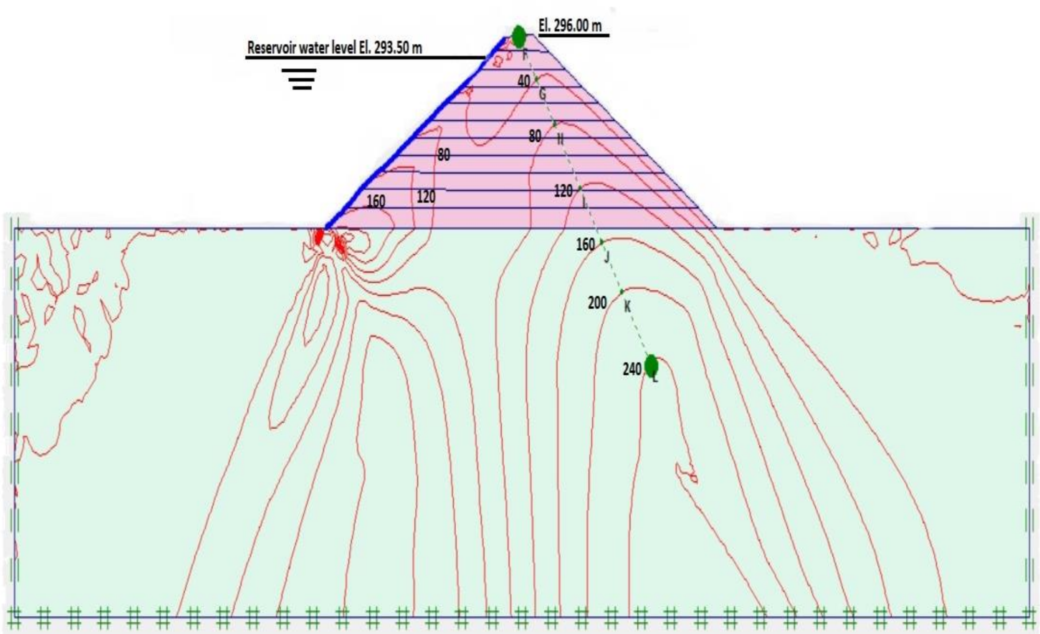

(*)Stress contours are calculated in Plaxis v8.2.

Figure 5.33 Shear Stress Contours for RI Condition (kPa)

CHAPTER 6

SUMMARY AND CONCLUSIONS

In this study; stress and settlement analyses of Aydın Karacasu Dam, the first concrete faced sand-gravel dam of Turkey, are conducted by using both Plaxis v8.2 and Phase2 2D finite programs. Results of analyses, obtained from these finite element programs, are compared with each other and observed ones recorded by DSİ. Some presumptions are taken into consideration during conduct analyses. These presumptions are as following;

- Concrete slab of Aydın Karacasu dam is assumed as impervious and not being exposed to any cracks.
- Thickness of the concrete membrane is assumed to be constant from the foundation of dam body to the crest. Thus, it is modeled as a single unit having 0.3 m thickness.
- The interaction between concrete face and sand-gravel fill dam is assumed to be perfect.
- In Plaxis v8.2, sand-gravel fill material is designed by utilizing soil hardening model (Duncan and Chang's) and also Mohr Coulomb Model is used in Phase2 analyses.
- Rock foundation of the Aydın Karacasu dam is assumed to be a rigid.
- The parameters are assessed by means of a search of available literature for hyperbolic model utilized for CFSGDs. They yield similar deformation behavior with Aydın Karacasu Dam. Then, parameters are modified by comparing the calculated and observed settlements taken from State Hydraulic Works to obtain

the best results. It is seen that the best compatible model parameters are those given in “Alternative 2” shown in *Table 4.5* (see *Section 4.2.2.1*).

At the end of the finite element analysis conducted by Plaxis v8.2 and Phase2 following conclusions are arrived,

- Some of the observed and calculated settlements, taken from same hydraulic settlement devices, are compatible when the analysis results are examined. Difference between the calculated and observed ones decreases with increasing elevations. On the other hand, some of the observed and calculated settlements differ in the magnitude. Poor quality of compaction or irregular readings taken from instrumentation devices during end of construction and reservoir impoundment may be the cause of those differences between observed and calculated vertical displacements.
- Horizontal displacements are not observed by DSİ for both at the end of the construction and during impoundment period. Thus, a comparison of horizontal deformation behavior of Aydın Karacasu Dam is not possible.
- It is seen from Plaxis v8.2 and Phase2 that total vertical stress distribution, total horizontal stress distribution and shear stress distribution are symmetrical with the dam centerline for the end of construction periods. This may be attributed to the fact that both downstream and upstream slopes are the same.
- For the end of construction condition, majority of the calculated values obtained from both finite element program results are compatible with observed settlement values. Maximum vertical settlement is found as 36,20 cm which corresponds to about 55% of the total dam height from the base by Plaxis v8.2 and it is found as 38.20 cm which corresponds to about 46% of the total dam height from the base by Phase2. These results verify that compressibility of the fill material decreases with increasing elevations.

- In the reservoir full condition, analyses results indicate that most of the calculated settlements are smaller than observed ones except settlements calculated in axis X_4-X_4. In axis X_4-X_4, maximum vertical settlement is found as 39,30 cm which corresponds to about 55% of the total dam height from the base by Plaxis v8.2 and it is also found as 40,00 cm which corresponds to about 46% of the total dam height from the base by Phase2. Results of analyses conducting in axes X_3-X_3 and X_4-X_4 are compatible with observed values obtained from DSİ. Results of RI analyses show that reservoir impounding has significant effect on regions closer to upstream membrane.
- Horizontal settlements of the Karacasu Dam are not measured by instrumentation devices. Therefore, comparison of calculated and observed settlement is not possible. It is seen from results of analyses conducted to predict horizontal deformation behavior of Aydın Karacasu Dam (see *Section 5*.4) that reservoir impounding has a noteworthy effect on regions closer to upstream membrane.
- As can be observed from *Figures 5.18-5.23* (see *Section 5.5*), shear stresses are seen symmetrical with respect to the dam axis and shear stress is zero at the dam axis for the end of construction condition. However, in reservoir full condition, water load affects the behavior of the dam body unsymmetrically. Dam body settles towards the downstream due to the impact of the water load. Negative shear stress of the upstream zone of the dam body is reduced. In contrast, positive shear stress occurring in the downstream zone of the dam body is increased. These stress changes are compatible with studies having similar deformation behavior with Aydın Karacasu Dam in the literature.

It is seen that some of the observed settlement data taken from hydraulic settlement devices are not reliable. For this reason, incompatible readings are not taken into consideration. Generally, soil deformations, under loading and unloading conditions during end of construction and reservoir impoundment periods, analyzed by using 2D finite element programs Plaxis v8.2 and Phase2. These programs yield similar results. It is suggested that, for future studies, 3D finite element analyses may be conducted by utilizing Plaxis 3D by importing model geometries from CAD data. Fattah et al., (2010) use finite element program called 3-DEEP to model a trial embankment built in Finland which can be of value in studying CFSGDs.

REFERENCES

1. Fanlie, Z. (2000). "Study on Application of Sand-gravel to Gudongkou Concrete Faced Rockfill Dam", CFRD Proceedings International Symposium on Concrete Faced Rockfill Dams, p.197~203, Beijing, China.

2. Ti, K. S., Huat, B. K., Noorzaei, J., Jaafar, M. S., Sew, G. S. (2009). "A Review of Basic Soil Constitutive Models for Geotechnical Application", Malaysia.

3. Salimi, N., Yazdanjou, V., (2008). "Effect of Gravel Content on the Shear Behavior of Sandy Soils", the 4th National Conference on Civil Engineering, Tehran.

4. Singh, B., Varshney, R. S., (1995). "Engineering For Embankment Dams", A.A. Balkema Publishers, Brookfield.

5. Haselsteiner, R., Ersoy, B., (2011). "Seepage Control of Concrete Faced Dams with Respect to Surface Slab Cracking", 6th International Conference on Dam Engineering, Lisbon, Portugal.

6. Clough, R. W., Woodward, R. J. (1967). "Analysis of Embankment Stresses and Deformations". *Journ. SMFD, ASCE*, vol. 93, no. SM4.

7. Duncan, J. M., Chang, C. Y., (1970). "Nonlinear Analysis of Stress and Strains in Soils", *Journ. SMFD, ASCE,* 96 (SM5): 1629-1653.

8. Anochie, J. K.,Boateng, (2007). “Advanced Testing and Characterization of Transportation Soils and Bituminous Sands”, Urbana, Illinois.

9. Cooke, J. B., (1984). “Progress in Rockfill Dams”. *Journ. Geotech. Engg.*, ASCE, vol. 110, no. 10.

10. Hydraulic State Works (2012), Design Guide of Embankment Dams.

11. Özkuzukıran, S., Özkan, M. Y., Yıldız, G. S., (2005). “Settlement Behavior of Concrete Faced RockFill Dams, A Case Study, Msc. Thesis, METU, Ankara.

12. Ünsever, Y. S., Özkan, M. Y., Yıldız, G. S., (2007). “An Analysis of Deformation Behavior of MuratlI Asphalt Faced Rockfill Dam”, Msc. Thesis, METU, Ankara.

13. TS 500, (2000). “Requirements for Design and Construction of Reinforced Concrete Structures”, Turkish Standards Institution (TSE).

14. Kondner, R. L., (1963). “Hyperbolic Stress-Strain Response. Cohesive Soils”, J. of Soil Mech. and Found. Div., ASCE, 89, SM1, 115-143.

15. Phase2 ver. 8.0, Material Model Manual, 2011.

16. Schanz, T., Vermeer, P. A., Bonnier, P. G., (1999). “The Hardening Soil Model: Formulation and Verification”, Beyond 2000 in Computational Geotechnics-10 Years of Plaxis, Balkema, Rotterdam.

17. Plaxis ver. 8.2, Material Model Manual, 2010 and 2013.

18. Cooke, J. B., Sherard, J. L., (1987). "Concrete-Face Rockfill Dam: I. Assessment", J. Geotechnical Engineering., ACSE, 113, 10, 1096-1112.

19. Fell, R., Hunter, G., (2003). "Rockfill Modulus and Settlement of Concrete Face Rockfill Dams", J. Geotech. Geoenv. Engrg., ASCE, 129, 10, 909-917.

20. Cooke, J. B., Sherard, J. L., (1987). "Concrete-Face Rockfill Dam: II. Design", J. Geotechnical Engineering., ASCE, 113, 10, 1113-1132.

21. Nobari, E. S., Duncan, J. M., (1972). "Movements in Dams due to Reservoir Filling", ASCE: Specialty Conf. On Performance of Earth and Earth Supported Structures, 797-815.

22. Bowles, J. E., P. E., S. E. (1997). "Foundation Analysis and Design", the McGraw-Hill Companies, Inc., Illinois.